



2013

**ACTIVITY REPORT**







2013  
**ACTIVITY REPORT**

© ALBA SYNCHROTRON 2014  
Ctra. BP 1413, km. 3,3 08190  
Cerdanyola del Vallès (Barcelona)  
Spain

Graphic design: Lucas Wainer.

## INDEX

07	FOREWORD
10	ALBA SYNCHROTRON, THE NEWEST SOURCE IN THE MEDITERRANEAN AREA
	SCIENTIFIC RESULTS
17	BIOSCIENCES
23	MATERIALS SCIENCE
32	CATALYSIS
38	MAGNETISM
46	INDUSTRY RESULTS
	ACTIVITY REPORTS BY DIVISION
48	EXPERIMENTS
53	ACCELERATORS
57	COMPUTING AND CONTROLS
61	ENGINEERING
67	COLLABORATION WITH EXTERNAL INSTITUTIONS
70	STUDENT TRAINING ACTIVITIES
72	WORKSHOPS AND SEMINARS
74	COMMUNICATIONS AND OUTREACH
78	FACTS & FIGURES



---

## FOREWORD

In recent years Spain has been developing several research facilities with the objective to align our country to other more advanced nations with much richer research activities. The ALBA synchrotron light source is one of the major installations devoted to that objective and it is the result of a fruitful collaboration of the Spanish Government and the autonomous administration in Catalonia.

This annual report is a proof of the capacity to construct an infrastructure of a very demanding technological content with a very tight schedule and within the approved budget. The quality of the installation allows the comparison of ALBA with the most advanced facilities of this kind in the world and the characteristics of the beamlines are state of the art in the corresponding experimental techniques.

The number and the origin of users during these first years of activities is a proof that the decision taken some years ago of constructing this facility was opportune and responded to a real demand of our research communities. We are convinced that ALBA will be an excellent instrument to enhance the quality of our research.

As persons responsible of the research in our administrations we want to express our gratitude to the teams that have made possible the high level of quality of ALBA and we are convinced that, even in difficult times, they will succeed in exploiting ALBA at the highest possible level.

### **CARMEN VELA**

*Secretary of State of Research, Development  
and Innovation*  
Ministry of Economy and Competitiveness  
Spanish Government

### **ANDREU MAS-COLELL**

*Minister of Economy and Knowledge*  
Catalan Government

---

Dear reader

This is the first ALBA Activity Report, a 3rd generation light source, funded by the Spanish Government and the Generalitat de Catalunya. It is aimed at highlighting the status, the scientific output, and the future programs of our young facility.

ALBA project was approved in 2003. The construction on a green field in a country with no experience in accelerator based large infrastructures signified a challenge, which has been successfully taken on by the ALBA team, headed by Joan Bordas under the chairmanship of Ramon Pascual. The original design of a 3 GeV light source, with low emittance and high flux, and a Phase I portfolio of seven beamlines, has become a reality, and our laboratory is welcoming users since two years ago.

This issue is dedicated to the years 2012-2013, describing therefore the first operation period, even if the facility started providing photons already in 2011, in which installation of the latest systems, beamline commissioning, and friendly users coexisted. May 2012 marks the first official user, arrived to ALBA after the selection of proposals of the first user call. By beginning of 2013 all Phase I beamlines were operational.

ALBA is nowadays offering Photoemission Spectroscopy, including a Near Ambient Pressure Photoemission station, Soft X-ray Microscopy, Macromolecular Crystallography Diffraction, High Resolution SAXS and WAXS, Powder Diffraction including High Pressure Station, EXAFS and XANES, Circular Magnetic Dichroism and Resonant Magnetic Diffraction. In the report you will find information on the first experiments performed in our facility and on the future plans.

Our users mainly hail from Spain, with an international component which shows a tendency to increase in the three user calls performed up to now. All Spanish Regional Community are represented, with a majority of Catalan ones, who profit also from the proximity. Universities and Research Centers are among our customers. Proprietary access is available and few private companies are already collaborating with us, while contacts with many others are paving the way for fruitful future utilizations of our instruments by private sectors.

Our staff is constantly evolving. A large part of it has been renewed as often happens when a facility crosses the frontier between construction and operation. A significant increase has been accomplished in the experimental division, which now has a complete team for each beamline, including also post-docs. The photo on the last page shows a good representation of the staff, whose young average age is one of ALBA richness.

Daily collaboration with national and international institutes provides a forum for exchanging experiences, developing technologies, and plan new experiments. ALBA position

---

in the environment of Barcelona, which houses universities, research institutions and technological companies, is a fortunate opportunity for development and technological transfer.

Several initiatives of outreach and information to the general public about our activities are constantly being developed at all levels by our staff. The most significant example is the organization of open days, which involve a large part of the ALBA workers on voluntary basis and is rewarded with an extremely great success from the point of view of visitors and especially of their enthusiasm.

The original plan of regular growth in terms of beamlines has suffered an arrest of few years due to the recent austerity situation. This stop has been productively used by ALBA staff to enter in the operation phase, facing and solving the typical problems of a new born facility. Some of these challenges are part of this report and their overcoming has strengthened and matured the whole project.

Even if this report is focused on the activity of the last two years, I take the opportunity to announce that the Phase II Beamline program has started in 2014 with the construction of MIRAS, a beamline dedicated to infrared spectro-imaging, and LOREA, dedicated to low-energy angular resolved photoemission with ultra-high resolution. Phase III Beamline program, for which the funding is still to be secured, consists of four extra Experimental lines, whose definition is in progress during this year.

We can consider that the exciting period of going from the construction to the operation period is now coming to an end, and we are now looking forward for the expansion of the facility in terms of beamlines in order to exploit the full capacity of the infrastructure, while producing scientific results at the frontier of knowledge.



I wish you to enjoy the reading,

Sincerely

**CATERINA BISCARI**

Director

# ALBA SYNCHROTRON, THE NEWEST SOURCE IN THE MEDITERRANEAN AREA

ALBA IS THE SPANISH 3<sup>RD</sup>-GENERATION SYNCHROTRON LIGHT SOURCE, LOCATED IN CERDANYOLA DEL VALLÈS (BARCELONA). IT IS A COMPLEX OF ACCELERATORS FOR ELECTRONS WHICH PRODUCE SYNCHROTRON LIGHT AND OF EXPERIMENTAL STATIONS WHERE THE PHOTONS ALLOW VISUALIZATION OF THE ATOMIC STRUCTURE OF MATTER AND THE STUDY OF ITS PROPERTIES.



## THE MACHINE

The electron beam energy is 3 GeV and the available photon energy ranges from infrared up to hard X-rays. Diffraction, spectroscopies and imaging techniques are offered in its seven state-of-the-art operational Phase-I beamlines.

Electron beam energy	3 GeV
Storage ring circumference	269 m
Natural horizontal emittance	44 nm rad
Nominal beam current	250 mA
Number of insertion straight sections	17
Number of Phase-I beamlines	7

Table 1. ALBA Synchrotron main parameters.

ALBA is composed of a linear accelerator (LINAC) – where electrons reach the energy of 100 MeV – and a low-emittance, full-energy booster – where electrons are accelerated to 3GeV, almost reaching speed of light. The booster and the storage ring are both hosted in the same tunnel and include 17 straight sections available for insertion devices.

## THE BEAMLINES

According to their scientific applications, ALBA beamlines can be divided into three groups:

### BIOSCIENCES

- MISTRAL, X-ray full-field transmission microscope for cryo-tomography of biological material of very high spatial resolution, producing 3D images of complete cells without the need of sample slicing.
- NCD studies crystalline samples with large (SAXS) and small (WAXS) periodicities. Very useful to analyze biological applications (fiber tissues and solutions) as well as polymers.
- XALOC is devoted to protein structure determination through X-ray crystallography.

### CONDENSED MATTER, especially magnetic and electronic properties and nanoscience.

- CIRCE, photoemission microscopy for chemical imaging of the surface and photoemission spectroscopy with samples at pressures up to 20 mbar for investigating surface chemical reactions and surfaces of liquid samples.

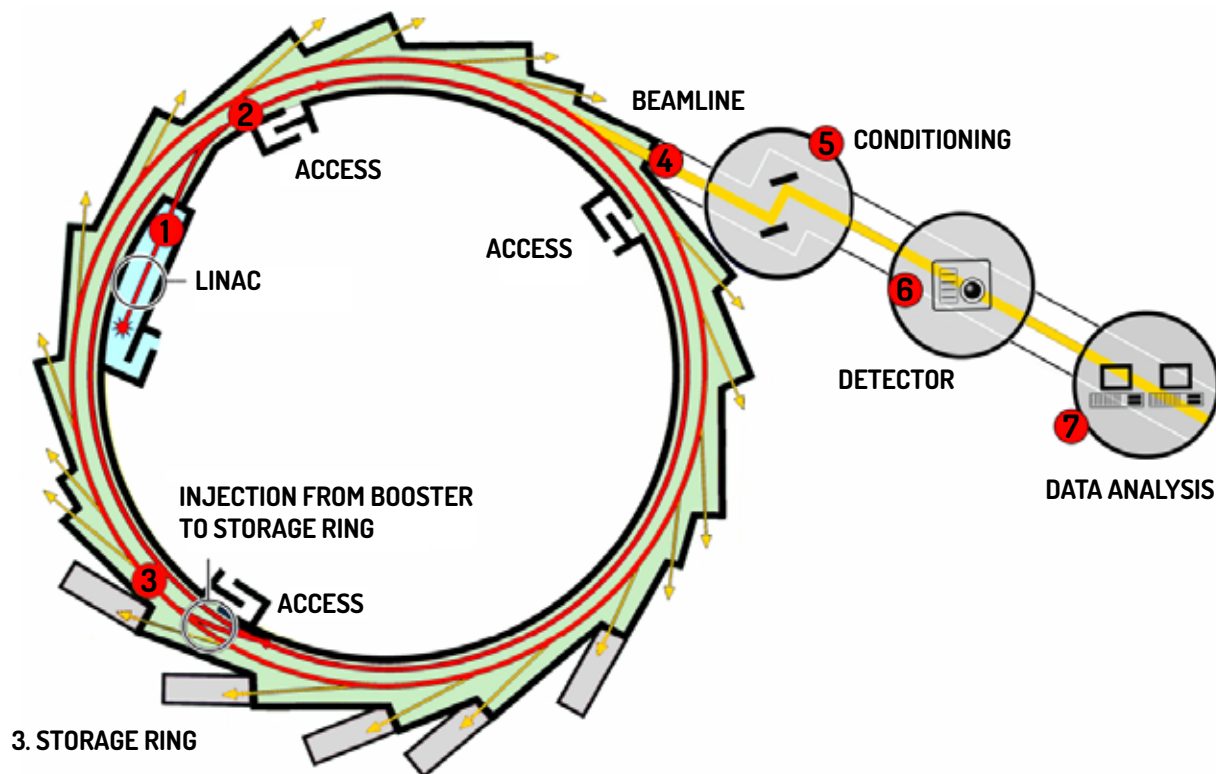


Figure 1. ALBA layout of the accelerators and beamlines.

- BOREAS, X-ray magnetic circular dichroism (XMCD) and X-ray magnetic linear dichroism (XMLD) techniques for the study of advanced magnetic materials. A 2nd experimental end-station is being developed for soft-X-ray magnetic scattering (SXRS).

**MATERIALS SCIENCE, with applications in chemistry, environment and cultural heritage, among others.**

- MSPD, powder diffraction beamline with two end-stations: diffraction under high pressure for analyzing the crystalline structure of matter under extreme pressure (up to ~50 GPa) and high resolution and high speed powder diffraction for the study of chemical kinetics, phase transitions, etc.
- CLÆSS, absorption spectroscopy for XANES/EXAFS during chemical reactions under conditions close to those relevant to industrial catalysis.

Two new beamlines have been approved in the second phase and are now in designing status:

- MIRAS, infrared microspectroscopy for the imaging of a very broad range of samples. This beamline is currently under construction and it is foreseen to be available for users at the end of 2016.
- LOREA, Low-energy ultrahigh resolution angular photoemission beamline for the understanding of the electronic structure of graphene-based material, topological insulators and other advanced materials. This beamline is currently in design status and will be available for users at the end of 2018.

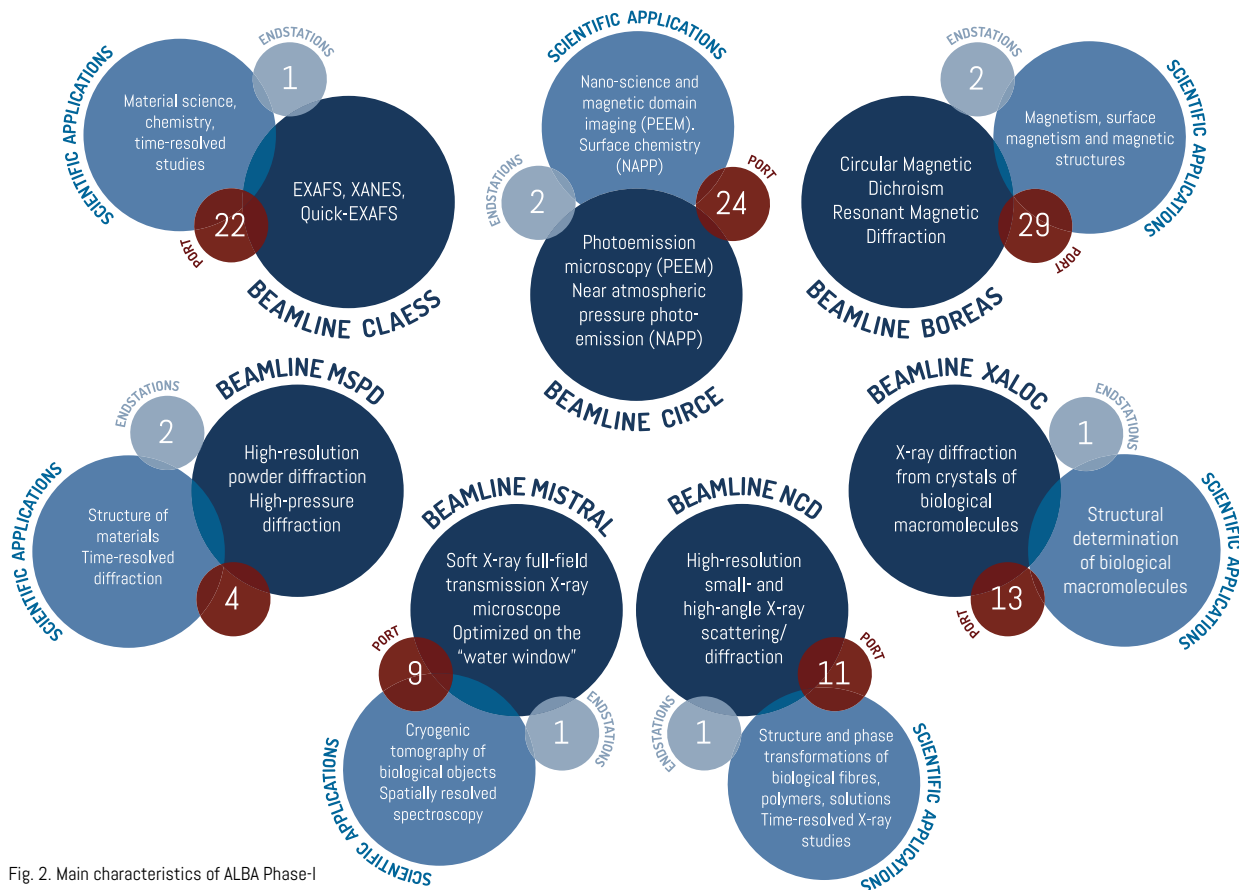


Fig. 2. Main characteristics of ALBA Phase-I

## THE USERS

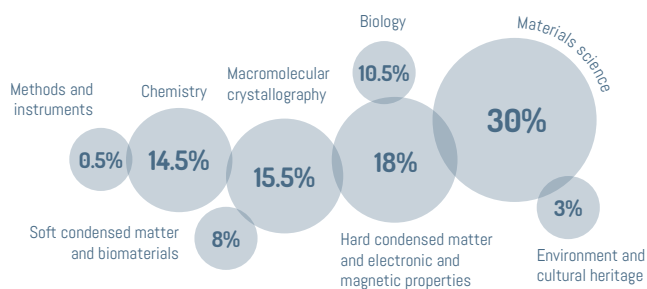
ALBA Synchrotron has the capability of producing above 5.000 hours of beamtime per year and is available for the public and the private sector to give service to more than 1.000 researchers every year.

In May 2012, ALBA received its first official user. Three user calls have been opened: 2011, 2012 and 2013. Beamtime is awarded to proposals based on technical feasibility and scientific excellence, after the evaluation of an international panel. An average overbooking factor of about 2, with a tendency to increase has been reached in the different calls, meaning that about 50% of proposals could only be taken on board. Industrial proprietary users have also performed experiments in ALBA, granted directly on the basis of technical and safety feasibility evaluations and ad-hoc beamtime allocation, wherein standard fees are applied.

### COUNTRY OF ORIGIN OF USERS



### RESEARCH AREA



### WHO ARE ALBA USERS?



## A BIT OF HISTORY...

### 90'S

The first attempt to obtain funding for a synchrotron light source in Spain was at the beginning of the 90's...

### 2003

... although it was in 2003 that the ALBA Synchrotron project was approved and funded in equal parts by the Spanish and the Catalan Administrations. For that purpose, the Consortium for the Construction, Equipping and Exploitation of the Synchrotron Light Source (CELLS) was created to manage the ALBA Synchrotron.

### 2006

Construction began in 2006, after few years dedicated to the design and training of a new team of experts, coming from Spain and abroad.



### 2010

The accelerator was ready and commissioned by 2010.



### 2011

Beamlines commissioning was completed in 2011-2012.



### 2012

First official users came in May 2012 and, at the end of the same year, first scientific paper was published containing data collected at MSPD beamline.



### 2013

By beginning of 2013, the seven beamlines have already received official users.



## GOVERNING BODIES

The Rector Council of the ALBA Synchrotron is the main decision-making body and usually meets twice a year. Its responsibilities are to ensure and supervise the

performance of the ALBA Synchrotron. The Rector Council delegates powers on the Executive Commission for managing the human and financial resources of the facility.

### RECTOR COUNCIL

#### CHAIRPERSON

##### ANDREU MAS-COLELL

Ministry of Economy and Knowledge –  
Regional Catalan Government

#### VICE CHAIRPERSON

##### LUIS DE GUINDOS JURADO

Ministry of Economy and  
Competitiveness –  
Spanish Central Government

#### SECRETARY

##### XAVIER URIÓS

Head of the Legal Advice Section.  
Department of Governance and  
Public Administrations –  
Regional Catalan Government

### EXECUTIVE COMMISSION

#### CHAIRPERSON

##### RAMON PASCUAL

Executive Commission Chairperson

#### SECRETARY

##### XAVIER URIÓS

Head of the Legal Advice Section.  
Department of Governance and  
Public Administrations - Regional  
Catalan Government

#### MEMBERS

##### CARMEN VELA OLMO

Secretary of State for Research,  
Development and Innovation –  
Spanish Central Government

##### M<sup>a</sup> LUISA PONCELA GARCÍA

General Secretary for Science,  
Technology and Innovation –  
Spanish Central Government

##### M<sup>a</sup> LUISA CASTAÑO MARÍN

Director General for Innovation and  
Competitiveness –  
Spanish Central Government

##### JOSÉ IGNACIO DONCEL MORALES

Deputy General Director of Planning  
of Scientific and Technical  
Infrastructures –  
Spanish Central Government

#### VICE SECRETARY

##### JORGE SÁNCHEZ VICENTE

State's Attorney head in Catalonia

##### ANTONI CASTELLÀ I CLAVÉ

General Secretary for Universities  
and Research –  
Regional Catalan Government

##### JOSEP MARIA MARTORELL I RODON

Director General for Research –  
Regional Catalan Government

##### LLUÍS JOFRÉ I ROCA

General Director of Universities –  
Regional Catalan Government

##### FERRAN SANCHO I PIFARRÉ

Rector of the Universitat Autònoma  
de Barcelona (UAB)

#### GUESTS

##### RAMON PASCUAL

Executive Commission Chairperson

##### CATERINA BISCARI

Director of CELLS

#### MEMBERS

##### M<sup>a</sup> LUISA CASTAÑO MARÍN

Director General for Innovation and  
Competitiveness –  
Spanish Central Government

##### JOSÉ IGNACIO DONCEL MORALES

Deputy General Director of Planning  
of Scientific and Technical Infrastructures –  
Spanish Central Government

#### VICE SECRETARY

##### JORGE SÁNCHEZ VICENTE

State's Attorney head in Catalonia

##### ANTONI CASTELLÀ I CLAVÉ

General Secretary for Universities  
and Research –  
Regional Catalan Government

##### JOSEP MARIA MARTORELL I RODON

Director General for Research –  
Regional Catalan Government

#### GUESTS

##### CATERINA BISCARI

Director of CELLS

---

## 2013 SCIENTIFIC ADVISORY COMMITTEE

The ALBA Scientific Advisory Committee (SAC) is a board of international renowned experts in the field of the synchrotron radiation, which participates in the strategic scientific direction of the ALBA Synchrotron with the aim of ensuring the quality and relevance of the research developed in ALBA. The members in 2013 were:

### JOHN HELLIWELL, CHAIR

---

Professor of Structural Chemistry at the University of Manchester (UK).

### OLIVER BUNK

---

Head of Laboratory for Macromolecules and Bioimaging of the Swiss Light Source (PSI), Switzerland.

### ANDY FITCH

---

Head of ID31 beamline High-resolution Powder Diffraction Beamline of the European Synchrotron Radiation Facility (ESRF), France.

### ENRIQUE GARCIA MICHEL

---

Full permanent professor of the Universidad Autónoma de Madrid (UAM), department of Condensed Matter Physics, Spain.

### PETER GUTTMANN

---

X-ray microscopy beamline scientist at U41-XM (BESSY II), Germany.

### AMOR NADJI

---

Director of Sources and Accelerators Division at Soleil Synchrotron (France).

### SAKURA PASCARELLI

---

Head of ID24 beamline Energy dispersive X-ray Absorption Spectroscopy of the European Synchrotron Radiation Facility (ESRF).

### CHRISTOPH QUITMANN

---

Director of the MAX-IV Laboratory in Lund, Sweden.

### NICK TERRILL

---

Principal beamline scientist on the Small Angle beamline I22 of Diamond Light Source (UK).

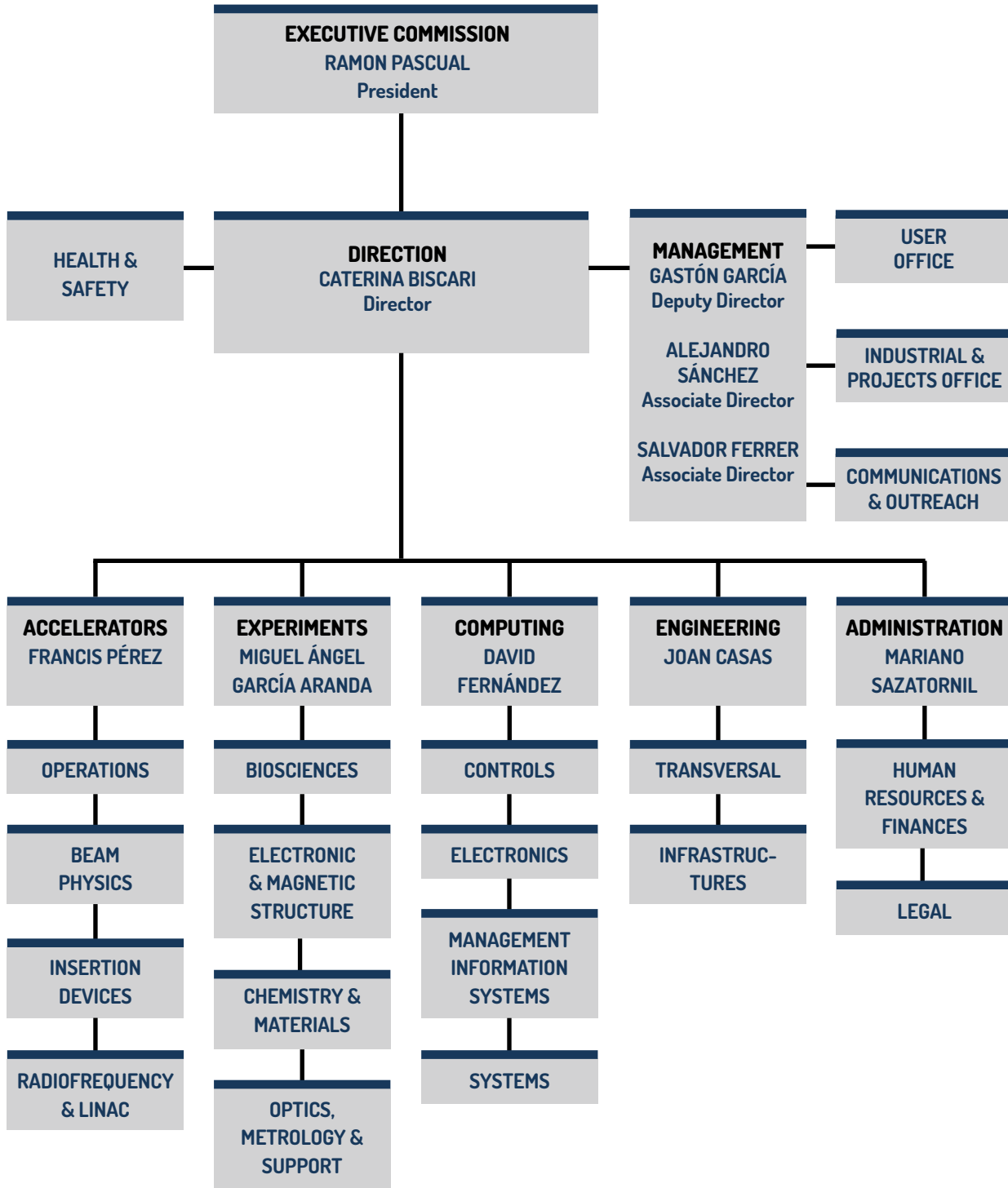
### RICHARD WALKER

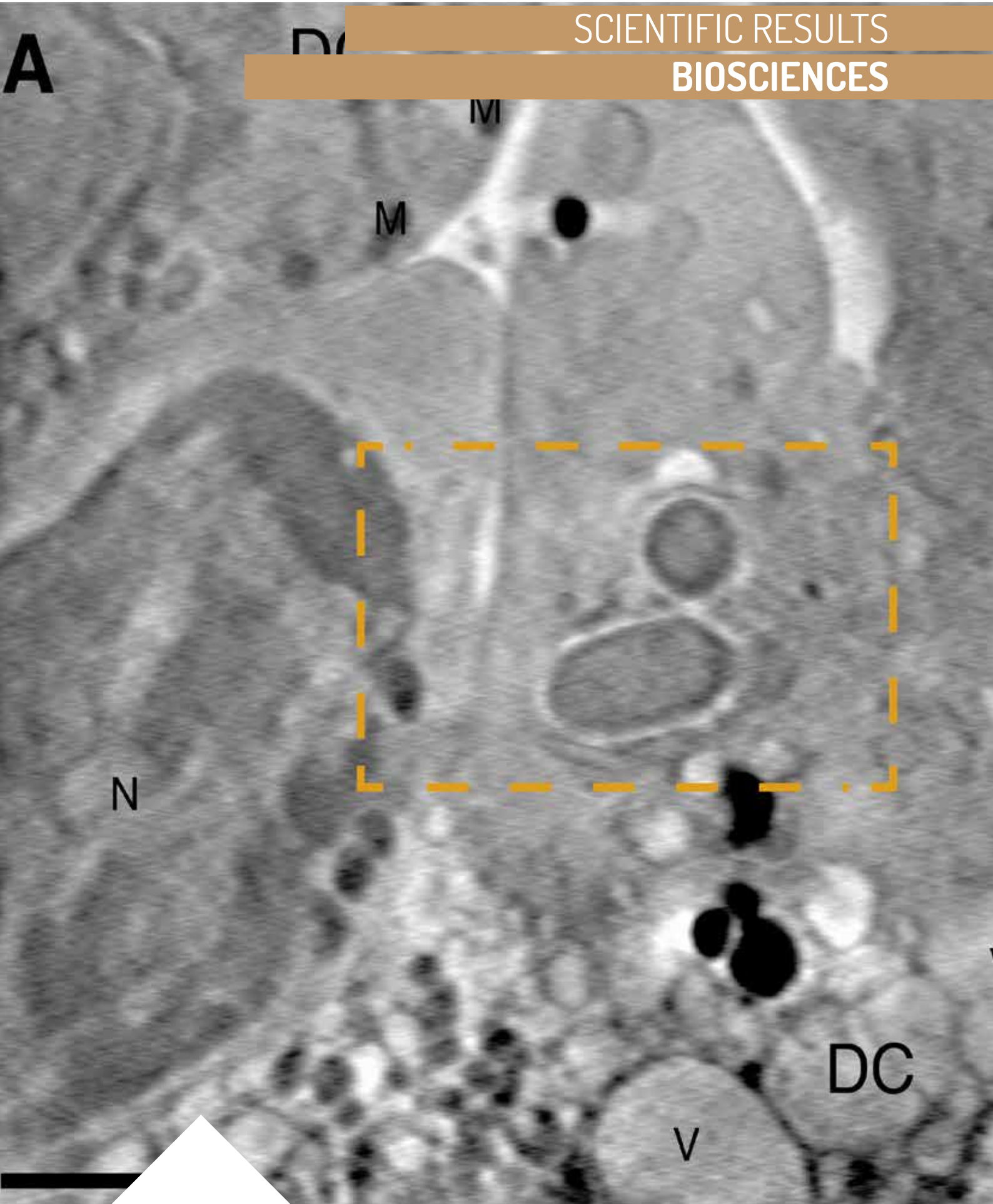
---

Technical director of Diamond Light Source (UK).

# ORGANIZATION CHART

ALBA Synchrotron is composed of 165 people, organized in six divisions: Management, Accelerators, Experiments, Computing, Engineering and Administration.





# UNVEILING A MOLECULAR MECHANISM THAT CONTROLS PLANT GROWTH AND DEVELOPMENT

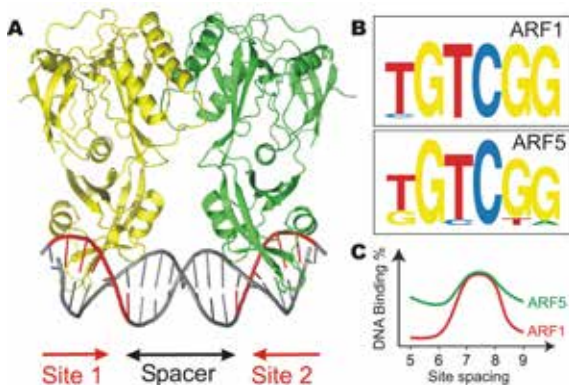
Structural Basis for DNA Binding Specificity by the Auxin-Dependent ARF Transcription Factors

*Cell* 56(3), 577 (2014)

**D. ROELAND BOER, ALEJANDRA FREIRE-RIOS, WILLY A.M. VAN DEN BERG, TERRENS SAAKI, IAIN W. MANFIELD, STEFAN KEPINSKI, IRENE LÓPEZ-VIDRIO, JOSE MANUEL FRANCO-ZORRILLA, SACCO C. DE VRIES, ROBERTO SOLANO, DOLF WEIJERS AND MIQUEL COLL**

Auxins are plant hormones that control growth and development, that is to say, they determine the size and structure of the plant. Among their many activities, auxins favor cell growth, root initiation, flowering, fruit setting and delay ripening. Auxins have practical applications and are used in agriculture to produce seedless fruit, to prevent fruit drop, and to promote rooting, in addition to being used as herbicides. The biomedical applications of these hormones as anti-tumor agents and to facilitate somatic cell reprogramming (the cells that form tissues) to stem cells are also being investigated. The effects of auxins in plants were first observed by Darwin in 1881, and since then this hormone has been the focus of many studies. However, although it was known how and where auxin is synthesized in the plant, how it is transported, and the receptors on which it acts, it was unclear how a hormone could trigger such diverse processes.

Fig. 3: The DNA-binding domains of ARF1 (shown in yellow and green) dimerize and in this way recognize the two binding sites on a DNA fragment (A). The recognized sites are similar between two distinct ARFs (ARF1 and ARF5, panel B). However, the two different ARFs distinguish between DNA fragments based on the distance between the two sites (C), that is on the length of the spacer.



At the molecular level, the hormone serves to unblock a transcription factor, a DNA-binding protein, which in turn activates or represses a specific group of genes. Some plants have more than 20 distinct auxin-regulated transcription factors. They are called ARFs (Auxin Response Factors) and control the expression of numerous plant genes in function of the task to be undertaken, that is to say, cell growth, flowering, root initiation, leaf growth etc.

Using the ALBA Synchrotron and the European Synchrotron in a joint study with researchers from the University of Wageningen (The Netherlands), the Institute of Molecular Biology of Barcelona (IBMB-CSIC, Spain) and the Institute for Research in Biomedicine

of Barcelona (IRB Barcelona, Spain), have elucidated the structural basis of the regulation of auxin-dependent gene expression. The atomic structure of ARFs bound to regions of DNA that control gene expression has revealed that the DNA-binding domain of ARFs recognize DNA as dimers. ARFs may have opposite effects on the production of genes, acting as activators or repressors. However, the study shows that the local recognition of DNA is highly similar for these functionally divergent ARFs, indicating that functional differences must be related to the formation of higher order structures that most probably involve distant regions within the genomic DNA.

## AUTHORS AFFILIATION

D. Roeland Boer,<sup>1,2,+</sup>  
Alejandra Freire-Rios,<sup>3,+</sup>  
Willy A.M. van den Berg,<sup>3,+</sup> Terrens Saaki,<sup>3</sup>  
Iain W. Manfield,<sup>4</sup> Stefan Kepinski,<sup>4</sup> Irene López-Vidrio,<sup>5</sup> Jose Manuel Franco-Zorrilla,<sup>5</sup> Sacco C. de Vries,<sup>3</sup> Roberto Solano,<sup>5</sup> Dolf Weijers,<sup>3,+</sup> and Miquel Coll<sup>1,2,+</sup>

1. Institute for Research in Biomedicine (IRB Barcelona), Barcelona, Spain

2. Institut de Biologia Molecular de Barcelona (IBMB-CSIC), Barcelona, Spain

3. Laboratory of Biochemistry, Wageningen University, Wageningen, the Netherlands

4. Astbury Centre for Structural Molecular Biology and Centre for Plant Sciences, Faculty of Biological Sciences, University of Leeds, UK

5. Genomics Unit and Department of Plant Molecular Genetics, Centro Nacional de Biotecnología-CSIC, Campus Universidad Autónoma, Madrid, Spain

+ These authors contributed equally to this work

## THE INHIBITION OF RAP PHOSPHATASE BY SPECIFIC PHR PEPTIDES

Structural basis of Rap phosphatase inhibition by Phr peptides

*PLoS Biology* 2013 11(3):e1001511

**FRANCISCA GALLEGO DEL SOL AND ALBERTO MARINA**

**Instituto de Biomedicina de Valencia CSIC, Valencia, Spain**

In microorganisms, two component signaling systems are widely used to sense and respond to environmental changes. The minimal machinery required for these systems is a sensor histidine kinase and an effector response regulator. However, auxiliary proteins, termed connectors, capable of modulating the activity of this machinery, are emerging as additional players in signaling process of high complexity.

Rap proteins conform to the prototypic connector family, and have been exhaustively studied in *Bacillus subtilis*, which expresses 11 chromosomal and five plasmid-encoded members. Raps are involved in complex signaling processes mediated by two-component systems, such as competence, sporulation or biofilm formation, by inhibiting the response regulator components involved in these pathways. Despite the high degree of sequence homology they can modulate response regulator activity in two completely different ways. One subset of Rap proteins display phosphatase activity to their target response regulators. The second subgroup blocks the action of the target response regulator by a direct interaction with their DNA binding domain, and works as an anti-activator. In addition, Rap activity is modulated by specific peptides named Phr. Their mature active form of Phr is a penta- or hexa-peptide generated from a ~40 amino-acid precursor by a post-transcriptional export-import process. *Phr* genes are situated immediately downstream of the genes encoding the Rap proteins to form rap-phr signaling cassettes, which are concurrently transcribed. How the Rap protein activity is regulated by its cognate Phr peptide and the exquisite specificity Rap-Phr still remains unknown.

To answer these questions, a team from IBV-CSIC formed by Francisca Gallego del Sol and Alberto Marina, has solved the X-ray crystal structure of RapF, a Rap family member that blocks response regulator ComA, alone and in complex with its inhibitory peptide PhrF (QRGM1) using X-ray diffraction techniques at the ALBA Synchrotron and at the ESRF Synchrotron.

These structures and complementary functional results reveal that PhrF blocks the RapF-ComA interaction by an allosteric mechanism since the PhrF-RapF contact induces a conformational change that is propagated to the ComA binding domain, which disrupts the binding-site of ComA and triggers its dissociation from RapF. Using a sequence analysis guided by the structure, the authors pinpointed two sets of residues responsible for peptide anchor and specificity, respectively. Then using direct mutagenesis techniques, they were able to alter RapF-Phr specificity by simply changing a single residue.

Knowledge of these key residues and the Rap inhibition mechanism open up the possibility of re-engineer Rap proteins, paving the way for reprogramming signaling pathways for biological and biotechnological applications.

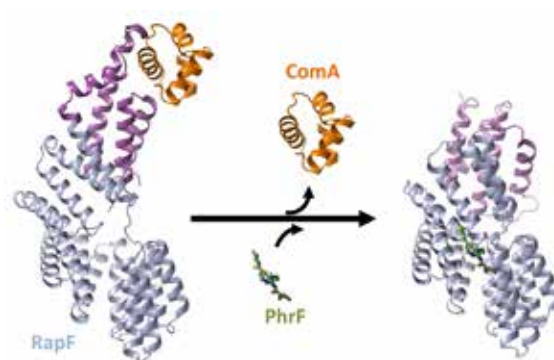


Fig. 4: Structure of RapF bound to its target ComA or to the inhibitory peptide PhrF. Binding of the inhibitory penta-peptide PhrF (green) to the TPR domain of RapF (blue) induce a conformational change in the target binding domain (magenta) of RapF that induce the release of the target protein ComA (orange).

## NEW INSIGHTS FOR FIGHTING CYSTIC FIBROSIS

Direct interaction of a CFTR potentiator and a CFTR corrector with phospholipid bilayers.  
*European Biophysics Journal* (2014)

**DEBORA BARONI, OLGA ZEGARRA-MORAN, AGNETA SVENSSON AND OSCAR MORAN\***

Cystic fibrosis (CF) is the most common lethal genetic disease in the Caucasian population. It is caused by mutations in the protein CFTR, responsible of the salt transport in epithelia. Recently, new drugs, named potentiators and correctors, are that target the basic CFTR protein defect and are expected to benefit cystic fibrosis patients. To optimize the substances so far proposed for human use, and to minimise the unwanted side effects, it is essential to investigate the possible interactions between the drugs and the cell components. Small angle X-ray scattering method and synchrotron radiation have been applied to analyse the effects of two representative drugs, the potentiator VX-770 (Ivacaftor), approved for human use, and the corrector VX-809 (Lumacaftor) in a model phospholipid membrane. It has been demonstrated that the penetration of these drugs into the model membrane, causes a destabilization of the membrane, that has to be taken into account for future drug development.

Phospholipid large unilamellar lipid vesicles (LUV) were exposed to synchrotron X-rays, obtaining small angle-X-ray scattering (SAXS) spectra of very high quality with good experimental statistics. Reciprocal space scattering data are related to the real space structure through a Fourier transform, with no loss of information.

SAXS data were fitted with the Fourier transform of a multi-Gaussian model [1] to estimate the electronic density  $\rho(r)$  of the LUV wall (Fig. 5). Qualitatively, the  $\rho(r)$  produce the familiar shape of a vesicle lipid bilayer wall. A model of the phospholipid vesicle bilayer is presented on the top of panel A in Fig. 5 showing a cross section of the control vesicle bilayer, without any substance. Note how the inner leaflet is depicted as rougher, i.e. a larger variation in head-group positions.

Addition of 1  $\mu\text{M}$  of CFTR-potentiator VX-770 induce a contraction of the external leaflet, and an expansion of the internal leaflet, resulting in a thickening of the LUV bilayer. The bilayer  $\rho(r)$  shape is also modified in the presence of the CFTR-potentiator. There is the appearance of a shoulder between the inner side of the bilayer that may host an object of about 15 Å (see the red line in Fig. 5B), that is the same length as the VX-770 molecule.

When phospholipid LUVs were treated with 3  $\mu\text{M}$  of the CFTR-corrector VX-809, we observed a displacement of the bilayer leaflets towards the external side, resulting in a thickening of the membrane. The shape of the  $\rho(r)$  is also slightly modified, as seen in Fig 5C, suggesting that the VX-809 molecules are distributed into the phospholipid bilayer.

The first outcome that can be drawn from this work is that both compounds, VX-770 and VX-809, applied at concentrations similar to those used when evaluating their biological actions

\* Corresponding author

in *in vitro* cellular preparations [2], cause modifications of the phospholipid bilayer. The  $\rho(r)$  profiles obtained from LUV treated with these compounds indicated that VX-770 and VX-809 enters into the lipid bilayer. These two compounds need to cross the plasma membrane to exert their action, and consequently must be soluble in the lipid phase. Thus, it is not surprising that both substances can enter the lipid phase of the bilayer.

In conclusion, the potentiator VX-770 and the corrector VX-809 may produce unwanted side effect by destabilizing the cell membranes. Therefore, it is necessary to keep in mind the unspecific physical-chemical effect of the substances developed for the treatment of the CF in humans to reduce the secondary effects of the drugs. Thus, future functional studies are needed to understand whether VX-770 and/or VX-809 cause a general reduction of the activity of membrane proteins and to what extent.

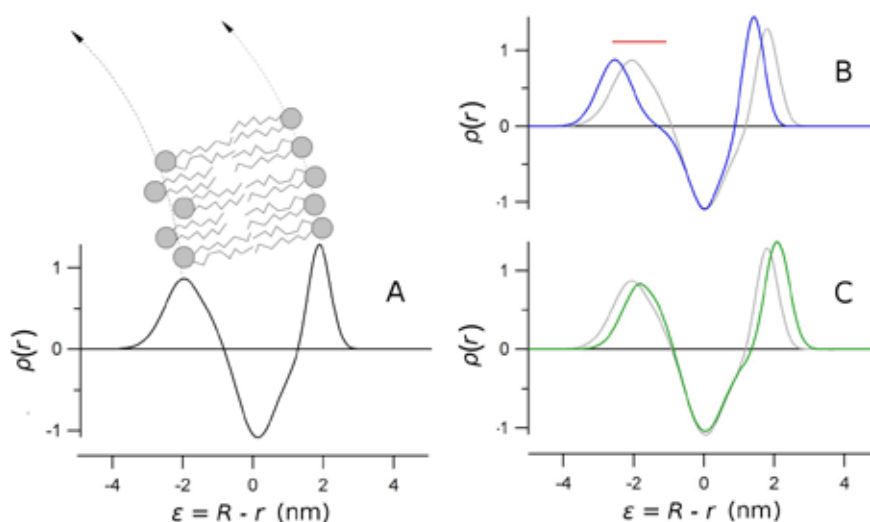


Fig. 5: The electronic density,  $\rho(r)$ , of the phospholipid bilayer models.  $\epsilon$  is the distance from the center of the bilayer, and  $R$  is the radius of the LUV;  $\rho(r)$  is expressed in arbitrary units. A: The calculated  $\rho(r)$  profile obtained from parameters for the untreated LUV bilayers, with a depiction of bilayer structure and arrangement. Circles represent plausible head-group locations. B and C: The  $\rho(r)$  of bilayers of the models corresponding to LUVs treated with 1  $\mu$ M VX-770 and 3  $\mu$ M VX-809, respectively. The  $\rho(r)$  of the untreated bilayer is shown in grey in each panel to enable better comparison.

## REFERENCES

- [1] Brzustowicz MR, Brunger AT. (2005) X-ray scattering from unilamellar lipid vesicles. *J. Appl. Cryst.* 38:126-131.
- [2] Gianotti A, Melani R, Caci E, Sondo E, Ravazzolo R, Galiotta LJV, Zegarra-Moran O. (2013) Epithelial sodium channel silencing as a strategy to correct the airway surface fluid deficit in cystic fibrosis. *Am J Respir Cell Mol Biol.* 49:445-452.

## ACKNOWLEDGMENTS

Partially supported by Fondazione per la Ricerca sulla Fibrosi Cistica (grant FFC4/2012) These experiments were performed at BL11 beamline at ALBA Synchrotron Light Facility with the collaboration of ALBA staff.

## AUTHORS AFFILIATION

Debora Baroni<sup>1</sup>, Olga Zegarra-Moran<sup>2</sup>, Agneta Svensson<sup>3</sup> and Oscar Moran<sup>1\*</sup>

1. Istituto di Biofisica, CNR, via De Marini, 6, 16149, Genova, Italy  
 2. Laboratorio di Genetica Molecolare, Istituto Giannina Gaslini, via Gerolamo Gaslini, 5, 16148 Genova, Italy  
 3. ALBA Synchrotron, Carretera BP 1413, 08290 Cerdanyola del Vallès, Barcelona, Spain

# BACTERIA TRANS-INFECT T LYMPHOCYTES THROUGH THE IMMUNOLOGICAL SYNAPSE

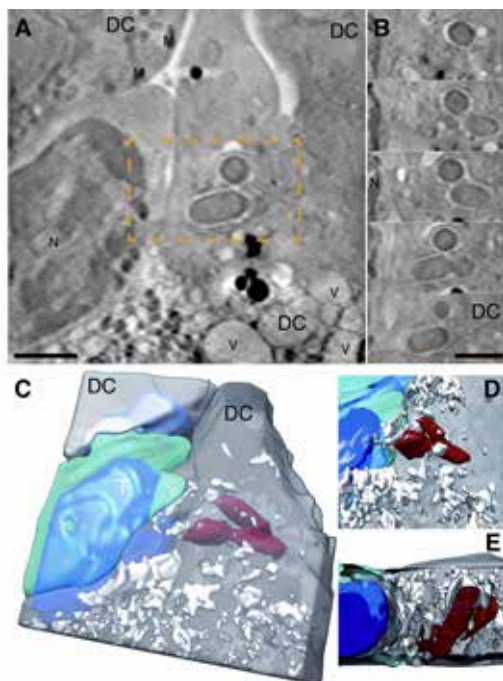
T cells kill bacteria captured by transinfection from dendritic cells and confer protection in mice

*Cell Host Microbe* 15: 611-622 (2014)

**A. CRUZ-ADALIA, G. RAMIREZ-SANTIAGO, C. CALABIA-LINARES, M. TORRES-TORRESANO, L. FEO, M. GALÁN-DÍEZ, E. FERNÁNDEZ-RUIZ, E. PEREIRO, P. GUTTMANN, M. CHIAPPI, G. SCHNEIDER, J.L. CARRASCOSA, F.J. CHICHÓN, G. MARTÍNEZ DEL HOYO, F. SÁNCHEZ-MADRID, E. VEIGA**

During infections, several bacterial species survive phagocytosis and disseminate systemically through infected antigen presenting cells (APC) such as dendritic cells (DC). It has been proposed that T cells could also serve as bacterial reservoir during infections in mice. However, taken into account that primary T cells are infected poorly *in vitro*, the route bacteria invade T cells remains unknown.

Fig. 6: A) Virtual slice of a tomogram showing an infected dendritic cell (DC) exposing internal bacteria near the immune synapse (IS) with a T cell (T). N labels the nucleus position of the T cell and V some vesicles. Bacteria are visible in the dashed yellow rectangle. B) Consecutive virtual slices every 460 nm showing the proximity of the three bacteria, in the yellow rectangle of A, to the IS with a T cell. Scale bars in A and B represent 2 microns. C, D and E) Volumetric representations of the tomogram in A and B. The T cell is represented in cyan and its nucleus is shown in blue. The dendritic cells (DC) are shown in grey and the bacteria in red.



In this research, it has been discovered that T cells are able to capture bacteria from dendritic cells (DC) by transinfection and kill the transinfected bacteria. These striking results show that T cells, the paradigm of adaptive immunity, have developed functions thought to be exclusive to cells of the innate immunity.

By analyzing in the laboratory at the Instituto de Investigación Sanitaria Princesa (Hospital de Santa Cristina) the differences between the T cells, it was observed that when these lymphocytes are transinfected with bacteria, they produce more inflammatory cytokines (i.e., IL-6, TNF-alpha and IFN-gamma) than non-infected cells and protect from bacterial infections *in vivo*.

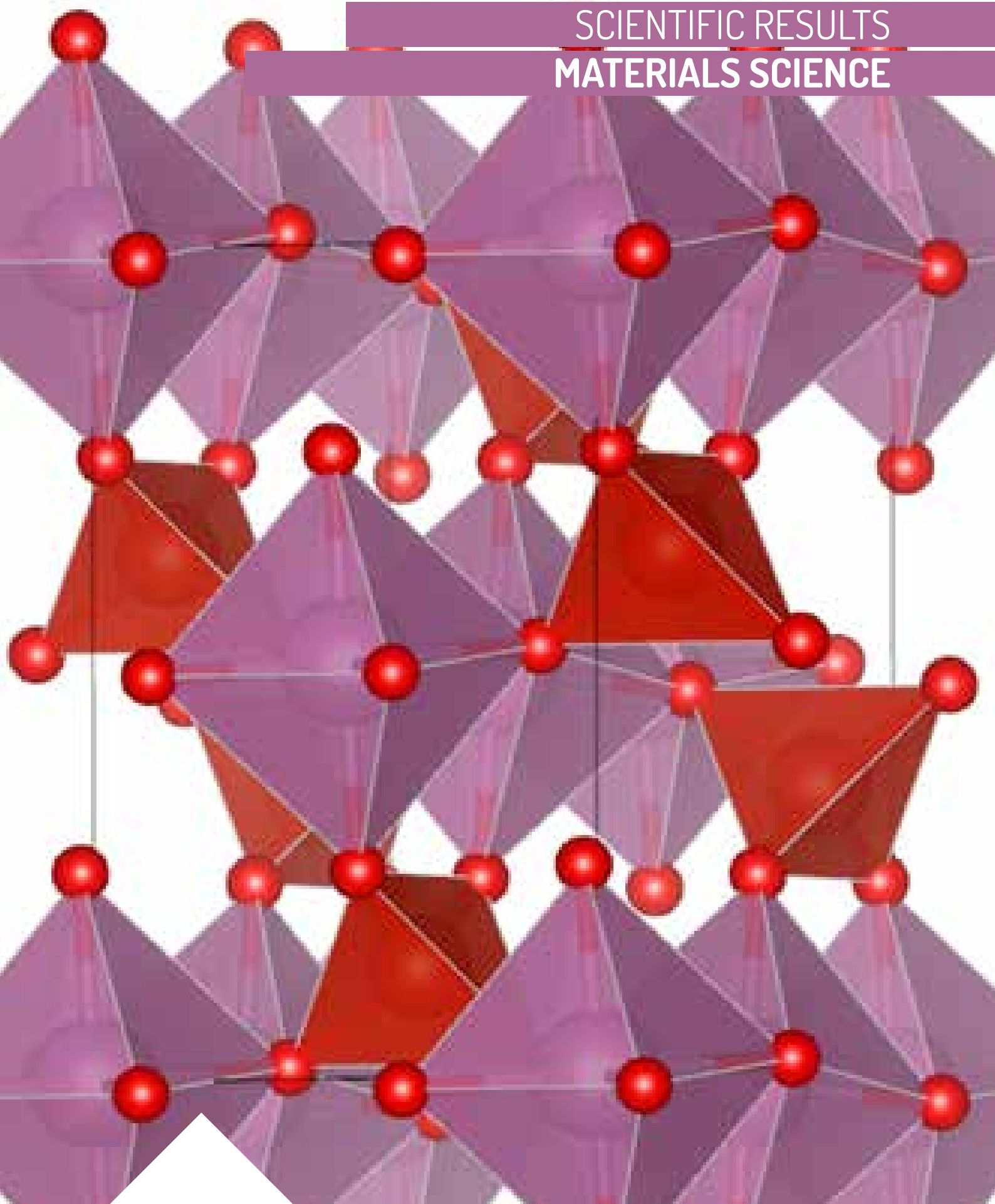
This study shows for the first time that T cells are able to capture and kill bacteria. Surprisingly, transinfected T cells kill the bacteria more efficiently than the DC.

## AUTHORS AFFILIATION

A. Cruz-Adalia<sup>1,2</sup>. G. Ramirez-Santiago<sup>1,2</sup>. C. Calabia-Linares<sup>2</sup>. M. Torres-Torresano<sup>1,2</sup>. L. Feo<sup>2</sup>. M. Galán-Díez<sup>1,3</sup>. E. Fernández-Ruiz<sup>2</sup>. E. Pereiro<sup>4</sup>. P. Guttmann<sup>5</sup>. M. Chiappi<sup>1</sup>. G. Schneider<sup>5</sup>. J.L. Carrascosa<sup>1,6</sup>. F.J. Chichón<sup>1</sup>. G. Martínez del Hoyo<sup>7</sup>. F. Sánchez-Madrid<sup>2</sup>. E. Veiga<sup>1,2</sup>

1. Centro Nacional de Biotecnología CSIC, Madrid, Spain
2. Instituto de Investigación Sanitaria Princesa, Hospital de la Princesa, Madrid, Spain
3. Microbiology and Immunology Department, Columbia University Medical center, New York, USA
4. ALBA Synchrotron, Cerdanyola del Vallès, Spain
5. Helmholtz-Zentrum Berlin für Materialien und Energie GmbH, BESSY II, Berlin, Germany
6. Instituto Madrileño de Estudios Avanzados en Nanociencia (IMDEA), Madrid, Spain
7. Centro Nacional de INvestigaciones Cardiovasculares (CNIC), Madrid, Spain

SCIENTIFIC RESULTS  
MATERIALS SCIENCE



# UNRAVELLING THE STRUCTURE OF AMPHIPHILIC PEPTIDE NANOCHANNEL ASSEMBLIES WITH X-RAY DIFFRACTION

Design, synthesis, and structural analysis of turn modified cyclo-( $\alpha\beta^3\alpha\beta^2\alpha$ )<sub>2</sub> peptide derivatives toward crystalline hexagon-shaped cationic nanochannel assemblies.  
*Crystal Growth & Design*, 13, 4355-4367 (2013)

**JOSÉ M. OTERO, MATTHIJS VAN DER KNAAP, ANTONIO L. LLAMAS-SAIZ, MARK J. VAN RAAIJ, MANUEL AMORÍN, JUAN R. GRANJA, DMITRI V. FILIPPOV, GIJSBERT A. VAN DER MAREL, HERMAN S. OVERKLEEF, AND MARK OVERHAND**

Amphiphilic peptide nanochannels are ingenious and sophisticated versions of *supramolecular nanotubes*, in which the hydrophobicity of the outer and inner surfaces are opposite. They have potential as synthetic ion channels, encapsulated drug delivery systems and other biotechnological applications in biology and pharmaceutical sciences, tissue engineering and development of nano-electronic devices. Nature also makes use of substances with ability to self-assemble in amphiphilic nanochannels: for example as a defence method against pathogens (i.e. cationic antibiotic peptides) or to allow a variety of molecules, from small ions to large macromolecules, to pass through membranes (i.e. pore-forming membrane proteins).

Inspired by the structure of the amphiphilic cyclopeptide gramicidin S, a natural antibiotic isolated from the bacterium *Bacillus brevis* which acts disrupting the membrane cells of some Gram positive and Gram negative bacteria as well as some fungi, the researchers developed a family of synthetic cyclopeptides with the aim of understanding and improving their ability to self-assemble into amphiphilic nanotubes.

It was found that cyclodecapeptides which contain two (*R*)-configuration  $\beta$ -amino acids, two (*S*)-configuration  $\beta$ -amino acids, two (*R*)-configuration  $\alpha$ -amino acids and four (*S*)-configuration  $\alpha$ -amino acids form amphiphilic nanotubes with a hexagonal cross section (Figure 7). The exterior surface of these nanotubes is highly hydrophobic and the tubes interact with each other to form a honeycomb-type molecular assembly. The pores of the nanotubes contain the cationic side-chains of the cyclopeptides, allowing water molecules or ions to easily pass through them.

When subtle changes to the aromatic side-chains of the parent cyclopeptide 1 were made to give compounds 2, 3 and 4, interesting alterations in the self-assembly of the monomers into crystallographic nanotubes were observed. While compound 1 assembled into double-helical hexagonal tubes, compound 2 crystallized as a linear stack of hexagonal discs of six

cyclopeptides. Compound 3 formed single helices in the crystal, with a hexagonal cross-section, while in compound 4 the double-helical stacking of monomers was recovered. However, in this case the peptides formed cylindrical nanotubes instead of the hexagonal ones obtained with the other compounds.

Finally, the researchers demonstrate how milligrams of long and narrow microcrystalline fibres of compound 1 can be readily obtained. These fibres have an average length of 200 to 300  $\mu\text{m}$  and are approximately 500-600 nm wide (figure 8) and could be useful as functional nanomaterials. Scanning probe electron microscopy studies performed with these ultra-thin needles elucidate their morphology, revealing a hexagonal cross-section, which was tentatively related with the honeycomb-like packing observed in the macro-crystals.

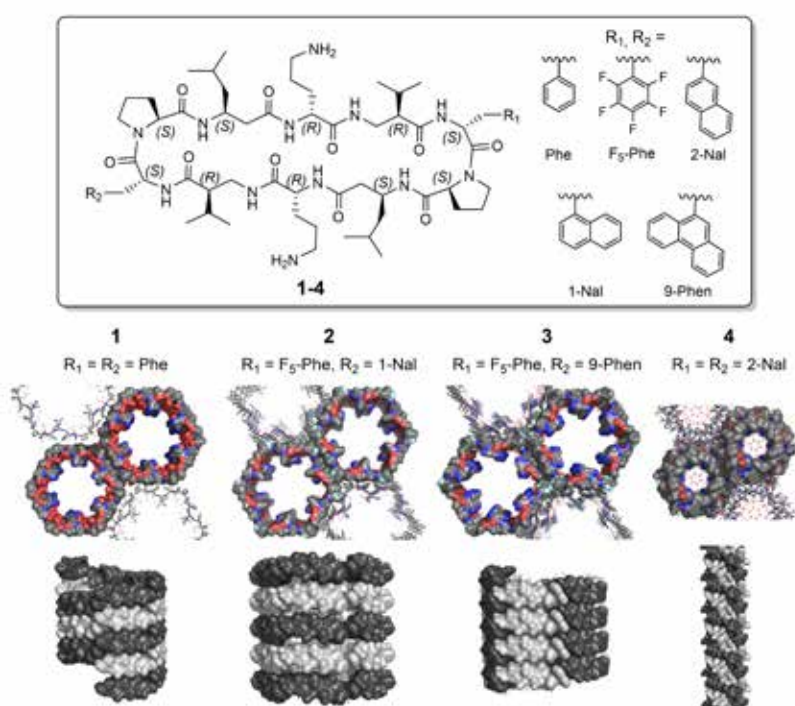


Fig. 7: Structures (upper row) and crystallographic nanochannels (top view in middle row and side view in bottom row) of the cyclo-( $\alpha^3\alpha\beta\alpha$ )<sub>2</sub> peptide derivatives 1-4.

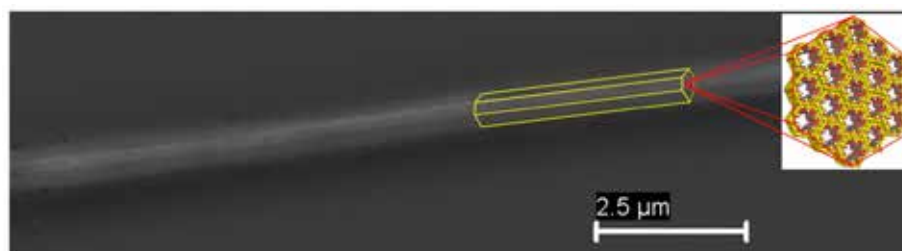


Fig. 8: Scanning probe electron microscopic image of one microcrystal of compound 1. Highlighted is its hexagonal-shaped morphology (600 nm wide approximately) and zoomed is a proposed nanotubes honeycomb aggregation for a 25 nm wide hexagonal-shaped portion of the fiber. The hydrophilic pore inner diameter is approximately 3 nm.

1. Bioorganic Synthesis Leiden Institute of Chemistry, Leiden University, P.O. Box 9502, 2300 RA Leiden, The Netherlands
2. Departamento de Bioquímica y Biología Molecular Facultad de Farmacia and Centro Singular de Investigación en Química Biológica y Materiales Moleculares, Universidad de Santiago de Compostela Campus Vida, E-15782 Santiago de Compostela, Spain
3. Unidad de Rayos X RIAIDT, Edificio CACTUS, Universidad de Santiago de Compostela Campus Vida, E-15782 Santiago de Compostela, Spain
4. Centro Nacional de Biotecnología (CNB-CSIC), c/Darwin 3, Campus Cantoblanco, E-28049 Madrid, Spain
5. Departamento de Química Orgánica Centro Singular de Investigación en Química Biológica y Materiales Moleculares and Unidad Asociada al CSIC, Universidad de Santiago de Compostela Campus Vida, E-15782 Santiago de Compostela, Spain

#### AUTHORS AFFILIATION

José M. Otero<sup>1,2</sup>,  
Matthijs van der Knaap<sup>1</sup>,  
Antonio L. Llamas-Saiz<sup>3</sup>,  
Mark J. van Raaij<sup>4</sup>,  
Manuel Amorín<sup>5</sup>, Juan  
R. Granja<sup>5</sup>, Dmitri V.  
Filippov<sup>1</sup>, Gijbert A. van  
der Marel<sup>1</sup>, Herman S.  
Overkleeft<sup>1</sup>,  
and Mark Overhand<sup>1</sup>

# STUDYING THE STRUCTURE DEVELOPMENT OF POLYMERS

Mesophase Formation in Random Propylene-*co*-1-Octene Copolymers.  
*Macromolecules*, 46, 8557-8568 (2013)

**JAVIER ARRANZ-ANDRÉS, ROSA PARRILLA, MARÍA L. CERRADA, ERNESTO PÉREZ**

Crystallization of polymers is a key area in polymer research since many properties are related to the capability of forming ordered structures. Mesophases are partially ordered states which are attracting a great interest for their characterization. We have investigated the formation of the mesophase in several propylene- *co*-1-octene copolymers by means of Fast Scanning Calorimetry and conventional DSC. X-ray diffraction experiments, with conventional and synchrotron radiation, were also performed on these copolymers, in order to establish the nature of the phases involved. It was concluded that the mesophase rate of formation depends very much on the comonomer content, in such a way that the copolymers with higher contents show rates low enough to be studied by conventional techniques, namely DSC or X-ray diffraction. For these high contents, the mesophase formation and its transformation into the most stable alpha modification on melting were ascertained by real-time variable-temperature synchrotron experiments.

In this work [1], the mesophase development has been investigated in random iPP copolymers with 1-octene. Three copolymers were studied, named as cP02, cP06 and cP09, with contents in 1-octene of 2.2, 5.6 and 8.9 mol%, respectively. The term mesophase is used for those phases with a degree of order intermediate between that of three-dimensional crystals and the non-ordered amorphous structures. Consequently, mesophases use to exhibit new remarkable properties in between those of the crystal and the amorphous polymer.

The formation (or inhibition) of ordered structures when cooling at very high rates is a rather attractive issue in Polymer Science, with interesting technological and scientific features. Mesophase development is specially relevant in isotactic poly(propylene), iPP. This polymer exhibits a fascinating polymorphism [2], and fast cooling, at rates higher than about 100 °C/s, leads to a metastable mesomorphic phase.

Fast Scanning Calorimetry, FSC, is a recent technique capable of reaching cooling rates of 4000 °C/s and heating rates higher than 40000 °C/s. Thus, the mesophase formation in iPP can be observed by FSC, but it is not possible to ascertain unequivocally the phases involved in the different transitions.

Fortunately, the mesophase formation rate is reduced significantly in iPP copolymers as the comonomer content increases, as it has been shown [3] in copolymers of propylene with 1-pentene, so that the analysis has been extended to copolymers with 1-octene in this work.

A commercial calorimeter (Mettler-Toledo, Flash DSC 1) was employed in the FSC analyses. The real-time synchrotron study, at variable temperature, was carried out on beamline BM11-NCD at ALBA (Cerdanyola del Vallés, Barcelona, Spain), by using a wavelength of 0.1283 nm (9.6617 keV) and an ADSC 210 detector. A Linkam stage, with a liquid nitrogen cooling system, provided the temperature control.

The results indicate that, as observed in Figure 9, the mesophase formation rate can be easily tailored in a very wide range of magnitude, depending on the comonomer content. Thus, the rates implicated for the copolymers with higher contents are low enough to be investigated with conventional Differential Scanning Calorimetry, DSC.

Additional real-time variable-temperature X-ray experiments with synchrotron radiation were carried out for the copolymers with high contents. The mesophase formation and its transformation into the most stable alpha modification on melting were ascertained. For instance, Figure 10 shows the diffractograms corresponding to the melting of a sample of cP06 rapidly cooled from the melt, where the mesophase is initially the dominant phase.

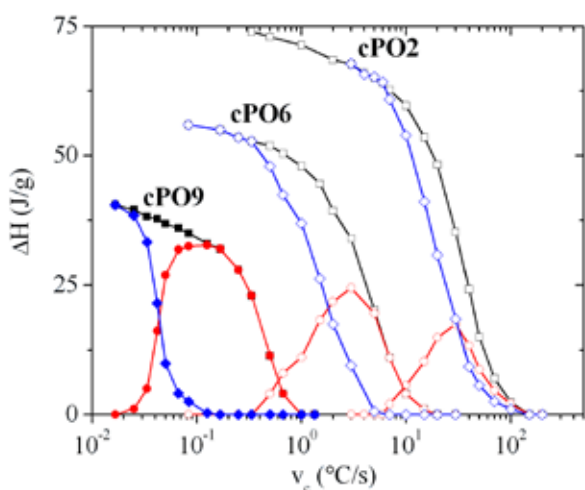


Fig. 9: Variation with the cooling rate of total (squares), meso (circles) and alpha crystals enthalpy (diamonds) for the three copolymers. Open symbols: FSC results; full symbols: conventional DSC.

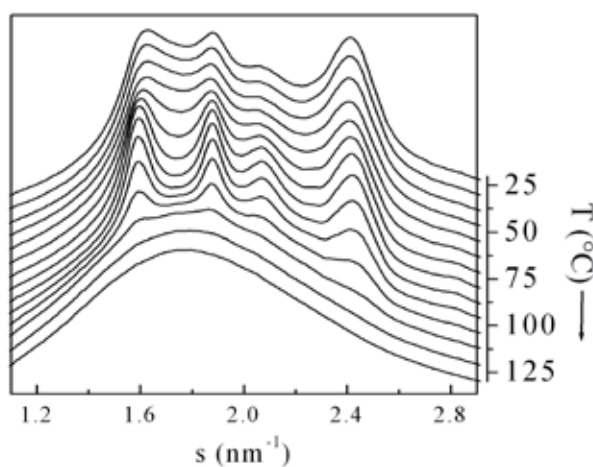


Fig. 10: Real-time variable-temperature synchrotron diffraction patterns for the heating, at 10 °C/min, of a sample of cP06 rapidly cooled from the melt.

## REFERENCES

- [1] Arranz-Andrés, J.; Parrilla, R.; Cerrada, M.L.; Pérez, E. *Macromolecules* 2013, 46, 8557.
- [2] a) Brückner, S.; Meille, S. V.; Petraccone, V.; Pirozzi, B. *Prog. Polym. Sci.* 1991, 16, 361; b) Natta, G.; Corradini, P. *Nuovo Cimento Suppl.* 1960, 15, 40; c) Turner-Jones, A.; Aizlewood, J. M.; Beckett, D. R. *Makromol. Chem.* 1964, 75, 134.
- [3] Pérez, E.; Gómez-Elvira, J. M.; Benavente, R.; Cerrada, M. L. *Macromolecules* 2012, 45, 6481.

## ACKNOWLEDGMENTS

We acknowledge the financial support of MICINN (Project reference MAT2010-19883). The synchrotron experiments were performed at beamline BL11-NCD at ALBA Synchrotron Light Facility with the collaboration of ALBA staff.

## AUTHORS AFFILIATION

Javier Arranz-Andrés,<sup>1</sup>  
Rosa Parrilla,<sup>2</sup> María L.  
Cerrada,<sup>1</sup> Ernesto Pérez<sup>1</sup>

1. Instituto de Ciencia y Tecnología de Polímeros (ICTP-CSIC), Juan de la Cierva 3, 28006-Madrid, Spain  
2. Centro Tecnológico Repsol, Móstoles, 28935-Madrid, Spain

# DISCOVERY OF A VANADATE POLYMORPH USEFUL FOR PHOTOCATALYTIC HYDROGEN PRODUCTION

New Polymorph of  $\text{InVO}_4$ : A High-Pressure Structure with Six-Coordinated Vanadium.  
*Inorganic Chemistry* 52, 12790–12798, (2013)

**D. ERRANDONEA\***, O. GOMIS, B. GARCÍA-DOMENE, J. PELLICER-PORRES, V. KATARI,  
S.N. ACHARY, A.K. TYAGI, AND C. POPESCU

Orthovanadates are important materials with applications in existing and future technologies. Recently they have attracted considerable attention due to potential usages in renewable energy and alternative green technology. Under moderate compression, these compounds transform to denser phases with novel properties, which could open the door to new applications. Consequently, high-pressure (HP) studies on orthovanadates have attracted large interest in the last lustrum. To shed more light on the understanding of their structural properties and in particular their pressure-induced phase transitions we studied  $\text{InVO}_4$  at ALBA.

Two novel phases are found in  $\text{InVO}_4$  by high-pressure XRD. One of them, found at  $P > 8$  GPa, has a crystal structure which implies a coordination increase for V. The phase transition involves changes in the electronic structure of  $\text{InVO}_4$  causing a band gap collapse. The crystal structure of the different phases and the RT P–V equations of state are determined.

We performed HP X-ray diffraction (XRD) experiments at beamline BL04-MSPD. We used a monochromatic X-ray beam ( $\lambda = 0.4246 \text{ \AA}$ ) focused down to  $20 \mu\text{m} \times 20 \mu\text{m}$ . A diamond-anvil cell was used to generate HP and XRD patterns were recorded on a Rayonix CCD detector. In the experiments we employed micron-size powders and 16:3:1 methanol-ethanol-water was used as pressure-transmitting medium. Pressure was measured using Cu as calibrant. Thanks to the high-brilliance photon beam and the micron-size beam spot available at BL04-MSPD, successful experiments were conducted at RT up to 24 GPa.

Fig. 11 shows selected HP XRD patterns. Up to 6.2 GPa all Bragg peaks can be indexed assuming the low-pressure orthorhombic  $\text{CrVO}_4$ -type structure. From this pressure up to 8.2 GPa we detected the coexistence of two novel phases. At  $P \geq 8.2$  GPa we found a phase transition to a phase with monoclinic symmetry. In Fig. 12 we compare the low-pressure orthorhombic and the high-pressure monoclinic structures. Details on the novel structure of  $\text{InVO}_4$  can be found in the published article [1]. It has been assigned to a distorted wolframite-type having an ordered arrangement of  $\text{InO}_6$  and  $\text{VO}_6$  polyhedral units. The discovered phase is the first known cation-ordered phase of  $\text{InVO}_4$  (and related vanadates) having V atoms in six coordination. Additionally, the HP phase is relatively incompressible as indicated by a large bulk modulus ( $B_0 = 168$  GPa). The low-pressure phase is more compressible ( $B_0 = 69$  GPa). The compressibility change is related to the increase of the packing efficiency associated to the transition, which is accompanied by a volume collapse of 14%. In both structures

\* Corresponding author

compression is highly anisotropic. The phase transitions discovered in the XRD studies have been confirmed by Raman spectroscopy [1].

An interesting output of the discovery of wolframite-type  $\text{InVO}_4$  (which could be recovered as a metastable phase) is that the new phase has a smaller band gap than the already known phases. This is a direct consequence of the presence of six-coordinated V and may lead to maximum efficiency for the splitting of water molecules by visible light, favoring technological applications like photocatalytic hydrogen production. The results obtained on  $\text{InVO}_4$  triggered subsequent studies in related vanadates. They were performed under similar conditions at BLO4-MSPD. They led to the discovery of new phases in  $\text{NdVO}_4$  and  $\text{LaVO}_4$  [2]. Additional studies on orthovanadates have been (and will be) carried out at ALBA.

Fig. 11: Typical XRD patterns of  $\text{CrVO}_4$ -type and wolframite-type structures of  $\text{InVO}_4$ . Refinements are shown. Residuals are shown.

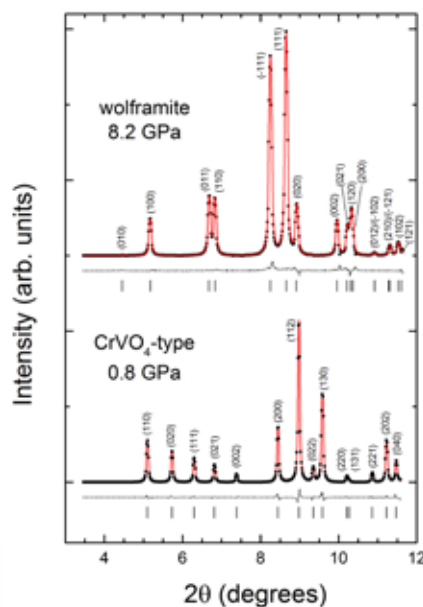


Fig. 12: Crystal structure of the low- (left) and high-pressure (right) phases. The coordination change of V can be clearly seen in the figure.



1. Departamento de Física Aplicada-ICMUV, Universidad de Valencia, MALTA Consolider Team, Edificio de Investigación, C/Dr. Moliner 50, 46100 Burjassot, Valencia, Spain
2. Centro de Tecnologías Físicas, Universitat Politècnica de Valencia, Camino de Vera s/n, 46022 Valencia, Spain
3. Chemistry Division, Bhabha Atomic Research Centre, Trombay, Mumbai 400085, India
4. ALBA Synchrotron, Cerdanyola, 08290 Barcelona, Spain

## REFERENCES

- [1] D. Errandonea, O. Gomis, B. García-Domene, J. Pellicer-Porres, V. Katari, S.N. Achary, A.K. Tyagi, and C. Popescu, *Inorg. Chem.* 52 (2013) 12790–12798.
- [2] D. Errandonea, C. Popescu, S.N. Achary, A.K. Tyagi, and M. Bettinelli, *Mat. Res. Bull.* 50 (2014) 279–284.

## ACKNOWLEDGMENTS

Research supported by Spanish MINECO (MAT2010-21270-C04-01 and CSD2007-00045) and done at ALBA as part of experiment 2012010170. The technical support of beamline staff is acknowledged as well as the logistic support of ALBA user office.

## AUTHORS AFFILIATION

Daniel Errandonea<sup>1</sup>, Oscar Gomis<sup>2</sup>, Braulio García-Domene<sup>1</sup>, Julio Pellicer-Porres<sup>1</sup>, Vasundhara Katari<sup>3</sup>, S. Nagabhusan Achary<sup>3</sup>, Avesh K. Tyagi<sup>3</sup> and Catalin Popescu<sup>4</sup>

# STRUCTURAL ORIGIN OF THE FERROELECTRIC PHASE TRANSITION IN CHARGE ORDERED $\text{LuFe}_2\text{O}_4$

Strong local lattice instability in hexagonal ferrites  $\text{RFe}_2\text{O}_4$  (R=Lu, Y, Yb) revealed by x-ray absorption spectroscopy  
*Physical Review B* 89, 045129 (2014)

**SARA LAFUERZA, JOAQUÍN GARCÍA, GLORIA SUBÍAS, JAVIER BLASCO AND VERA CUARTERO**

$\text{RFe}_2\text{O}_4$  compounds (R = Ho-Lu and Y) show a variety of electric and magnetic phase transitions ascribed to the occurrence of charge ordering (CO) of  $\text{Fe}^{2+}$  and  $\text{Fe}^{3+}$  ions. These oxides crystallize in a hexagonal cell ( $R\bar{3}m$  space group) consisting of an alternating stacking of triangular nets of R-O layers and Fe-O double layers along the c-axis. The formal valence of iron (+2.5) implies that an equal amount of  $\text{Fe}^{2+}$  and  $\text{Fe}^{3+}$  occupies the same site in the triangular lattice.

Within this family,  $\text{LuFe}_2\text{O}_4$  is the most studied compound. It undergoes a phase transition at about  $T_{\text{CO}} \approx 320$  K that was attributed to the  $\text{Fe}^{2+}/\text{Fe}^{3+}$  CO, which would originate electric dipoles in the geometrically frustrated triangular Fe lattice giving rise to ferroelectricity [1]. Besides, it shows ferrimagnetic ordering below  $T_{\text{N}} \approx 240$  K being a potential multiferroic material. Although a large number of papers have been published in  $\text{LuFe}_2\text{O}_4$  trying to explain the CO mechanism for multiferroicity, recent experimental works indicate that it is not ferroelectric [2]. This result questions the proposed  $\text{Fe}^{2+}/\text{Fe}^{3+}$  CO as the basis for the magnetoelectric properties of the  $\text{RFe}_2\text{O}_4$  systems. X-ray absorption spectroscopy (XAS) is a valuable tool to directly probe the existence of CO as it provides the incoherent addition of the x-ray absorption near edge structure (XANES) spectra of all the iron atoms in the sample.

We have performed a complete XAS study of the  $\text{RFe}_2\text{O}_4$  series (R = Lu, Y, Yb) and the isostructural compound  $\text{LuFeCoO}_4$  at the Fe K-edge. XANES and extended x-ray absorption fine structure (EXAFS) spectra were measured as a function of temperature from 100 K to 390 K crossing the CO transition on both isotropic and oriented powder samples. Conventional unpolarized and polarized spectra, *i.e.* with the x-ray's polarization vector parallel and perpendicular to the hexagonal c-axis, were obtained separately. The experiment was carried out at beamline BL22-CLAESS of ALBA. The quick energy scanning mode was employed to collect the spectra with typical acquisition time per point of about 0.5 s.

One of the key points was determining whether a complete charge disproportionation into  $\text{Fe}^{2.5-\delta}$  and  $\text{Fe}^{2.5+\delta}$  with  $\delta=0.5$  can describe the experimental XANES spectra. If there is coexistence of  $\text{Fe}^{2+}$  and  $\text{Fe}^{3+}$  valence states as in heterogeneous mixed-valence compounds, the XANES spectrum of  $\text{LuFe}_2\text{O}_4$  should agree with the 1:1 addition of the individual XANES spectra of appropriate  $\text{Fe}^{3+}$  and  $\text{Fe}^{2+}$  reference compounds. Figure 13b shows that the simulation resulting from the linear combination 1:1 of the XANES spectra representative of the  $\text{Fe}^{2+}$  and  $\text{Fe}^{3+}$  states does not reproduce the experimental one. Taking into account the empirical chemical shift ( $\Delta E$ ) between  $\text{Fe}^{2+}$  and  $\text{Fe}^{3+}$  of 4 eV [3], we conclude that the

maximum charge disproportionation between  $\text{Fe}^{2.5+\delta}$  and  $\text{Fe}^{2.5-\delta}$  atoms in  $\text{LuFe}_2\text{O}_4$  is  $\delta = 0.25$ . The same result applies to  $\text{YbFe}_2\text{O}_4$  and  $\text{YFe}_2\text{O}_4$  compounds and therefore, we conclude the absence of ionic  $\text{Fe}^{3+}$  and  $\text{Fe}^{2+}$  species in the mixed-valence  $\text{RFe}_2\text{O}_4$  ferrites.

The polarized EXAFS spectra have allowed us to analyze the local structure separating the different contributions mixed up in the unpolarized data. The best fit results show that the five oxygen atoms of the first coordination shell are at nearly the same distance but with a large Debye-Waller factor, revealing a high instability in the Fe local structure. Neither the interatomic distances nor the Debye-Waller factors of the first oxygen coordination shell change significantly with temperature at  $T_{\text{CO}} \approx 320$  K for  $\text{LuFe}_2\text{O}_4$  indicating that the dynamical structural distortion of the high temperature symmetric hexagonal phase freezes upon cooling down. Thus, the local structure instability of the mixed valence  $\text{Fe}^{+2.5}$  is at the origin of the CO transitions.

## REFERENCES

- [1] N. Ikeda *et al.*, Nature (London) 436, 1136 (2005)
- [2] S. Lafuerza *et al.*, Phys. Rev. B 88, 085130 (2013)
- [3] J. García *et al.*, J. Synchrotron Rad. 17, 386 (2010)

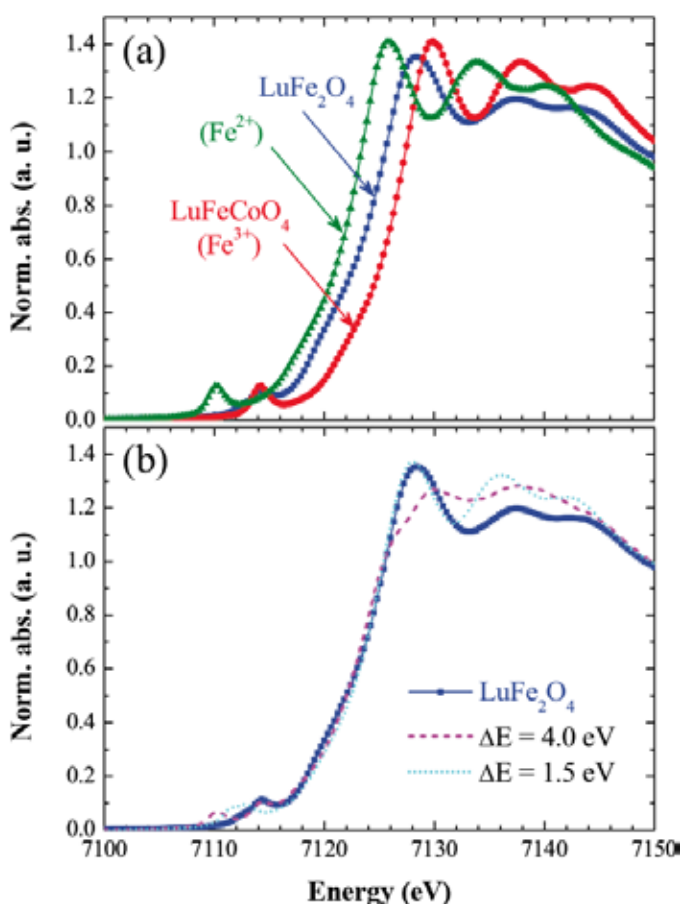


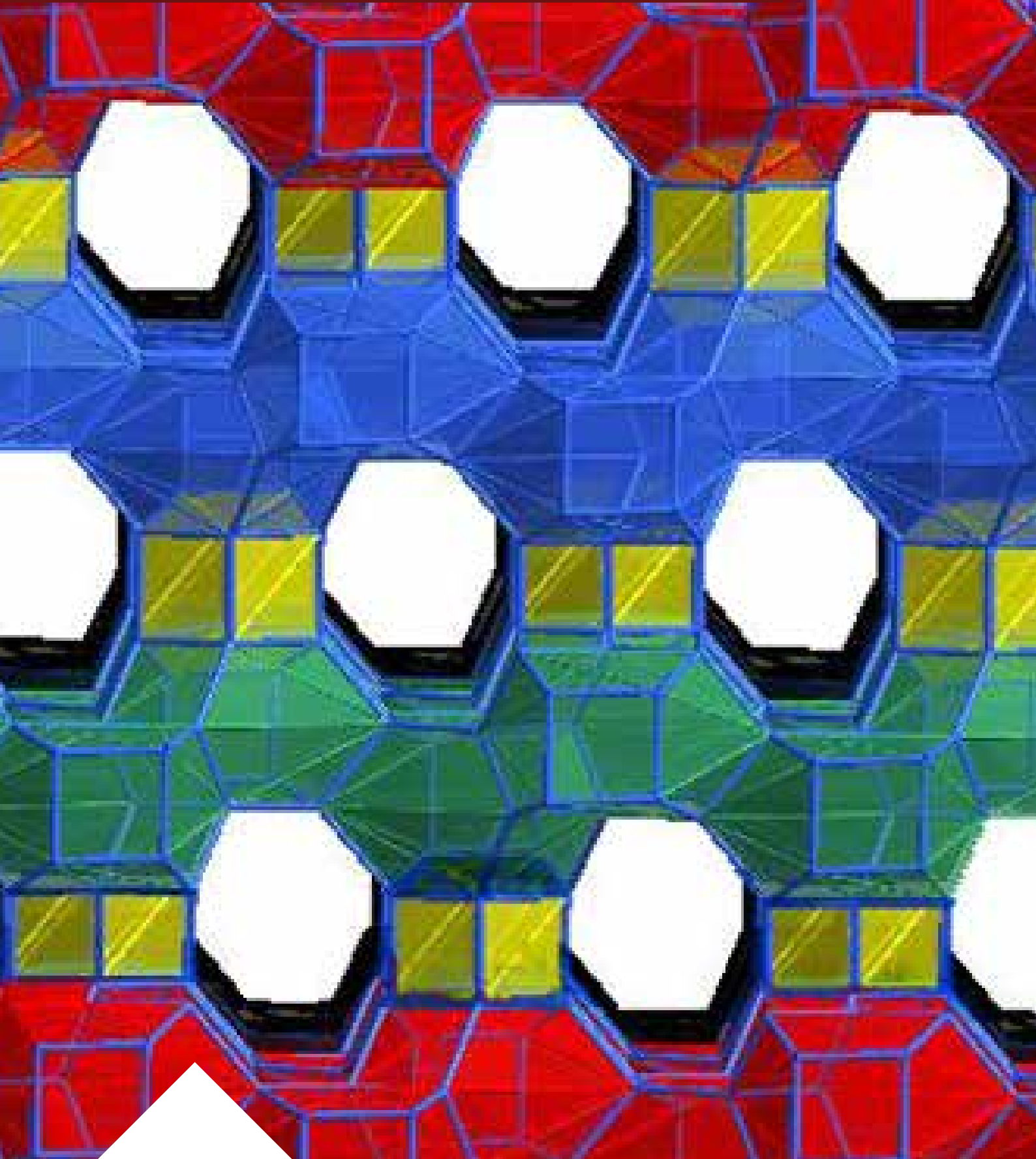
Fig. 13: (a) Experimental XANES spectrum at the Fe K-edge for polycrystalline  $\text{LuFe}_2\text{O}_4$  compared with XANES spectra of  $\text{Fe}^{+3}$  (from  $\text{LuFeCoO}_4$ ) and  $\text{Fe}^{+2}$  (extrapolated from the  $\text{Fe}^{3+}$  spectrum by the shift of  $-4\text{eV}$ ). (b) Comparison between the experimental XANES of  $\text{LuFe}_2\text{O}_4$  and two simulated spectra obtained from the 1:1 addition of the  $\text{Fe}^{+3}$  and  $\text{Fe}^{+2}$  spectra with different chemical shift ( $\Delta E$ ) among them.

## AUTHORS AFFILIATION

Sara Lafuerza<sup>1</sup>, Joaquín García<sup>2</sup>, Gloria Subías<sup>2</sup>, Javier Blasco<sup>2</sup> and Vera Cuartero<sup>1</sup>

1. European Synchrotron Radiation Facility, 38043 Grenoble, France  
 2. Instituto de Ciencia de Materiales de Aragón, 50009 Zaragoza, Spain

SCIENTIFIC RESULTS  
**CATALYSIS**



## HOW XAFS HELPS TO UNDERSTAND THE STRUCTURE OF THE ACTIVE SPECIES IN A REAL Au/TiO<sub>2</sub> CATALYST

Low-Temperature Oxidation of Carbon Monoxide with Gold(III) Ions Supported on Titanium Oxide. *Angewandte Chemie* 53, 3245-3249 (2014)

**ILYA SINEV, DENNIS GROSSMANN, WOLFGANG GRÜNERT**

Despite the remarkable potential of supported gold catalysts, the nature of their active sites is under debate even for a reaction as simple as CO oxidation. Regarding the Au oxidation state in them, most researchers favor Au(0) at the perimeter between metal cluster and support. Typical mechanisms involve reaction of oxygen activated on the support with CO adsorbed on perimeter sites, e.g. on slightly positively charged clusters Au<sub>n</sub><sup>δ+</sup>. Activation of both reactants by exposed Au sites on the nanoparticles has been also proposed.

The study was made with an Au/TiO<sub>2</sub> catalyst made by deposition-precipitation, without subsequent calcination. AuL<sub>III</sub>-edge XAFS was measured at HASYLAB, Hamburg, Germany (X1, fluorescence) and at ALBA (CLÆSS beamline, transmission). Spectra from self-supporting pellets wrapped in Kapton tape were measured at liquid nitrogen temperature (X1) or at room temperature (CLÆSS). The catalyst was investigated in the as-prepared state, after CO oxidation at room temperature, after heating in He flow at 623K, and after subsequent treatment in air at 623 K.

The XAFS signature of the initial catalyst is reported in Figure 14. XANES shows the gold completely in the +3 state. In EXAFS, there is no shell beyond the nearest Au-O coordination. This may be thought to suggest the gold to be atomically dispersed. Actually, it shows just that there is no order beyond the first shell – no ordered Au oxide, hydroxide, no metallic particles from Au(III) autoreduction. Indeed, high angle annular dark field scanning transmission electron microscopy (HAADF-STEM) showed most of the gold in small (ca. 2nm) disordered gold patches although isolated Au ions were also detected [1]. IR spectra of CO adsorption onto this sample at 90 K revealed Ti<sup>4+</sup> sites while Au<sup>3+</sup> could be hardly detected – most of it apparently being blocked by adsorbed water. Nevertheless, CO was slowly oxidized by gas-phase oxygen at 90 K, apparently by the Au<sup>3+</sup> exposed.

After CO oxidation at room temperature, linear combination analysis of the XANES showed 87% of the gold still in the +3 state, i.e. the catalysts achieved their very high activities [1] with a small minority of Au reduced to Au(0). Though not resulting from in-situ work, the low reduction degree is a reliable fact because possible experimental artifacts (storage, exposure to light or X-rays) would enhance the Au reduction degree. In EXAFS, the metal Au-Au coordination was hardly discernible. The spectrum could be reproduced by superimposing the initial spectrum with the one obtained after He, 623K in the 87/13 ratio. IR spectra of the

same sample showed intense signals from CO on perimeter sites between neutral and charged Au clusters ( $\text{Au}_n$ ,  $\text{Au}_n^{\delta+}$ ) and  $\text{TiO}_2$  support.  $\text{CO}/\text{Au}^{3+}$  became visible only after partial desorption of CO from AuO-related sites. STEM images remained mostly the same, but with rare relatively big metallic particles [1].

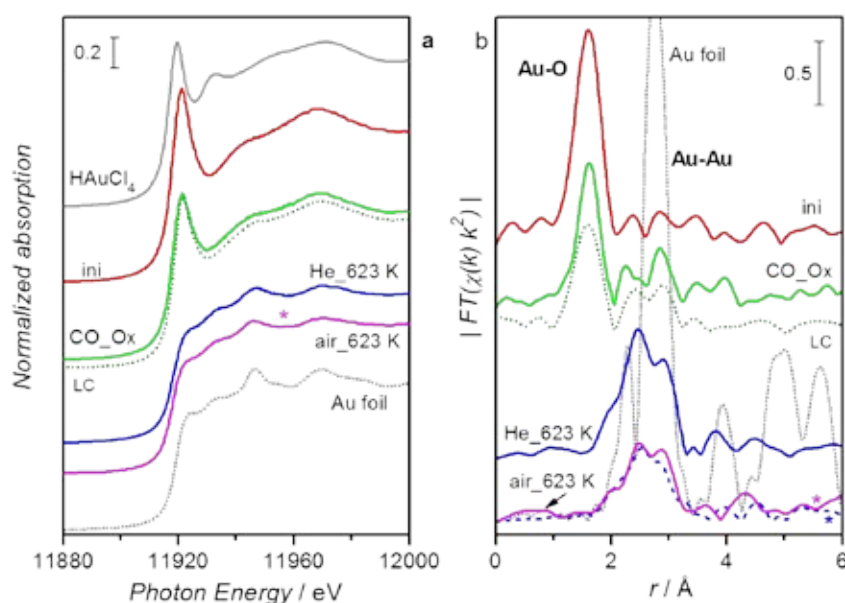
## REFERENCES

- [1] W. Grünert, D. Großmann, H. Noei, M.M. Pohl, I. Sinev, A. De Toni, Y. Wang, and M. Muhler, *Angew. Chem. Int. Ed.* 53 (2014) 3245.  
 [2] W. Grünert, D. Großmann, H. Noei, M. M. Pohl, I. Sinev, A. De Toni, Yuemin Wang, M. Muhler, *Chemie-Ing-Techn.*, submitted.

After He, 623 K, XAFS clearly showed the complete reduction of gold (Fig. 14), but the Au-Au coordination was still small. The resulting Au-Au C.N. of 8 [1] indicates particles of 1.2-1.3 nm size although the spherical model used for the evaluation is certainly inadequate at such sizes and EXAFS probably underestimates sizes of very small supported particles because of support-induced static disorder. HAADF-STEM showed Au in particles <2nm, oli-gomers, and even single atoms [1, 2], which have to be metallic according to XAFS. IR showed coexistence of CO adsorbed at the perimeters of  $\text{Au}_n$  and  $\text{Au}_n^{\delta+}$  at 90 K. The catalyst was highly active also in this state, but with a changed conversion-temperature dependence, apparently due to a transition of active sites from  $\text{Au}^{3+}$  to  $\text{Au}(\text{O})$ . Oxidation in air at 623 K deactivated the catalyst significantly but not completely. While Au remained in the zero oxidation state, IR of adsorbed CO showed the  $\text{Au}_n^{\delta+}$  state strongly attenuated and HAADF-STEM showed Au oligomers and atoms almost completely missing. From this, we confirm  $\text{Au}_n^{\delta+}$  as another active site for CO oxidation [1, 2].

Our XAFS data provide instructive examples for the interplay between methods required to solve such problems. Regarding XAFS, the XANES contributions were even more important and reliable than those of EXAFS. None of the other methods could identify the actual Au oxidation state: IR detects only exposed sites and remains qualitative if extinction coefficients are unknown, electron microscopy is blind for oxidation states. While the conclusions from XANES were supported by EXAFS (no  $\text{Au}-\text{Au}^0$  initially, no  $\text{Au}-\text{O}$  after thermal treatments), the information on population of coordination spheres was prone to misinterpretation (initial state: no order beyond first sphere – but STEM reveals particles; He, 623 K: ca. 1.5 nm particles, but STEM detects particles, oligomers, and single atoms). The case shows again that data of the averaging technique EXAFS can be of high value but have to be related to results of complementary methods.

Fig. 14: Au  $L_{III}$  XAFS spectra of Au/TiO<sub>2</sub> catalyst in different states. a) near-edge structure (XANES), references for Au<sup>III</sup> ( $\text{HAuCl}_4$ ) and Au<sup>0</sup> (Au foil) given for comparison, "LC" labels result of linear combination analysis, b) extended X-ray absorption fine structure (EXAFS), with Au foil as reference. All spectra measured at 77K except for those marked by \*, which have been measured at room temperature.



## AUTHORS AFFILIATION

Wolfgang Grünert<sup>1</sup>,  
 Dennis Großmann<sup>1</sup>,  
 Ilya Sinev<sup>1</sup>

1. Laboratory of Industrial Chemistry, Ruhr-University Bochum, Germany

## DETERMINATION OF THE STRUCTURE OF A NEW MICROPOROUS ZEOLITE

A new microporous zeolitic silicoborate (ITQ-52) with interconnected small and medium pores.  
*Journal of the American Chemical Society* 136, 3342-3345 (2014)

**RAQUEL SIMANCAS, JOSE LUIS JORDÁ, FERNANDO REY, AVELINO CORMA, ÁNGEL CANTÍN, INMA PERAL, CATALIN POPESCU**

Zeolites are microporous crystalline materials with a regular structure of pores that allows the entrance of molecules through and permits chemical reactions depending on the topology of their structural pores. The structure acts as a sieve, enabling the molecules to pass through only if they are smaller than the pores. This is why they are frequently used in many catalytic processes, having a great impact on several industries such as the petrochemical, fine chemical production and air separation.

In this research, members of the Instituto de Tecnología Química (UPV-CSIC) from Valencia have synthesized this new zeolite (named ITQ-52) using amino-phosphonium cations as organic structure-directing agents (OSDA) to control the size and shape of the pores.

High resolution diffraction experiments were performed at beamline 04-MSPD of ALBA for solving the structure of zeolite ITQ-52 (see Fig. 15). Knowing the structure of the new zeolite helps researchers to find possible applications of the new material by matching the pore geometry with the chemicals, intermediate states and products involved in the target process.

Possible processes for application of this new zeolite ITQ-52 could be alkylation of aromatics or selective separation of hydrocarbons, in which the pore structure is of paramount importance. The main conclusion of this research is the demonstration of the effectiveness of amino-phosphonium cations to be used as structure directing agents for creating new zeolitic catalysts with improved performance.

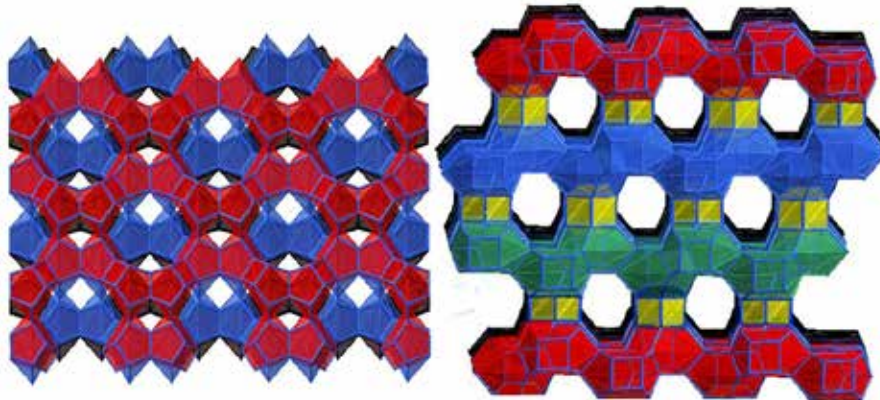


Fig. 15: The structure of ITQ-52 can be described as a stacking of layers. Each layer (in a different color in the figure) contains the large pores, while the stacking forms the smaller ones.

### AUTHORS AFFILIATION

Raquel Simancas<sup>1</sup>, Jose Luis Jordá<sup>1</sup>, Fernando Rey<sup>1</sup>, Avelino Corma<sup>1</sup>, Ángel Cantín<sup>1</sup>, Inma Peral<sup>2</sup>, Catalin Popescu<sup>2</sup>

1. Instituto de Tecnología Química (UPV-CSIC), Universidad Politécnica de Valencia–Consejo Superior de Investigaciones Científicas, Av. de los Naranjos s/n, 46022 Valencia, Spain  
2. ALBA Synchrotron, Cerdanyola del Vallès, Barcelona, Spain

# AMBIENT PRESSURE XPS STUDIES OF RhPd-BASED CATALYSTS FOR HYDROGEN PRODUCTION

N.J. DIVINS, C. ESCUDERO, V. PÉREZ, J. LLORCA\*

The structure of heterogeneous catalysts is essentially dynamic and depends on the composition of the surrounding environment. Thus, their surface structure and composition may be modified when the gaseous conditions change in order to adapt their electronic properties and geometry to the new surrounding environment, originating the catalytic phenomenon.

In this work, we have studied the reorganization of RhPd alloyed nanoparticles when they are exposed to different gaseous environments. RhPd nanoparticles constitute the active phase of a highly active, selective and stable catalyst towards the production of H<sub>2</sub> from bioethanol reforming with steam. The ethanol steam reforming reaction (ESR),  $C_2H_5OH + 3 H_2O \rightarrow 6 H_2 + 2 CO_2$ , represents a very attractive route for hydrogen generation from a renewable and widespread source (bioethanol) without net CO<sub>2</sub> emissions that is being currently intensively investigated [1,2].

The excellent performance of this system supported over metal oxides for the ESR was first reported in 2008 [3]. At the same time, Tao et al. studied by ambient pressure X-ray photoelectron spectroscopy (AP-XPS) the rearrangement of RhPd model nanoparticles (15 nm in diameter) under different gaseous environments (NO, O<sub>2</sub>, and CO and NO mixtures) at the Advanced Light Source (Berkeley, USA) [4]. These authors detected the migration of Rh and Pd atoms and found that a core-shell structure developed depending on the atmosphere tested. During our investigations, we wanted to focus on the reorganization and changes experienced by our RhPd bimetallic nanoparticles (NPs) (5 nm in diameter) under the reforming catalytic atmosphere.

We carried out Ambient Pressure X-ray PhotoElectron Spectroscopy at the NAPP branch of the CIRCE beamline in ALBA [5]. The NAPP endstation is equipped with a hemispherical electron energy analyzer that can operate at a sample pressure range from UHV up to 25 mbar thanks to a differential pumping system which ensures a pressure difference of 10<sup>9</sup> between detector and sample. Therefore the usual characterization capabilities of XPS are extended to the study of gas-solid and gas-liquid interphases, with applications to in-situ characterization of heterogeneous catalysts, corrosion processes, wetting, fuel cells, photovoltaics, etc.

The experiments were performed at 0.05 mbar and 573-823 K under different gaseous environments such as O<sub>2</sub>, H<sub>2</sub>, and ethanol + water. Three different photon energies (hν) of 670, 875 and 1150 eV were used in each case to obtain high resolution XP spectra of Rh 3d, Pd 3d, O 1s and C 1s. The photon energies selected account for inelastic mean free paths (IMFPs) of Rh 3d and Pd 3d photoelectrons of ca. 0.7, 0.9 and 1.2 nm, respectively [6], which allowed us to perform a depth profile of the RhPd NPs and analyze different volumes of the NPs. The volumes defined by these IMFPs from the boundary of the nanoparticles represent approximately 25, 34 and 44% of their total volume, respectively.

\* Corresponding author

The first results show that during the oxidizing treatment the surface of the bimetallic nanoparticles showed a Rh/Pd ratio close to unity and no substantial differences between the different depths were detected. Under H<sub>2</sub> reduction a migration of Pd towards the surface was clearly observed. At the same time, Rh and Pd suffered a strong reduction and ca. 75% of both metals were present in the metallic state. During the performance of the ESR reaction in the analysis chamber, a new restructuring of the bimetallic system was detected as Rh atoms migrated towards the surface. The outer region of the NP experienced a strong reduction and ca. 90% of Rh and Pd were found in the metallic state (figure 16). This reducing effect is ascribed to the reducing effect of the hydrogen generated during the ESR reaction. This was corroborated studying the RhPd nanoparticles under pure H<sub>2</sub> at the same temperature. Rhodium and Pd did not reorganize and the outmost layers did not substantially change their oxidation state, whereas the inner layers got more reduced. Therefore, we demonstrate that bimetallic systems suffer reorganization under reforming conditions, which may help designing more effective catalysts by mimicking the resulting structure of the nanoparticles under reaction.

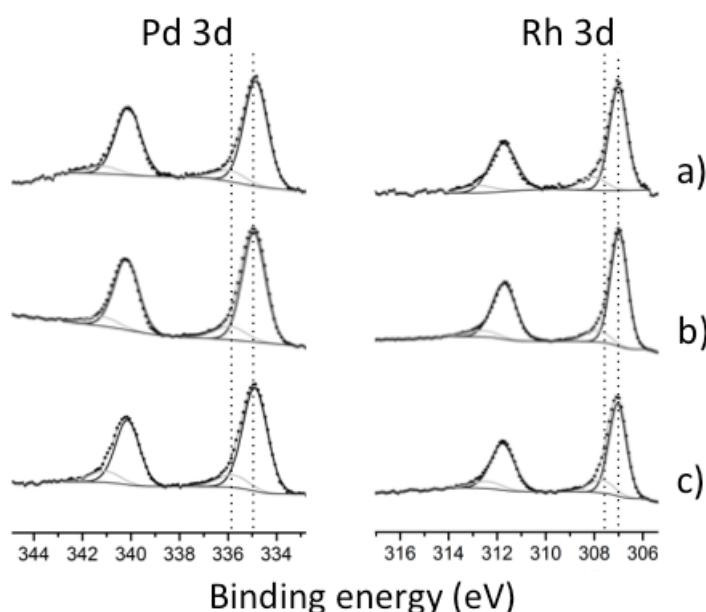


Fig. 16 Depth-profile ambient pressure XP spectra of Pd-Rh nanoparticles during the ethanol steam reforming reaction, at pressure= 5 10<sup>-2</sup> mbar. Metallic and oxidized components of each peak are shown in the deconvolution. Rhodium migration towards the surface was observed during the reaction and both metals were mainly reduced.

1. Institute of Energy Technologies and Centre for Research in NanoEngineering, Technical University of Catalonia. Diagonal 647, 08028 Barcelona, Spain.  
2. ALBA synchrotron, Cerdanyola del Vallès, Spain.

## REFERENCES

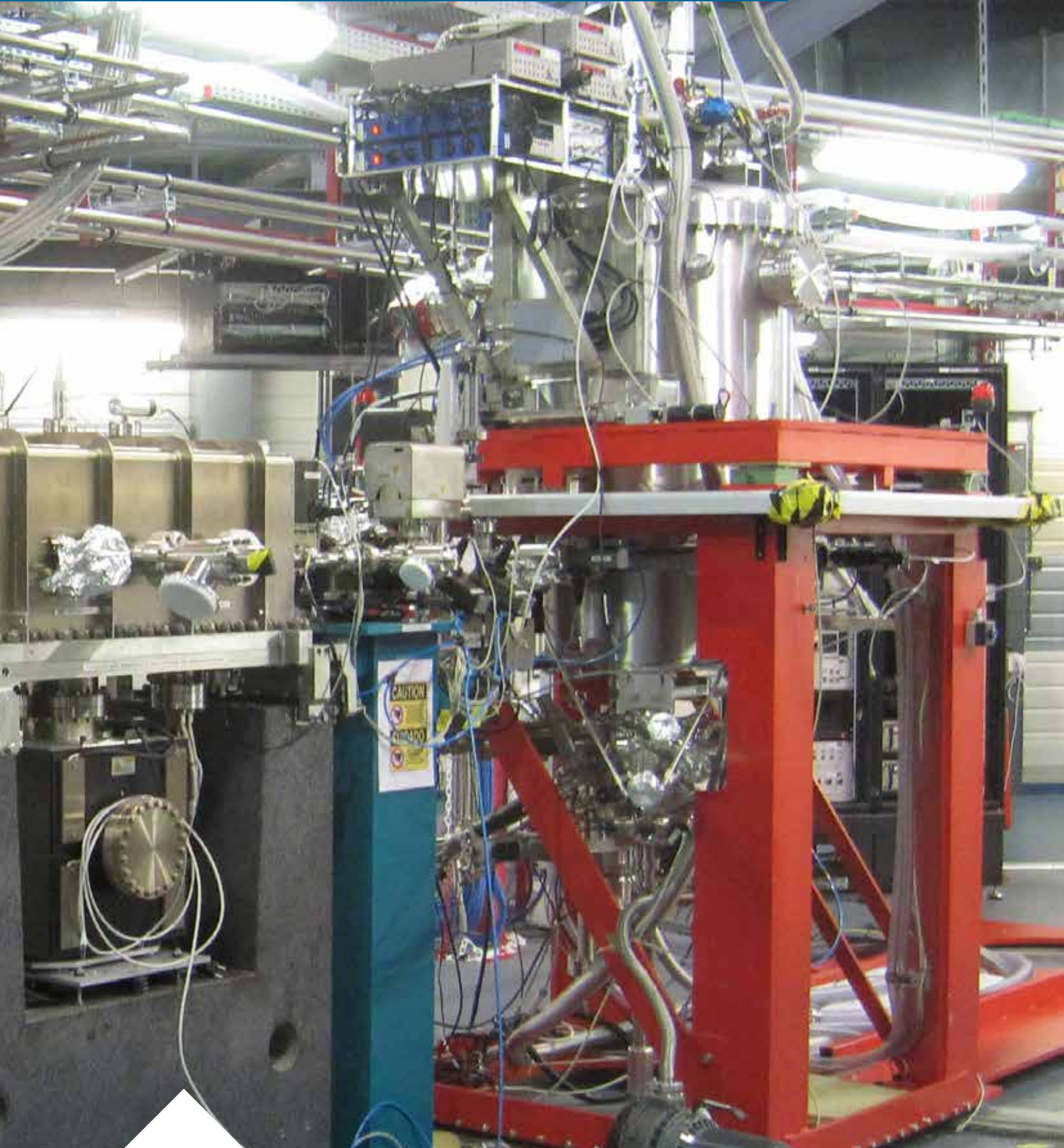
- [1] N. J. Divins, E. López, Á. Rodríguez, D. Vega, and J. Llorca, "Bio-ethanol steam reforming and autothermal reforming in 3- $\mu$ m channels coated with RhPd/CeO<sub>2</sub> for hydrogen generation," *Chem. Eng. Process. Process Intensif.*, vol. 64, pp. 31–37, 2013.
- [2] E. López, N.J. Divins, A. Anzola, S. Schbib, D. Borio, J. Llorca, "Ethanol steam reforming for hydrogen generation over structured catalysts", *International Journal of Hydrogen Energy*, vol. 38, p. 4418-4428, 2013.
- [3] H. Idriss, M. Scott, J. Llorca, S. Chan, W. Chiu, P.Y. Sheng, A. Yee, M. Blackford, S. Pas, A. Hill, F. Alamgir, R. Rettew, C. Petersburg, S. Senanayake, and M. Barteau, "A Phenomenological Study of the Metal-Oxide Interface: The Role of Catalysis in Hydrogen Production from Renewable Resources," *ChemSusChem*, vol. 1, no. 11, pp. 905–910, 2008.
- [4] F. Tao, M. E. Grass, Y. Zhang, D. R. Butcher, J. R. Renzas, Z. Liu, J. Y. Chung, B. S. Mun, M. Salmeron, and G. A. Somorjai, "Reaction-Driven Restructuring," *Science*, pp. 932–934, 2008.
- [5] V. Pérez-Dieste, L. Aballe, S. Ferrer, J. Nicolàs, C. Escudero, A. Milán, and E. Pellegrin; *J. Phys.: Conf. Ser.*, 425 (2013) 072023.
- [6] C. J. Powell and A. Jablonski, *NIST Electron Inelastic-Mean-Free-Path Database - Version 1.2*. Gaithersburg, MD: National Institute of Standards and Technology, 2010.

## AUTHORS AFFILIATION

N.J. Divins<sup>1</sup>, C. Escudero<sup>2</sup>, V. Pérez<sup>2</sup>, J. Llorca<sup>1</sup>

# SCIENTIFIC RESULTS

## MAGNETISM



# A STEP FORWARD IN UNDERSTANDING MAGNETIC Co/CoO NANOSTRUCTURES

Direct Observation of Rotatable Uncompensated Spins in the Exchange bias System Co/CoO-MgO  
*Nanoscale* 5, 10236 (2013)

**C. GE, X. WAN, E. PELLEGRIN, Z. HU, S. M. VALVIDARES, A. BARLA, W.-I LIANG, Y.-H. CHU, W. ZOU, AND Y. DU**

Computer hard disks use electromagnetic recording systems. To do so, they use “heads” to write or read onto or from the different disks, respectively. These heads are composed of layers made of ferromagnetic and antiferromagnetic materials. In the core of each layer, the electrons spins carry the magnetic moment of the atoms. In this study, it has been discovered that cobalt nanostructures in a non-magnetic host material show a surprisingly high “exchange bias” effect.

The exchange bias occurs when a ferromagnetic material (FM) and an antiferromagnetic material (AFM) get in touch and, as a result, there is a strong magnetic interaction between them. This effect has a great impact on magnetic recording systems. Nowadays, the exchange bias is used to pin the magnetic moments within the magnetic reference layer in spin valve readback heads.

The researchers designed and produced samples consisting of Co/CoO core-shell nanoparticles (~4 nm diameter Co metal core and CoO shell with ~1 nm thickness) embedded in a non-magnetic MgO matrix. Cobalt is one of the most used materials in modern magneto-electronics, because of its outstanding magnetic properties. This Co/CoO system exhibits a surprisingly large exchange bias field  $H_E \approx 2460$  Oe and a large coercive field  $H_C \approx 6200$  Oe at  $T = 2$  K, which is in sharp contrast to the small exchange bias and coercive field in the case of other non-magnetic  $Al_2O_3$  or C matrix materials reported in previous studies.

Using the brilliant circular polarized soft X-ray beam of the BOREAS beamline, they measured the soft x-ray magnetic circular dichroism (SXMCD) of the samples and a ferromagnetic signal originating from the nominally antiferromagnetic CoO shell could be observed (see fig. 17). This finding gives direct evidence for the existence of rotatable interfacial uncompensated Co spins in the CoO shell, thus supporting the uncompensated spin model as a microscopic description of the exchange bias mechanism.

This research will contribute to a better understanding of the magnetic exchange bias systems used for magnetic information storage devices. These systems enable the production of smaller hard disks with a higher information density.

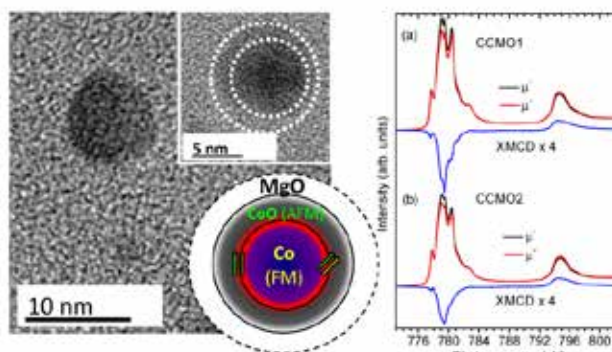


Fig. 17: Left panel: TEM pictures of samples analyzed at the BOREAS beamline. Samples consisted of a ~4 nm diameter Co metal core and a CoO shell with ~1 nm thickness. The red zone in the insert shows the magnetic interaction area between FM Co core and the AFM CoO shell, where the “exchange bias” effect takes place. Right panel: Co2p absorption edges demonstrating the ferromagnetic properties of the nominally antiferromagnetic CoO shell (top) and the Co metal core (bottom).

## AUTHORS AFFILIATION

C. Ge<sup>1,2</sup>, X. Wan<sup>1</sup>, E. Pellegrin<sup>3</sup>, Z. Hu<sup>4</sup>, S. M. Valvidares<sup>3</sup>, A. Barla<sup>5</sup>, W.-I Liang<sup>6</sup>, Y.-H. Chu<sup>6</sup>, W. Zou<sup>1</sup>, and Y. Du<sup>1</sup>.

1. National Laboratory of Solid State Microstructures and Department of Physics, Nanjing University, Nanjing 210093, China
2. Department of Physics, Jiangsu Institute of Education, Nanjing 210013, China
3. ALBA Synchrotron, Carretera BP 1413, km 3.3, E-08290 Cerdanyola del Vallès, Spain
4. Max Planck Institute for Chemical Physics of Solids, Nöthnitzer Straße 40, D-01187 Dresden, Germany
5. Istituto di Struttura della Materia, ISM CNR, S.S. 14 km 163.5, Area Science Park Basovizza (Ts), I-34149 Trieste, Italy
6. Department of Materials Science and Engineering, National Chiao Tung University, Hsinchu 30010, Taiwan.

# XMCD-PEEM IMAGING OF ROOM TEMPERATURE MAGNETOELECTRIC EFFECT IN $\text{La}_{2/3}\text{Sr}_{1/3}\text{MnO}_3$

D. PESQUERA<sup>1</sup>, M. FOERSTER<sup>2</sup>, B. CASALS<sup>1</sup>, G. HERRANZ<sup>1</sup>, L. ABALLE<sup>2</sup>, J. FONTCUBERTA<sup>1</sup>

Nanometric magnetic domains are important ingredients in microelectronic memories, e.g. magnetic hard disks drives or non-volatile magnetic RAM, as sensors in automotive industry and in new, programmable magnetic logic elements. Switching their magnetization  $M$  (e.g. to write information) is a crucial task for which two different approaches are used: a) local magnetic fields (Oersted fields), exhibiting a poor scaling behavior when reducing the device size, and b) transfer of electron spin angular momentum to  $M$  (spin transfer torque) with better scaling behavior but needing high current densities. Both methods rely on the flow of electric current, which invariably results in undesirable energy consumption and heat dissipation through Ohmic losses. Therefore the manipulation of magnetization  $M$  by a pure electric field (voltage) without current would be a key step towards more effective devices and continues to be a focus of research.

Although in some (multiferroic) materials an intrinsic coupling of magnetic and electric polarization can be found, this effect is usually small and restricted to low temperatures, making it hard to use in a practical device. On the other hand, heterostructures comprising of one magnetic and a second, ferroelectric material have shown much larger effects. There are different mechanisms through which a ferro- or piezoelectric material can influence a ferromagnetic material, for example by changing its anisotropy through elastic deformations (by the piezoelectric effect [1, 2]) or by charge doping [3].

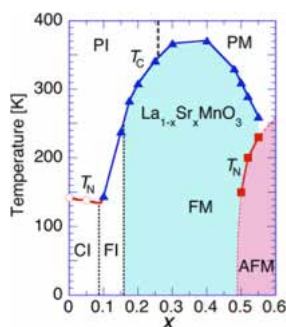


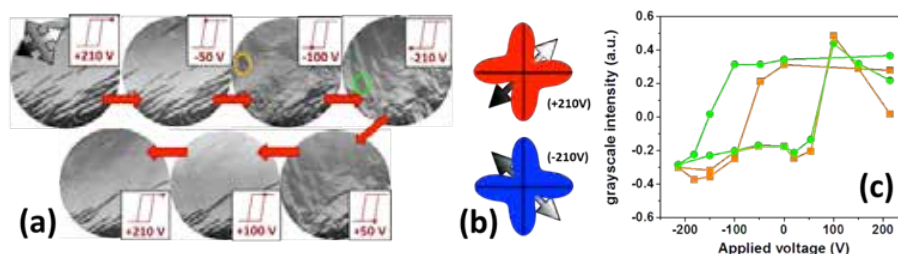
Fig. 18.  $\text{La}_{1-x}\text{Sr}_x\text{MnO}_3$  phase diagram for varying Sr doping  $x$  (from [5]).

$\text{La}_{1-x}\text{Sr}_x\text{MnO}_3$  is a family of oxides that display a rich phase diagram depending on the hole ( $\text{Mn}^{4+}$ ) concentration, whose proportion depends on the content of  $\text{Sr}^{2+}$  replacing  $\text{La}^{3+}$  in the perovskite lattice (Fig. 18).  $\text{La}_{2/3}\text{Sr}_{1/3}\text{MnO}_3$  (LSMO) is a ferromagnetic, metallic oxide which is bounded by insulating ferromagnetic or antiferromagnetic regions in the phase diagram. Thus we can expect this material to be also very susceptible to extrinsic charge doping, for instance by the polarization charge of a proximity ferroelectric material effectively influencing the Mn valence states (see e.g. [3]). Moreover, the 3d-bandwidth, which is intimately linked to the Mn-O-Mn bond configuration, is extremely sensitive to changes in their topology. Indeed, for the same amount of doping, ferromagnetic or antiferromagnetic phases can be obtained [4]. Thus, the magnetic properties of an LSMO-piezoelectric heterostructure are expected to be strongly dependent on the piezoelectric substrate state through interfacial coupling effects generated by charge doping and/or strain.

20 nm thick LSMO films were deposited on  $[\text{Pb}(\text{Mg}_{0.33}\text{Nb}_{0.67})\text{O}_3]_{0.72}-[\text{PbTiO}_3]_{0.28}$  (PMN-PT) piezoelectric substrates in (001) orientation. The sample was mounted on a specially built holder to include electrical top and bottom contacts. The substrate was poled in-situ using a bias unit floating at the 20kV of the high voltage rack made by the ALBA electronics group. Referencing the sample top to the PEEM start voltage we were able to image the sample while applying up to 250V bias voltage across the sample, with the LSMO layer acting as top electrode.

The sample was imaged in the PEEM with low energy (secondary) photoelectrons emitted upon illumination with X-rays tuned to the Mn-L<sub>3</sub> absorption edge. The absorption cross section and thus the electron emission depends on the relative orientation of the local magnetization *M* and the beam direction, with opposite sign variations for left and right handed circular polarization. Thus, subtracting images with opposite polarization, we obtain an image with only magnetic contrast. This magnetic imaging mode is called XMCD-PEEM (X-ray Magnetic Circular Dichroism - PhotoEmission Electron Microscopy).

As shown in Fig. 19, the evolution of the LSMO thin film magnetization upon electrically poling the PMN-PT ferroelectric substrate was followed. The intensity gray scale corresponds to the local magnetization as indicated by the arrow inset. One can immediately appreciate in Fig. 19 that the LSMO magnetization displays an in-plane uniaxial character. The uniaxial anisotropy most likely results from the domain texture of the PMN-PT substrate, which overrides the genuine biaxial magnetocrystalline anisotropy of LSMO. Moreover, one can observe: a) a dramatic modification of the magnetic domain structure of LSMO upon polarization switching of the underlying ferroelectric substrate (the observed switching electric field for the magnetic configuration around  $\pm 75$  V coincides with the ferroelectric coercivity of the PMN-PT substrate); b) a non-symmetric magnetization response for V+ and V-, and c) a remarkable reversibility of the magnetic domain structure after switching (for instance when comparing the two images taken at +210 V).



Results b) and c) are emphasized in Fig. 19c where we show the XMCD intensity vs applied voltage of selected areas (circles in Fig. 19a). Data in this plot illustrate that the magnetic switching induced by the E-field poling occurs at the coercive field of PMN-PT and, most remarkably, the magnetization returns to the initial direction after completion of the cycle. To help understand the observations, we have included in Figure 19b schematic contour plots of the magnetic anisotropy at the highest applied voltages (+210 V and -210 V).

We note that a uniaxial in-plane easy axis is in agreement with expectations for LSMO modulated by the domain morphology of the underlying ferroelectric domains of PMN-PT, which is largely modified at its coercive field.

These results could give new insight into the mechanism of interface ferromagnetic-ferroelectric coupling, such as the balance between elastic deformation of LSMO resulting from the piezoresponse of the PMN-PT substrate, field-effect-related charge modulation of LSMO, and magnetic pinning at ferroelectric domain walls.

1. Institut de Ciència de Materials de Barcelona (ICMAB-CSIC)  
2. ALBA Synchrotron Light Facility

## REFERENCES

- [1] M. Buzzi et al., PRL 111, 027204 (2013)
- [2] S. Finizio et al., Phys. Rev. App. 1, 021001 (2014)
- [3] CAF Vaz et al., Applied Physics Letters, 97, 042506 (2010)
- [4] D. Gutierrez et al. Phys Rev B 89, 075107 (2014)
- [5] Y. Tokura et al., J. Magn. Mater., 200, 1 (1999)

## ACKNOWLEDGMENTS

We gratefully acknowledge the help of the CIRCE support staff (J. Prieto, N. González, F. Becheri) and of the ALBA electronics group, especially A. Fontserè, A. Sánchez and O. Matilla.

Fig. 19: (a) XMCD-PEEM images of an LSMO thin film taken at the Mn-L<sub>3</sub> absorption edge with field of view 50  $\mu\text{m}$ . The gray scale magnetic contrast corresponds to the magnetization as indicated by the inset figure in the first panel. Consecutive images (along the red arrows) were taken with different out of plane voltage applied to the piezoelectric PMN-PT substrate as indicated. For each XMCD-PEEM image, the inset indicates the position of ferroelectric polarization versus applied field on generic hysteresis loop. Schematics at (i), (ii) and (iii) show the simplified magnetic anisotropy energy contour as deduced from the XMCD-PEEM images at  $\pm 210$  V and the change of the easy magnetization axis. (b) Schematic magnetic anisotropy energy contours illustrating the effective uniaxial easy magnetization direction and its rotation for different voltages. (c) XMCD-PEEM grayscale intensity vs applied voltage of selected areas (marked by orange and green circles in (a)) showing reversible magnetic switching behavior.

## AUTHORS AFFILIATION

D. Pesquera<sup>1</sup>, M. Foerster<sup>2</sup>, B. Casals<sup>1</sup>, G. Herranz<sup>1</sup>, L. Aballe<sup>2</sup>, J. Fontcuberta<sup>1</sup>

# IMAGING 60 NM DIAMETER MAGNETIC BUBBLES

**A. SORRENTINO, C. BLANCO, C. QUIROS, E. PEREIRO, M. VELEZ, J.M. ALAMEDA,  
J. ESTEVE, M. DUCH, S. FERRER**

Magnetic films or multilayers with perpendicular anisotropy are essential components of computers and other devices in modern technology. Films that are magnetically hard tend to form up and down magnetization domains in the absence of an external applied magnetic field. The morphology and dimensions of the domains and also the possibilities of manipulating them are important aspects for applications of magnetic devices. How stable the domains are and how difficult is to change the magnetization in magnetic films are relevant practical questions.

Beamline 9 Mistral offers the possibility of high resolution imaging of domains using the microscope and the circular magnetic dichroic absorption contrast. Thanks to the stability of the microscope and beamline optics, it is possible to achieve detailed information on the changes of a specific magnetic domain when a pulsed magnetic field is applied. In this study, it has been demonstrated that the effect of magnetic pulses can alter the microscopic structure of the domains at remanence. Depending on the magnitude of the pulsed field, either maze, bubbles or intermediate situations have been observed.

The samples analyzed were thin films (80 nm thickness) of  $\text{Co}_5\text{Nd}$  alloys grown by sputtering techniques at the University of Oviedo and were deposited on silicon nitride membranes fabricated at the Centro Nacional de Microelectrónica (CNM-CSIC), located in Bellaterra, that fit exactly the geometry of the microscope sample holder. The pulses of magnetic fields were created with a microcoil developed at ALBA. They could achieve  $\pm 1$  T as a maximum amplitude and had a duration of about 15  $\mu\text{s}$ . The 1 T field is intense enough to test the magnetic behavior of the films in stringent conditions of practical applications.

Panel a of figure 20 displays the characteristic labyrinth domains which are the most common magnetic structure at remanence after applying saturation pulses either positive or negative. Black and white domains correspond to inward and outward perpendicular magnetizations. The inset is the Fourier transform which shows a ring pattern indicating azimuthal disorder. The inverse of the radius of the ring gives the lateral correlation length of the distribution which is about 120 nm.

The new and somewhat surprising result observed is displayed in panel b. Applying pulses of selected amplitudes below the saturation of the perpendicular magnetization, resulted in a bubble domain structure with a very narrow distribution of the dimensions of the bubbles which

had a diameter of about 60 nm. The bubbles have mostly 6 fold and also 5 fold coordination and do not display long range order as shown by the annular shape of the Fourier transform in the inset.

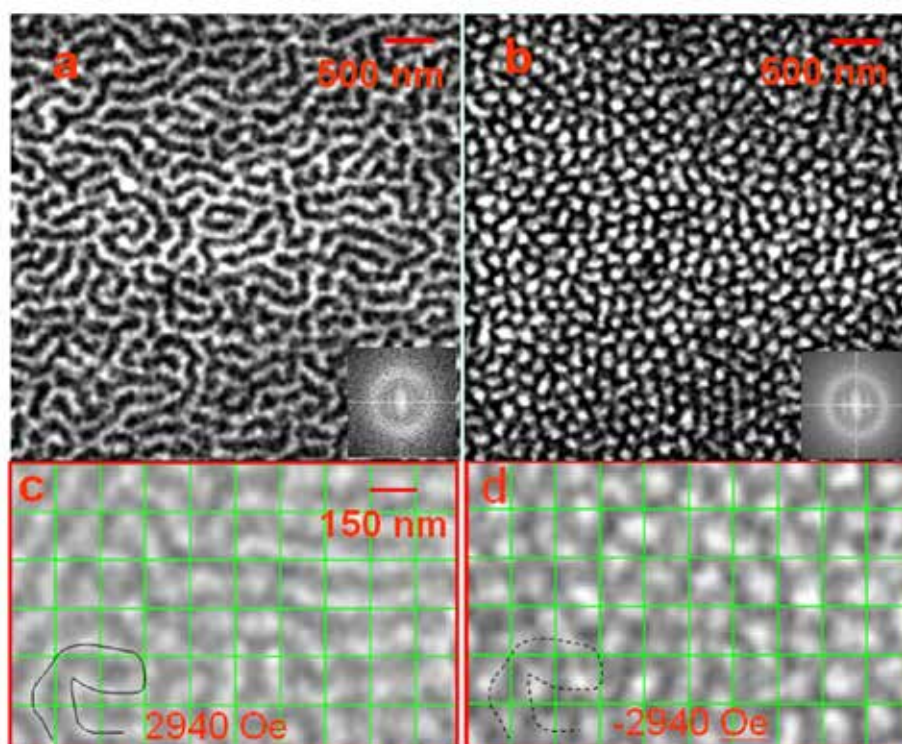


Fig. 20: (a): characteristic labyrinth domains (b) bubble domain structure. The insets are the corresponding Fourier transforms. (c) and (d) are the same region of the sample evolving from maze (c) to bubble (d) domains. The curved linear domains break and form magnetic dots.

These are the initial results of a systematic exploration of the different domain topologies that will be carried on the near future.

1. Universidad de Oviedo, Oviedo, Spain
2. Centro Nacional de Microelectrónica (CNM – CSIC), Bellaterra, Barcelona, Spain
3. ALBA Synchrotron, Cerdanyola del Vallès, Spain

#### AUTHORS AFFILIATION

Carlos Quiros<sup>1</sup>, Cristina Blanco<sup>1</sup>, Maria Velez<sup>1</sup>, Jose M. Alameda<sup>1</sup>, Jaume Esteve<sup>2</sup>, Marta Duch, Salvador Ferrer<sup>3</sup>, Andrea Sorrentino<sup>3</sup>, Eva Pereiro<sup>3</sup>

# RESONANT SOFT X-RAY REFLECTIVITY AND SCATTERING CAPABILITIES AT ALBA BEAMLINE 29

**BL29 STAFF, ALBA SYNCHROTRON**

*MaReS*, the resonant scattering endstation at ALBA BL29, is soon to become available for user experiments. The endstation, a technically cumbersome multicomponent system under final completion and commissioning, is aimed to be a world-class instrument for the finest scientific research on this field. Presently, *MaReS* major components have been delivered and most are commissioned: its multi-axis cryomanipulator (VG Scienta, UK), the sample and detector reflectometer circles (PINK, Germany), its UHV chamber (in-house design, manufactured by VCS, Italy), the magnet rotary circle (McAllister, US), 4-blade entrance slits (JJXray, Denmark), in-vacuum CCD (XCAM, UK), and a remarkable High-Temperature Superconducting magnet (manufactured by HTS-110, New Zealand). Related in-house work and design by ALBA has been considerable, including detector arms under manufacturing and other subsystems such as the endstation final support, magnet positioning arm and loads of cabling work due Fall 2014.



Fig. 21: BL29 resonant scattering endstation, MaReS at first tests with beam on March.

In summary, *MaReS* endstation will be available for UHV reflectometry studies with sample cryo-cooling capability down to 20K in the next cycle of official user experiments, starting Jan'2015. Additional instrumentation under completion and with pending tests and commissioning such as the CDD arm or magnet will be made available in successive experiment cycles. The reflectometer with sample cryo-cooling capability combined with the versatile photon energy range and polarization control of the beamline, including fast on-the-fly energy scans has already many possibilities, as evidenced by first tests with beam on last March discussed in the following. (see Fig. 21)

A resonant X-ray reflection or scattering experiment monitors the X-ray intensity reflected or dispersed by the specimen under investigation after reflection (or sometimes transmission) of the incoming X-ray beam. Measurements typically fall in either of two categories illustrated with the following study of a {CoSi/Si} magnetic multilayer [1].

In the case of reflectometry or related scattering measurements, Fig.22 (right), the reflected intensity is analyzed as a function of the angle of incidence and/or dispersion. The archetypical case is the specular reflectivity measurement, where sample and detectors are rotated to span an extended range of equal X-ray incidence and exit angles. Such a measurement is well-known to provide depth-profile information on the sample, because the intensity arises from the vertical distribution of charge density and contains information on, among other aspects, vertical periodicities such as a multilayer period.

A reflectance spectra such as those on Fig22(left) are *resonant measurements* of the reflected or scattered intensity as a function of the incoming soft X-ray photon energy this time at a fixed incidence angle. Data of this kind looks alike -and is closely related to- absorption spectra (XAS, NEXAFS), because the reflected/scattered intensity presents pronounced resonances at photon energies crossing atomic core levels giving signal enhancements well over one order of magnitude. The shown reflectance spectra at the Cobalt L-III and Silicon K- edge enclose information on the magnetic and chemical state of Cobalt atoms on the Cobalt Silicide layer, as well as of the Silicon atoms on both the Co-Si layer and Si layer.

Fig 22 shows reflectivity scans from the multilayer at the Co L pre -edge and Si K pre-edge photon energies. The good quality of the data along 5 decades of intensity is demonstrating the good mechanical behavior of the reflectometer.

In summary, soft X-ray resonant scattering techniques are powerful approaches that can provide unique information on the vertical and lateral profile of charge, chemical, magnetic or orbital electronic degrees of freedom on materials[2]. The scientific scope includes magnetic, superconductors, oxides, multiferroics, ferroelectrics, polymers, graphene and other C and Si based materials, typically in bulk, thin film, multilayered or nanostructured form.

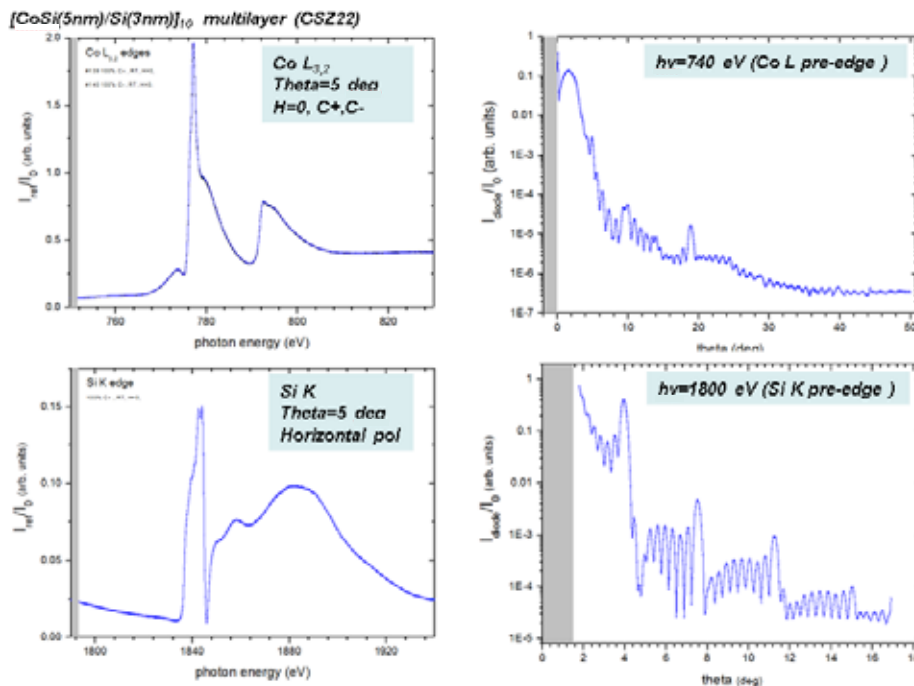


Fig. 22: Data taken in first test with beam of the MaReS scattering endstation checking a CoSi/Si 10-period multilayer. Left: Reflectance spectra taken at fixed incident angle across Co, Si absorption edges. Right: extended specular reflectivity for fixed photon energies at the pre-edge of Cobalt, Silicon white lines, respectively.

## REFERENCES

Link to beamline webpages: [www.cells.es/beamlines/bl29](http://www.cells.es/beamlines/bl29)  
 [1] - Resolving antiferromagnetic states in amorphous Co-Si / Si multilayers by soft x-ray resonant magnetic scattering, S. M. Valvidares, C. Quirós, A. Mirone, J. -M. Tonnerre, S. Stanescu, P. Bencok, Y. Souche, L. Zárata, J. I. Martín, M. Vélez, N. B. Brookes, and J. M. Alameda, Phys. Rev. B 78, 064406 (2008)  
 [2] Native SrTiO 3 (001) surface layer from resonant Ti L 2,3 reflectance spectroscopy, S. M. Valvidares, M. Huijben, P. Yu, R. Ramesh and J. B. Kortright , Phys. Rev. B 82, 235410 (2010)

## NOTE:

A Si photodiode has been used for the Reflectivity measurements. Proper normalization and further measurements have to be done, particularly for suitable background correction of the reflectance spectra at the Si K edge.

## ACKNOWLEDGMENTS

Samples courtesy of C. Quiros (Ov. Univ.). Special acknowledgements to J.B.Kortright (LBNL), E. Gullikson for advice and suggestions. S. Ferrer is specially thanked for suggestions and continuous support. Technical support by ALBA Computing and Engineering Divisions, and ALBA administration is also acknowledged.

# INDUSTRY RESULTS

ONE OF THE MAIN GOALS OF ALBA IS TO CONTRIBUTE TO THE INDUSTRY COMPETITIVENESS BY USING THE LATEST SYNCHROTRON LIGHT TECHNIQUE DEVELOPMENTS. THIS CONTRIBUTION RANGES FROM UTILIZING THE LIGHT BEAMTIME UP TO JOINT EQUIPMENT DEVELOPMENTS.



Industrial users have profited from beamtime from the very beginning of the operation thanks to the ALBA performance techniques, to the increasing relevance of the R&D and innovation activities within the industrial companies and to the extensive outreach activities performed in previous years.

The initially small number of private users is steadily increasing. They are both national and multinational companies covering a variety of sectors such as pharmaceutical, adhesives, semiconductors, pigments, etc... In the case of the pharmaceutical area, the polymorphs of Active Pharmaceutical Ingredients share the same chemical composition but may show different physiochemical properties affecting to its bioavailability. The characterization of such polymorphs using synchrotron light techniques is especially relevant. In the material science research area, some industrial customers were interested in the development of innovative adhesives with better or new properties while others were interested in

the characterization of semiconductor samples to better understand and improve their functionality.

These studies were mainly carried out using techniques such as powder diffraction, absorption and emission spectroscopies or photoemission electron microscopy at the MSPD, CLAESS or CIRCE beamlines respectively. In Figure 23, two simple pie chart cakes of the beamlines and the research sectors distribution of the industrial experiments performed during 2013 are shown.

Although ALBA is a very young facility strong industrial relationships have been already established. In some cases it involves collaboration agreements which include scientific personnel financed by the companies. That long term relationships are a big step forward for ALBA and for the companies.

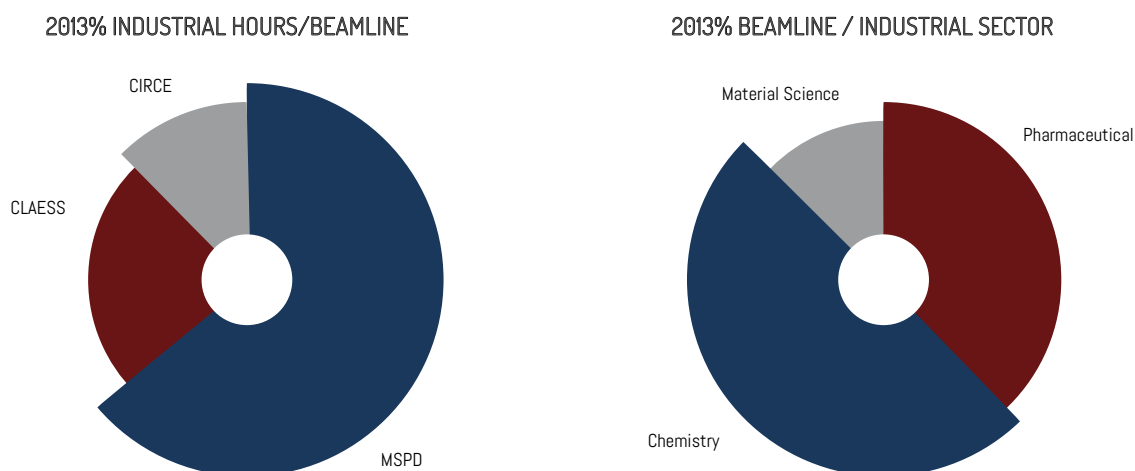
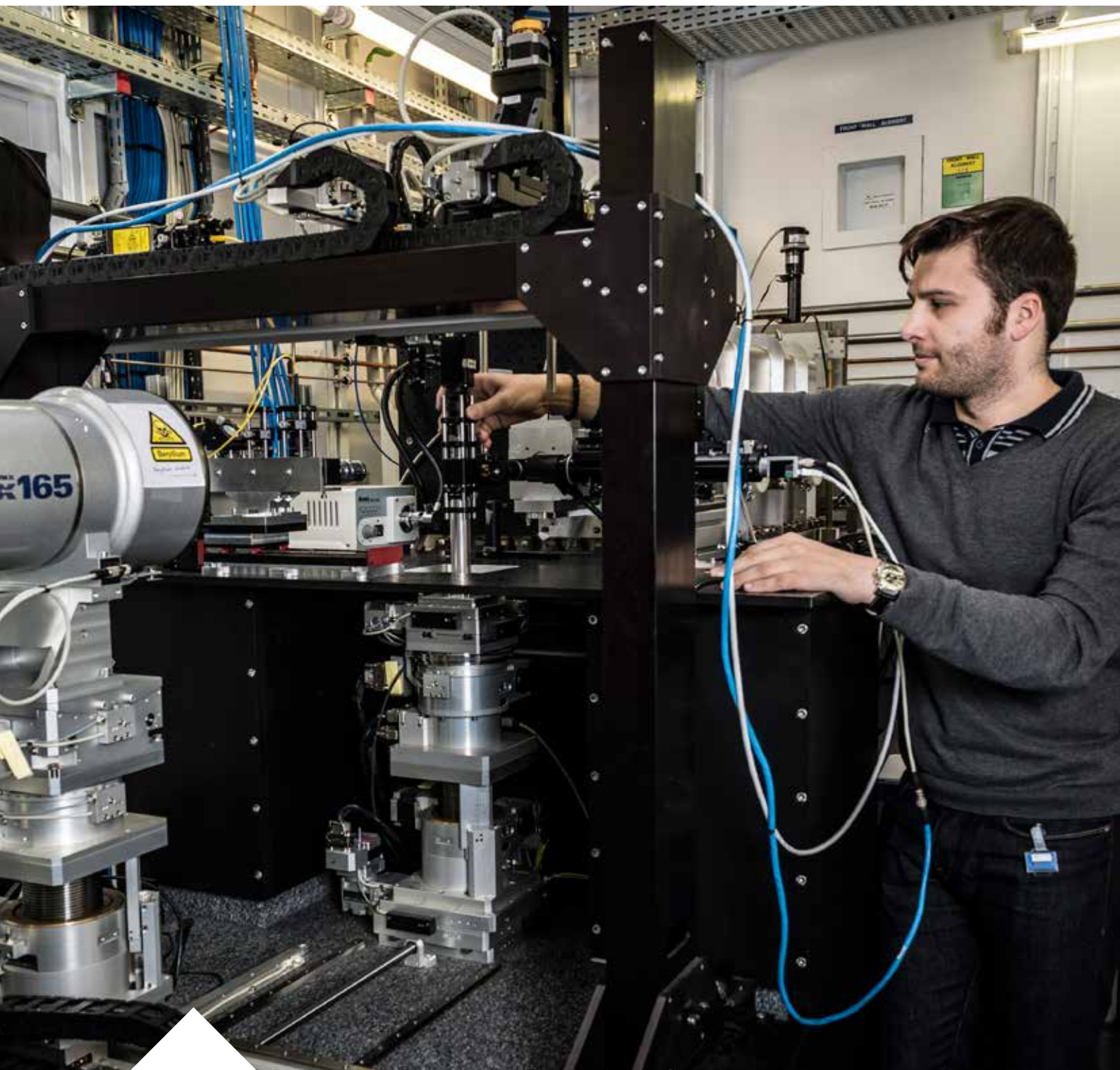


Fig. 23 Pie chart cakes of the beamlines used (left) and the industrial sectors (right) involved in the industrial experiments.

# ACTIVITY REPORTS BY DIVISION

## EXPERIMENTS

IN 2013 THE EXPERIMENTS DIVISION HAS DEVELOPED NEW INSTRUMENTATION TO FULFILL TECHNICAL REQUIREMENTS OF THE BEAMLINES. HERE WE PRESENT A SUMMARY OF SELECTED RELEVANT DEVELOPMENTS.



## INLINE PRESSURE CALIBRATION SETUP

CATALIN POPESCU AND IGORS SICS

A new setup for high pressure calibration inside the diamond anvil cell (DAC) using ruby fluorescence method has been developed in-house. In contrast to commercially available devices using a flipping mirror to switch between the visualization mode and fluorescence measurement mode (resulting in non-simultaneous operation), ALBA design employs a set of dichroic filters and a beamsplitter that separates beampaths of the coaxial illumination, visible image, laser light and ruby fluorescence emission. This enables simultaneous fluorescence spectra measurement with a continuous in-situ sample visualization, although at the expense of deteriorating color information in the visible image.

Visual observation module of this system consists of a CCD camera and a coaxial LED based illuminator, which combine their optical paths via beamsplitter. Magnified sample area is visualized on a PC monitor allowing to point a laser beam at a selected specific area of the sample under the scrutiny.

A high power laser generates a beam in the blue visible region (445 nm) that is coupled into the system via fiber optic of 50  $\mu\text{m}$  diameter using a very short focal length lens. Collected beam is reflected by a first dichroic mirror, with a cutoff at 470 nm, into a Motic microscope 20X objective which focuses beam onto the ruby sample inside the DAC. Laser beam spot has a diameter of around 20  $\mu\text{m}$  after focusing, which is highly suited for the tiny ruby chips (10-30  $\mu\text{m}$ ). Ruby fluorescence is collected in the backscattering geometry by the same objective. It passes through the first dichroic mirror in transmission mode and is subsequently reflected by a second dichroic mirror, with a cutoff at 690 nm. Light is focused onto a fiber coupler by a lens and is transmitted to the spectrometer module via fiber optic. Fluorescence

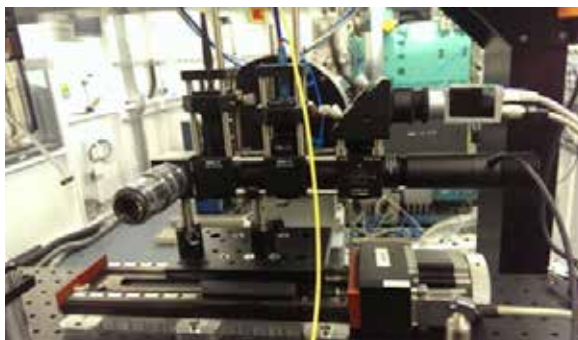


Fig. 24: The inline pressure calibration system using the ruby fluorescence method.

peak wavelength from the spectrometer reading is directly related to the pressure that ruby sample is exposed to. C. Popescu, I. Sics, et al., communication in preparation.

## CHARACTERIZATION, OPTIMIZATION, AND SURFACE PHYSICS ASPECTS OF IN-SITU PLASMA MIRROR CLEANING

ERIC PELLEGRIN

Although the graphitic carbon contamination of synchrotron beamline optics has been an obvious problem since several decades, the basic mechanisms underlying the contamination process as well as the cleaning/remediation strategies are not understood and the corresponding cleaning procedures are still under development. In this study, we report on an analysis of remediation strategies all based on in-situ low-pressure RF plasma cleaning approaches, including a quantitative determination of the optimum process parameters as well as their influence on the chemistry as well as the morphology of optical test surfaces. It appears that optimum results are obtained for a specific pressure range as well as for specific combinations of the plasma feedstock gases, the latter depending on the chemical aspects of the optical surfaces to be cleaned.

The basic approaches presently known regarding synchrotron optics cleaning procedures include ex-situ as well as in-situ setups, all of them using either oxygen radicals, hydrogen radicals, or ozone as chemically active cleaning agents. Among the ex-situ setups, UV lamps are used as ozone generators and efforts are now being made to integrate these lamps inside the vacuum chambers in order to avoid mirror extraction and subsequent bakeout. From an ozone generation efficiency point of view, these processes must be performed at oxygen partial pressures of about 100 mbar or higher, which classifies this method among the high-pressure approaches balancing ozone production efficiency against mean free path lengths.

For the low-pressure (i.e., less than 0.1 Torr or 0.133 mbar) in-situ setups, most applications so far have been using various types of plasma sources which exist in a wide variety as well as commercial components. Nevertheless, a basic distinction can still be made for the basic types such (i) DC discharge and (ii) RF plasma sources, where the latter includes both capacitive as well as inductively coupled plasma sources (i.e., CCP and ICP sources). From an application point of view, the above diversity

has led to a considerable amount of different approaches within the synchrotron and the Extreme Ultraviolet (EUV) lithography communities during the last decades, which are difficult to be compared due to the above multitude of inherent degrees of freedom. Last but not least, the complexity of plasma physics and the associated diagnostics have so far resulted into a poor plasma process control and, consequently, to a poor understanding of the physics and surface chemistry involved in the cleaning process. Some very peculiar “voodoo” approaches that are currently being used in practical synchrotron life are basically a result from this somewhat deplorable situation.

The present study is an attempt to gain some better insight into the RF plasma cleaning process and thus to obtain a better control on the process parameters in view of safer and more efficient cleaning processes. This does also allow for including other reflective coatings than gold - especially in the case of UV/VUV/XUV beamlines with a high sensitivity with respect to carbon contaminations - in view of keeping the flexibility required during the beamline design phase for achieving an optimum beamline performance.

In Fig. 25, we show a typical result from a test mirror consisting of an optically polished single-crystalline Si substrate and a gold reflective coating. The photograph on the left hand side shows the mirror after applying an intentional contamination with amorphous carbon via a sputtering process, whereas the photograph on the right hand side shows the same mirror after cleaning in an oxygen/argon plasma for about two hours with a carbon cleaning rate of about 3 Å/minute. After such an optimized cleaning process, the carbon contamination is fully removed down to the sub-monolayer level while the morphology (micro-roughness) and chemistry (chemical purity) of the optical surface are back to the pristine state of the mirror.

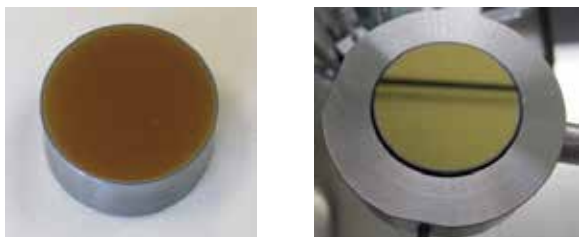


Fig. 25: Results from an oxygen/argon plasma test cleaning: The photographs on the left and right hand sides show the carbon-contaminated Si/Au test mirrors before and after the cleaning process, respectively.

*J. Synchrotron Rad.* (2014) 21, 300–314

E. Pellegrin<sup>1</sup>, I. Šics<sup>1</sup>, J. Reyez-Herrera<sup>1</sup>, C. Perez-Sempere<sup>1</sup>, J. J. Lopez Alcolea<sup>1</sup>, M. Langlois<sup>1</sup>, J. Fernandez Rodriguez<sup>1</sup>, and V. Carlino<sup>2</sup>

1. CELLS-ALBA, Carretera BP 1413, km 3.3, E-08290 Cerdanyola del Vallès, Spain.  
2. Ibss Group Inc., 1559B Sloat Blvd., Suite 270, San Francisco, CA 94132, USA.

## NANOMETER ACCURACY MIRROR CORRECTION USING A MINIMUM SET OF SPRING ACTUATORS

JOSEP NICOLAS

X-ray mirrors can be corrected to nanometer accuracy by introducing a controlled deformation of the mirror substrate. The deformation is introduced by springs for which the position and compression is derived from the initial figure error by means of an elastic deformation model.

The Optics laboratory has developed a technique to improve the figure error of X-ray mirrors by introducing a deformation of the mirror substrate that compensate the polishing error. The deformation of the mirror is controlled by a reduced set of spring actuators, whose position and strength is derived from the initially measured figure error of the mirror. For reaching sub-nanometer accuracy, the technique requires three main elements: precise metrology, for determining the figure errors that have to be compensated, an accurate model of the mirror deformations as a function of the introduced forces, and a set of spring correctors capable of introducing the required forces with enough resolution and stability. The required metrology is provided by the Alba-NOM, an instrument capable of providing accurate measurements of the figure error of optical surfaces for a wide range of radii of curvature, and for optics up to 1.5 m long. The optimization of the instrument allows obtaining measurements with uncertainties better than one nanometer [1]. The Optics lab also has the algorithms to optimize the position and force required for the correction.

This technique has been successfully used for optimising the refocusing optics of the macromolecular crystallography beamline at ALBA (BL13-XALOC). It consists in a pair of elliptically bent mirrors, in Kirkpatrick-Baez configuration, with optical lengths of 300 mm and 600 mm, respectively. Their slope errors have been reduced from 240 nrad to 55 nrad, and from 210 nrad to 80 nrad, respectively [2]. The agreement between the optimized profile and the predicted by the deformation model was better than 1 nm. In-situ measurements, using the pencil beam method confirm that the figure error is preserved after installation and commissioning, and after more than two years of operation, including many bending and unbending cycles.

ALBA is currently developing a high accuracy mirror bender, equipped with spring correctors capable of reducing the residual figure error of the surfaces below one nanometer, and providing selectable focusing position by means of a high accuracy motorized bending mechanism. The proposed

system is conceived to be scalable in length, being the first prototype one meter long; and to operate in vertical or horizontal deflection. The minimum distance between actuators is 22 mm. and the force resolution is in the order of 0.01 N, at any longitudinal position of the mirror. The first prototype is currently being characterized at the optics laboratory, and we foresee to have a completely corrected mirror by the end of 2014.

#### REFERENCES

- [1] Nicolas, J; Martínez, J C; Characterization of the error budget of the Alba-NOM, Nucl. Instr. Meth. Phys. Res. A, Volume 710, p. 24-30 (2013)
- [2] Nicolas, J; Ruget, C; Juanhuix, J; Benach, J; Ferrer, S; Focusing and defocusing using mechanically corrected mirrors at the MX beamline at Alba, J. Phys. Conf. Ser., 425, p.52016 (2013)

## INTEGRATING UHV AND HIGH-TEMPERATURE SUPERCONDUCTING MAGNETS FOR X-RAY SYNCHROTRON BASED EXPERIMENTS

MANUEL VALVIDARES

A X-ray resonant magnetic scattering experiment typically monitors the X-ray intensity reflected or dispersed by the specimen under investigation after reflection -or sometimes transmission- of the incoming x-ray beam. Measurements usually analyze the dependence of such intensity as either a function of the angle of reflection for a fixed photon energy, or either as a function of the x-ray photon energy at a fixed angle of reflection (or scattering). In such measurements, the challenge is to achieve the largest possible magnetic field while maintaining large optical access to the sample to allow extended angle reflectivity measurements, for example. So far a compromise between field intensity and angular acceptance has to be reached. Our pioneering instrument development has opened a new direction by integrating inside a UHV a superconducting magnet. Such magnet has to be light enough to be rotated synchronously with the sample with high precision, should allow a very large optical access, and be compatible with chamber dimensions and space required for detectors. All these requirements have been achieved by the conceived HTS magnet at the limit of the technical feasibility, whose challenging detailed design and manufacturing has been successfully accomplished by a team made by the world leading company on HTS magnets,

HTS-110 Ltd based in Wellington, New Zealand together with staff researchers at ICMAB-CSIC and ALBA. The magnet operation has been demonstrated satisfactory and it is waiting some in-house designed heavy load mechanical tools required for its integration and positioning on the scattering chamber of BL29. Final assembly and tests are foreseen for end of 2014, with aims that the system will get ready for user operation on the 2nd half of 2015. Further details are given in Figure 26.

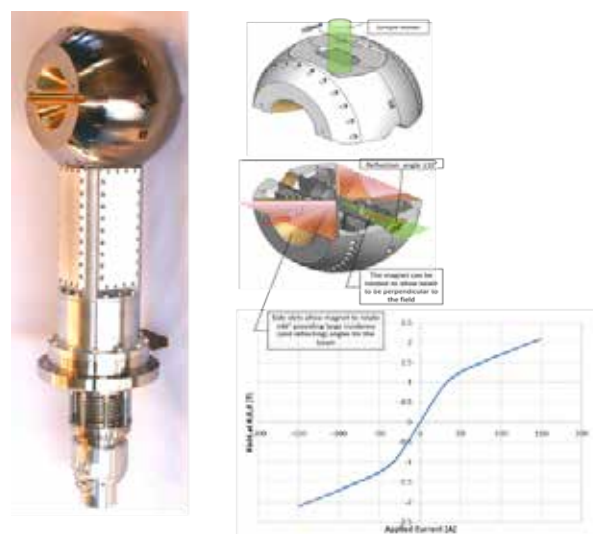


Fig. 26. Left: photo of the UHV HTS magnet; Top-right) Exploded CAD sectional view of the magnet indicating its large optical access for x-ray scattering measurements, and the upper slot for sample manipulator; bottom-right) magnetic field performance measured in the acceptance tests with a Hall probe, achieving a 2 Tesla magnetic field for an applied current of 150 Amps in the HTS coil pack.

*Journal of Physics: Conference Series* 425 (2013) 102003, 11th International Conference on Synchrotron Radiation Instrumentation (SRI 2012). IOP Publishing  
S M Valvidares, S. Ferrer, E Pellegrin, ALBA Synchrotron Light Facility. Cerdanyola del Valles.  
X. Granados, X Obradors, ICMAB-CSIC. Bellaterra.  
Z Lazić, V Chamritski, D Pooke, HTS-110 Ltd, Lower Hutt, New Zealand

#### ACKNOWLEDGMENTS

We acknowledge funding of this equipment via the Program "Diseño, viabilidad, acceso y mejora de Instalaciones Científicas y Técnicas Singulares" del Ministerio de Ciencia e Innovación, ICTS-2009-02.

Additional technical, administrative and management support: C. Colldelram, C. Ruget, J.F. Moreno, L. Nikitina, R. Martín, A. Crisol, S. Forcat, F.Farre, Y. Nikitin, X. Serra, X. Fariña, T. Camps, O. Matilla, J. Ferrer, F. Trujillo, M. Rodríguez, L. Campos, C. Reyero, M. Sazatornil, G. García.

# ON-AXIS SAMPLE IMAGING SYSTEM (OASIS)

IGORS ŠICS

X-ray experiments involving inhomogeneous samples in the size range of micrometers require instrumentation allowing selection and visualization of sample area under scrutiny. It is of a great advantage if the visual monitoring can be performed simultaneously with the x-ray experiment. Such instrument, essentially being a microscope, has to be integrated into the x-ray experiment setup.

An imaging setup was designed (see Figure 27) for this purpose using components of a commercially available NAVITAR 6000 UltraZoom system and Basler acA1300-30gc color CCD camera. It has been destined for use at CLAES and MSPD beamlines.

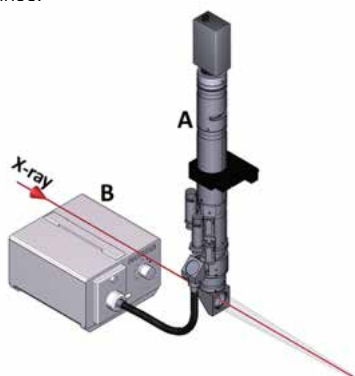


Fig. 27: 3D model of the OASIS system. Image shows configuration employing a coaxial illumination: (A) modified NAVITAR lens; (B) halogen light source with fiber-optic light guide.

System employs a 45° tilted mirror with a Ø1.5mm opening machined in its center. Mirror deflects the image of the sample into the lens while x-ray beam passes through the hole in the mirror. Such configuration allows observing sample from the perspective of the incident x-ray beam (“on-axis”), thus avoiding parallax errors and distortions present in other “non on-axis” arrangements.

Zoom and focusing adjustments of the lens are motorized allowing for a remote control of these parameters during an x-ray experiment.

Table 2. Optical parameters of the assembled system

	Low magnification	High magnification
Magnification (M)	0.71X	4.5X
Numerical aperture (NA)	0.023	0.071
Max resolution	14.5µm	4.7µm
Field of view (FOV)	6.75 x 5.06mm	1.065 x 0.89mm
Working distance (WD)	47mm	47mm

Either a coaxial or an oblique illumination mode can be set up (oblique – using semi-rigid fiber-optic light guides or coaxial – using built-in beamsplitter), depending on the experimental requirements and sample surface specifics.

OASIS is mounted on a motorized linear stage based XYZ positioning system for a remote position adjustment.

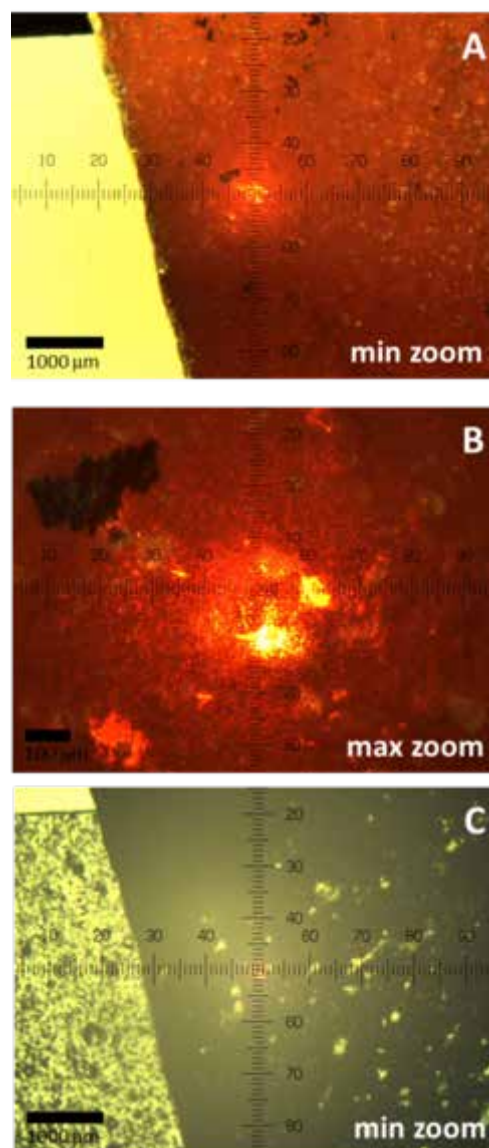


Fig. 28: Images of OASIS commissioning with a fragment of ceramic pottery as a sample: (A) lens at minimum magnification setting, (B) lens at maximum magnification. (C) lens at minimum magnification with coaxial illumination of the sample. Red spot in images laser simulating an x-ray beam passing through the hole in the 45° mirror.

# ACTIVITY REPORTS BY DIVISION

## ACCELERATORS

THE ACCELERATOR DIVISION OPERATES THE ALBA ACCELERATORS ON A DAILY BASIS AND IT ALSO DESIGNS AND IMPLEMENTS ITS IMPROVEMENTS AND UPGRADES. ALBA HAS THREE ELECTRON ACCELERATORS ALL REQUIRED TO PROVIDE A PHOTON BEAM TO THE USERS. THE LINAC, IS A LINEAR ACCELERATOR IN WHICH ELECTRONS ARE GENERATED AND ACCELERATED UP TO 100 MeV. THESE ELECTRONS ARE THEN INJECTED INTO THE BOOSTER WHERE THEY ARE FURTHER ACCELERATED TO 3.0 GeV AND FINALLY TRANSFERRED TO THE STORAGE RING, WHERE THEY EMIT SYNCHROTRON RADIATION. IN THE FOLLOWING PAGES A SUMMARY OF THE MAIN ACTIVITIES PERFORMED THIS YEAR BY THE ACCELERATOR DIVISION IS PROVIDED.



## OVERVIEW

During 2013 the CELLS accelerators have operated 2972 h for the beamlines and about 1200 h for machine development and further improvements. Table 3 shows the main parameters of the storage ring, followed by a table with the beam sizes and beam divergences at the source points (see Table 4).

Energy	3 GeV
Circumference	268.8 m
Operating current	125 mA
Emittance	4.6 nm-rad
Coupling	0.5%

Table 3: Main storage ring characteristics.

		$\sigma_x$ [um]	$\sigma_y$ [um]	$\sigma'_x$ [um]	$\sigma'_y$ [um]
BL09	MISTRAL	49.3	27.8	109.0	1.2
BL04	MSPD	130.0	4.9	474	4.7
BL11	NCD	129.7	4.6	46.9	4.0
BL13	XALOC	130.0	4.5	47.5	3.8
BL22	CLAESS	130.2	54	47.5	4.6
BL24	CIRCE	130.0	6.0	474	4.5
BL29	BOREAS	130.0	4.8	474	4.1

Table 4: Beam sizes and divergences at the source points. Values are given at the centre of the straights for the ID BLs and at the center of the bending magnet for BL09.

## 2013 ACCELERATOR OPERATION

2013 can be considered the first fully operational year of the facility. Initially there had been 3540 hours of operation scheduled for the beamlines. A major interruption of the original calendar was necessary to overcome a failure of the general cooling system, which forced a shutdown of almost three months. After a major re-schedule the operating hours for the beamlines were lowered to 3069 h, of which 2972 were delivered. With respect to the initial schedule beam availability was 83.8% and disregarding the problem of the cooling MTBF was 25 h and the mean time to have the beam back was 0.8 h.

The storage ring has run typically with a current of 120 mA in decay mode with 2 injections per day separated by 12 h. The filling pattern used at ALBA is composed of 10 trains of 32 consecutive bunches, with a gap in between of 24 ns. Figure 29 shows a typical image of the beam filling pattern.



Figure 29: FCT image of the beam filling pattern at the SR.

## FAST ORBIT FEEDBACK SYSTEM

In today's storage ring light sources the photon beam should be stabilized in position and angle to less than 10% of the beam size and beam divergence. This is achieved at ALBA with the slow orbit feedback system which corrects the orbit at a repetition rate of 0.3 Hz. In order to stabilize the beam at higher frequencies, up to 100 Hz, ALBA is developing a fast orbit feedback system (FOFB) which should be ready for 2014.

The FOFB system uses 88 beam position monitors and 88 horizontal and vertical correctors. Correction is distributed on 16 nodes, one per machine sector. Each node includes a sniffer board for BPMs data reception, a processing CPU for correction calculation and the corrector power supplies controllers. The FOFB is already running during machine development time and current activities are dedicated to develop a user's friendly interface and to provide a robust system for operation.

## IMPROVEMENTS ON THE RELIABILITY OF THE RF SYSTEM

The Radio Frequency (RF) system of the ALBA storage ring consists of 6 HOM damped cavities fed by 12 80 kW Inductive Output Tubes (IOTs). In the past the RF system has suffered many interruptions due to water interlocks. During 2013 a delay relay of 0.5 s. has been installed in the RF plants and a dramatic decrease on the number of water interlocks has been observed.

## TOP-UP INJECTION

ALBA has been designed for top-up injection. One of the benefits of top-up operation is the improved beam stability at the beamlines due to the electron beam current in the storage ring being constant at the level of a few per mil.

In 2012 safety simulations were already done and proved that injection onto the ALBA storage ring with the front ends open is safe. During 2013 the injection system for the control system has been modified and the beamlines have already tested the new injection mode. It is expected that the ALBA will enter in top-up during 2014 (see Figure 30). A view of the inner part of the tunnel is given in Figure 31.

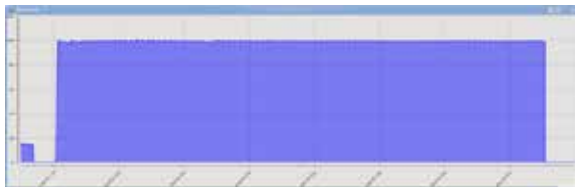


Fig. 30: SR current during a 8 h top-up test

## COUPLING REDUCTION

During the design phase of ALBA it was proposed and later implemented a global coupling correction scheme based on 2 families of skew quadrupoles: one on each transversal plane. Soon it was realised that this scheme will not be sufficient and in 2013 a campaign to equip the 32 skew quadrupoles with individual power supplies was launched and completed. With the new local correction scheme it has been shown that

the storage ring coupling can be decreased to 0.1%, from the typical value of 0.6% which is used during routine operation.

A lower coupling, which means that tilt errors on the machine are corrected with a combination of skew quadrupoles, results in a reduction of the vertical beam size and consequently on a lower vertical emittance. Figure 32 show the beam sizes with two different couplings.

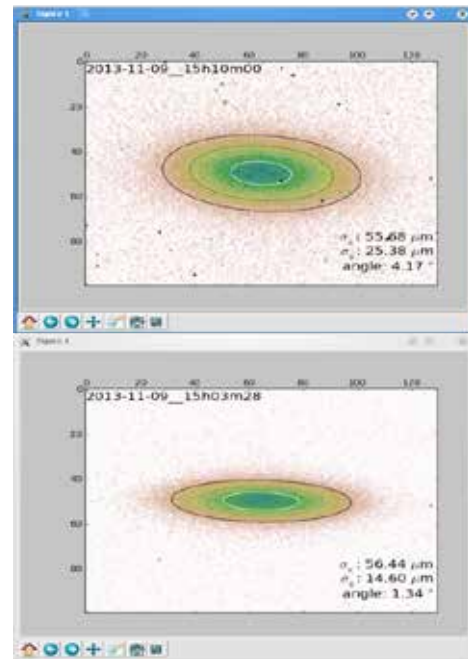


Figure 32 (top) typical beam size when running with a coupling of 0.5 %. The image below corresponds to a reduced coupling of 0.1 %. Note the reduction in the vertical beam size from 25.4 micrometers down to 14.60 micrometers.



Fig. 31: Interior of ALBA's tunnel: booster (on the left) and storage ring (on the right).

## IDS CORRECTION

The two wigglers installed at ALBA have required extra correction of the orbit distortion produced when opening/closing the gap. The ID group has monitored the correction required, and has built, installed and commissioned the additional coils needed. At this moment distortion in the orbit when opening/closing the gap of the wigglers at ALBA is kept below 30  $\mu\text{m}$ .

## SR EMITTANCE MEASUREMENTS USING AN X-RAY PINHOLE

The Storage Ring emittance is inferred after transverse beam size measurements, which are carried out using an x-ray pinhole camera. As such, it produces an image of the electron beam with a magnification factor (in this case, 2.24) given by the system design. This is done using the x-rays produced when the electron beam traverses a dipole using the experimental set-up located in FE34 and described in Fig. 33.

The x-rays go through an Aluminum window of 1mm thickness that separates the vacuum from the atmospheric pressure. Once in-air, the x-rays hit a Copper filter, whose thickness can be varied between 0 and 5mm to harden and attenuate the x-rays as desired (usually, we chose to work with x-rays of 45keV to decrease the diffraction effect). The Tungsten pinhole is a square aperture of  $10 \times 10 \mu\text{m}$  located at about 6 m from the source point. Finally, more than 13 m away, the x-rays impinge into a YAG:Ce screen, which is a scintillator material that converts the hard x-rays into visible light photons. The image produced in the screen is captured by a CCD camera, analyse to consider optical effects, and then a 2-d Gaussian fit to precisely infer the transverse beam sizes is performed.

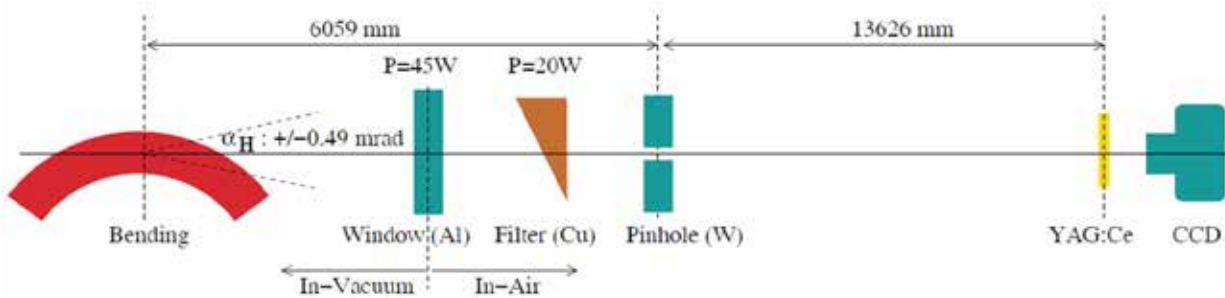


Figure 33. Sketch of the FE34, the ALBA pinhole, with the location of its main components (distances are not to scale). The magnification is given by the ratio source-to-pinhole distance (6.06 m) vs pinhole-screen distance (13.63 m).

From the beam size measurements and the Twiss parameters obtained from the ALBA lattice model, we can calculate the horizontal and vertical emittance, as well as the local machine coupling. Figure 34 shows an example of this calculation, which provides emittances of  $(\epsilon_x, \epsilon_y) = (4.67, 0.020) \text{ nm} \cdot \text{rad}$ , in very good agreement with the theoretical results of  $\epsilon_x = 4.6 \text{ nm} \cdot \text{rad}$  and a global coupling of 0.5%. The pinhole is continuously working during ALBA operation to monitor the beam emittance online.

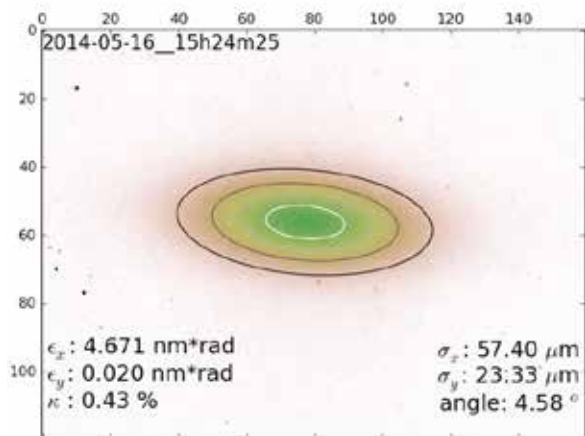


Figure 34. Example of the pinhole image, with the calculation of beam sizes and corresponding emittances. The horizontal and vertical axis are shown in pixels.

# ACTIVITY REPORTS BY DIVISION

## COMPUTING AND CONTROLS

THE COMPUTING AND CONTROLS DIVISION DEVELOPS AND OPERATES A BROAD PORTFOLIO OF SERVICES THAT RANGE FROM CABLING AND ELECTRONIC EQUIPMENT, CONTROL SYSTEMS FOR THE ACCELERATORS AND THE BEAMLINES, TO IT INFRASTRUCTURES, IT SERVICES AND INFORMATION SYSTEMS, ACTIVELY PARTICIPATING IN EUROPEAN SYNCHROTRONS COLLABORATIONS TO DEVELOP NEW SOLUTIONS.



## SARDANA AND TANGO, A MAJOR CONTRIBUTION OF ALBA

The division manages projects and services following PRINCE2 methodologies and ITIL best practices, by means of web applications. These management tools enable executive documents such as bellow graphics, which summarize the efforts of the whole year. Since 2013, we have been successfully combining PRINCE2 project management methodology with SCRUM iterative and incremental agile software development framework for software projects. While both emphasize the importance of customer involvement, one focuses on the customer benefits, business justification and project control, whereas the other offers an agile and systematic approach to the daily tasks, through constant re-prioritizations and frequent releases. Test Driven development and continuous integration also enhance the reliability and performance of our software products.

ALBA is one of the core developers of Tango, one of the major contributors, and member of the collaboration since late 2004. Since then, the synchrotron, accelerators and beamlines have been built and commissioned and are now in operation. It is now a major installation using Tango as a software bus in all accelerators, beamlines and laboratories. In addition, the Sardana SCADA, including the macro execution environment, standard step scans, and graphical interfaces, has been successfully commissioned in all beamlines and accelerators. Sardana is now an international collaboration having DESY in Germany, MAXIV in Sweden and Solaris in Poland as main partners. Parts of Sardana, such as Taurus, have also become very popular and a standard in the Tango collaboration.

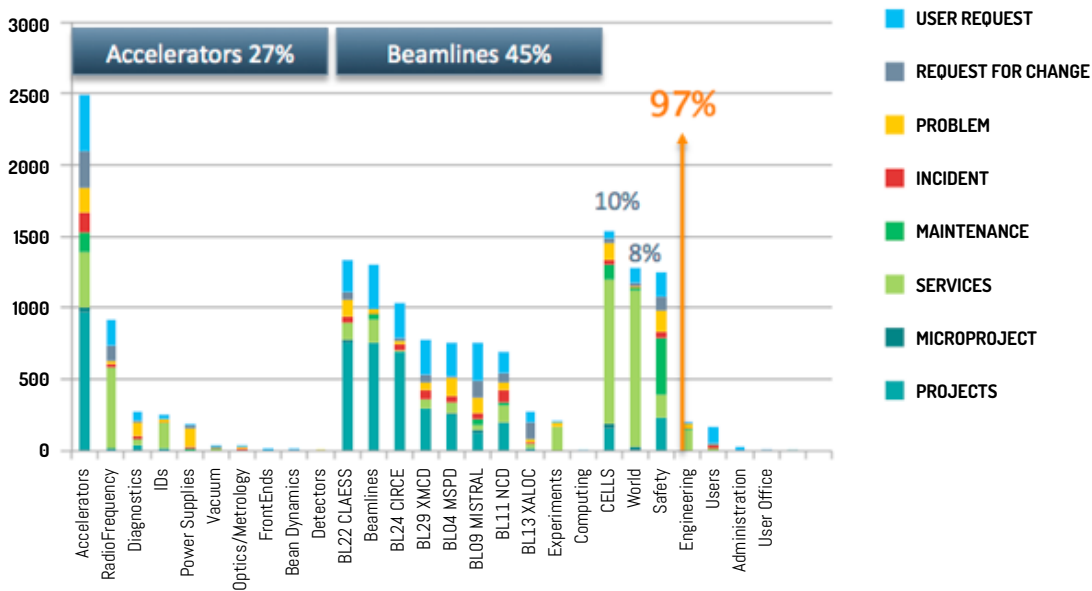


Figure 35: 2013 distribution of the Computing and Controls manpower in hours per (internal) customer

## TOP UP IN FINAL STAGE AND FAST ORBIT FEEDBACK IN COMMISSIONING

In 2013, we have implemented the first version of the Fast Orbit FeedBack (FOFB) based on standard quadruple core processors installed in sixteen of the existing compact PCI computers devoted to the control system of the accelerators. This reaches a sample frequency of 5 kHz. This system, together with TOP-UP, was in commissioning in 2013 and is to be in operation along 2014. The procurement process for the next generation of Fast Orbit Feedback at 10 kHz involving Field Programmable Arrays (FPGAs) has also concluded in 2013. In the context of TOP-UP, the Control system of the Linac has been extended from the standalone Labview application to the fully integrated Tango control with Taurus graphical Interfaces, see Figure 36. The Personnel Safety System (PSS) has been modified (with the consequent certification) to include the new safety conditions for TOP-UP.



Figure 36: The Taurus Graphical User Interface for TOP-UP

## ALBA UNDERTAKES CONTINUOUS SCANS FOR BEAMLINES

ALBA is moving to continuous scans. Today, most of the experiments benefit from this technique in half of our beamlines, and we are working on the software tools in Sardana and hardware interfaces and developments to make it the standard data acquisition technique, which is indeed suitable for most experiments in most beamlines. In a continuous scan, also called fly scan or quick scan,

the data acquisition takes place during the motion of one or several motors at synchronized intervals. The synchronization can happen at equidistant time intervals, naturally assuming a constant speed in all movable axes, or at arbitrary defined positions of the master axes. In BL29 as an example, the continuous scans reduced the typical time for a scan from 30 minutes to 5 minutes, resulting in better data sets and new possibilities unmanageable with slower step scans. These acquisition times are being reduced further while the framework is made more generic.

## ELECTRONICS DESIGNS: THE ALBA ELECTROMETER

The ALBA Electrometer (ALBA Em) is in use since the beginning of the operation. All beamlines have several units, used for both diagnostics and data acquisition. The project has been very successful with units in operations in other synchrotrons. In 2013, the project entered in a new phase with a complete new design and far more functionalities, capabilities and higher performance. The project, now named ALBA Em#, has been conceived to match the data acquisition requirements, synchronization, timestamps, and buffering to be integrated in the generic continuous scans of a beamline.

This new phase involves a new version of current amplifier design, which has already shown as good results as the high-end amplifiers in the market. In addition, it covers a complete redesign of the digital acquisition part that will increase the accuracy and speed of the analog to digital converters and will enable new digital processing capabilities based in FPGA technology. The ALBA Em# will be able to handle data acquisition and synchronization at higher speed and accuracy, increasing its synchronization capabilities and integration with the Control System. One of the most interesting objectives is being able to implement high bandwidth closed loop systems for the stability of the beam in the kHz range.

## CUSTOM PROTOTYPES

While some developments are used in all beamlines and accelerators and are suitable for many applications, not only in synchrotrons, some experiments need "ad hoc" developments. One example is an experiment at BL09

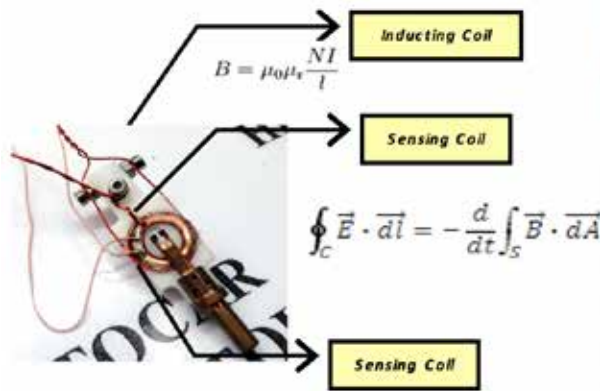


Figure 37: Picture of the coil on the left and the installation in the microscope on the right.

(S. Ferrer et al.) that consists in measuring the effect of high magnetic pulses on the microscopic structure of the domains. The challenge is to get a magnetic field of about 2 Tesla in a microscope in vacuum with a maximum diameter of the coil of 1 cm. Due to heating conditions, the solution required short pulses of high currents, with the complexity of managing eddy currents and measuring the resulting field. The project resulted in a prototype, see Figure 37, which achieves customizable pulses that are synchronized with the control system, and reaches peak currents of 1500 Amperes, with fields of 1.3 Tesla and 100  $\mu$ s pulse lengths.

## A NEW DEVELOPMENT IN DETECTORS FOR DIAGNOSTICS

In 2013 we have carried out a collaboration with the Instituto de Microelectrónica de Barcelona (IMB-CNM-CSIC) to design, manufacture and characterize 10 $\mu$ m thickness photodiodes conceived as diagnostics devices in transmission. The first requirement came from BL13 where the first proof of concept was carried out. The transmissivity of these devices will improve 90% in energy ranges of 10 keV, see Figure 38. The characterization, mechanization and operation of such thin devices engage a number of challenging technical issues. In addition to the development carried out in 2013, a funded program under the EDI program of FCRI (Fundació Catalana de Recerca, Generalitat de Catalunya) is today in progress to promote the commercialization of these devices.

## INFORMATION TECHNOLOGIES AND MANAGEMENT INFORMATION SYSTEMS

On the Information Technologies and Management Information Systems, the efforts go also to the support of the beamlines

and accelerators as well as users and central services. Ethernet is both the field bus used in accelerators and beamlines as the main interconnection to internet and intranet. We have about 3500 wire connections and a wireless infrastructure covering the whole facility. Virtualization is also one of the key priorities in the central services. Most controls and central servers such as web, Tango hosts, or network services run on virtual machines. In 2013, the data center has incorporated 15 new servers from Fujitsu, adding extra capabilities in high performance computing, and client (Virtual Desktop) and server virtual hosting. We made special effort to provide high availability to the most critical systems. The whole CAD system was migrated to Teamcenter/NX, reinstalling all clients and acquiring and replacing most CAD workstations.

ALBA User Office Portal is in production since 2011. Yet, in 2013, we delivered new customized workflows for the scientific, technical and safety evaluation, as well as new utilities such as an on-line safety training, site access management, experimental reports or publication records. The balance between requirements from users, scientist, safety officers and reviewers, and requirements from external entities such as PANData and ICAT, although complex, is also prioritized.

More information on ALBA Computing website: <http://computing.cells.es/>

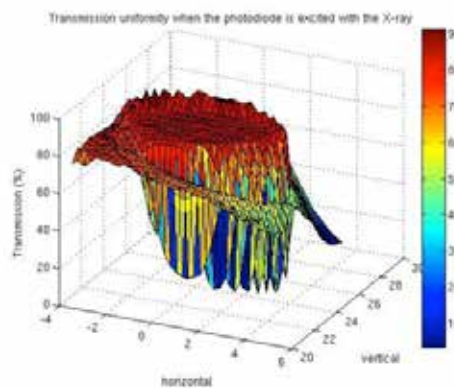
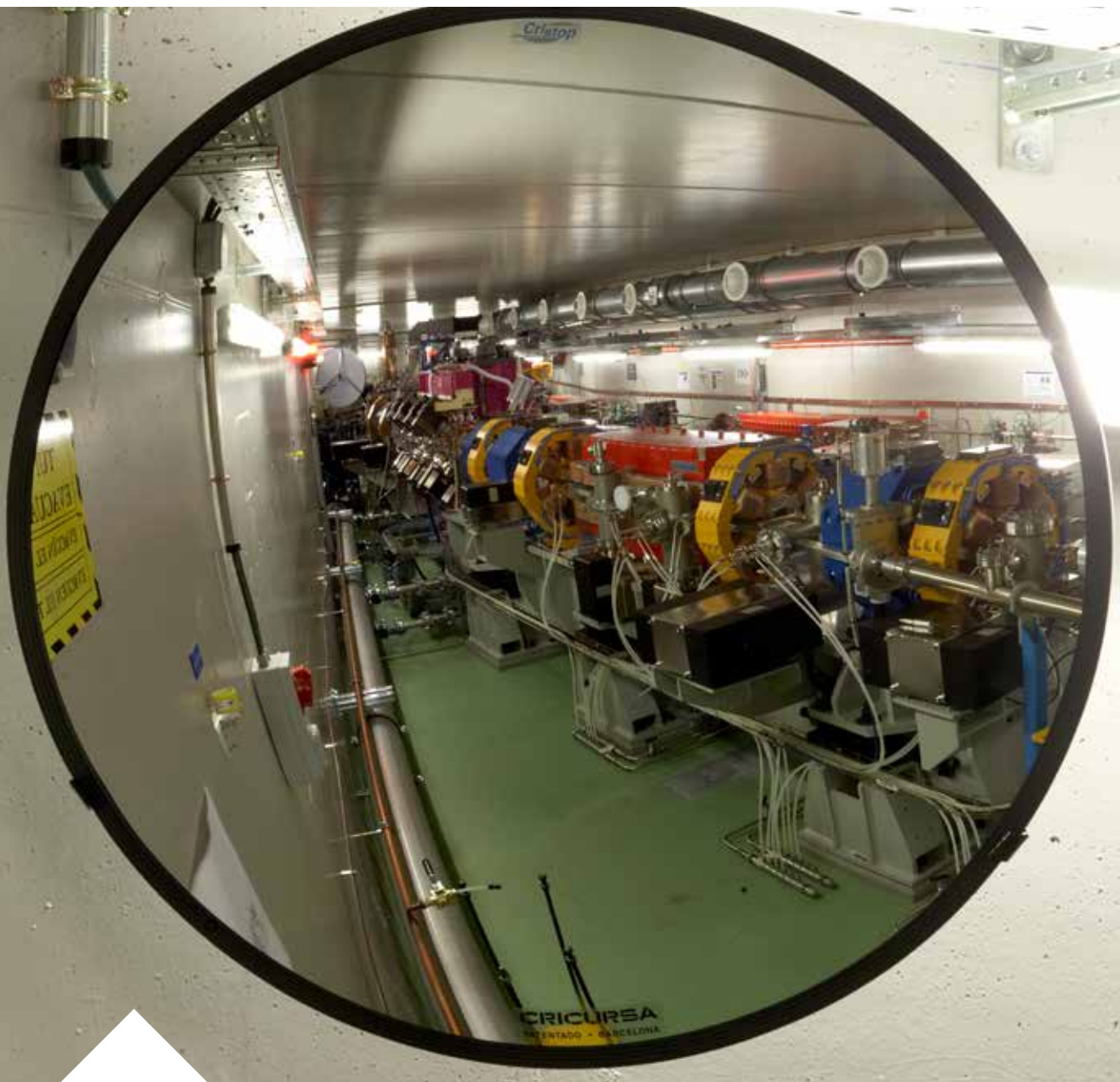


Figure 38: 3D view of the characterization of the transmission of the diodes

# ACTIVITY REPORTS BY DIVISION

## ENGINEERING

THE ENGINEERING DIVISION IS FORMED BY A TEAM OF 32 MULTIDISCIPLINARY ENGINEERS AND TECHNICIANS THAT GIVE SUPPORT TO THE OTHER DIVISIONS AND THE FACILITY ITSELF. WE ARE ORGANIZED IN TWO SECTIONS: THE INFRASTRUCTURES SECTION (IS) - DEVOTED TO NEW CIVIL ENGINEERING PROJECTS AND MAINTENANCE - AND THE TRANSVERSAL SECTION (TS) - COMPOSED BY SURVEY & ALIGNMENT ENGINEERS, VACUUM, CRYOGENICS AND PRECISION MECHANICS ENGINEERS, TECHNICIANS, CALCULISTS, CAD SYSTEM MANAGER & DRAFT-MAN AND GOODS STORAGE & LOGISTICS -.



# CONDITION BASED MAINTENANCE SYSTEM FOR ALBA

In the context of the Spanish CDTI program Support to the Industry of Science, the externally co-funded project CBM4ALBA addressed a feasibility study on the application of novel concepts for Condition Based Maintenance (CBM). The project itself was a mean for Industrial Capacitation (IC) as well.

The CBM system/solution concept was structured in three main areas or functional elements (see Figure 39): (1) a system to measure equipment status and performance, (2) a system to monitor alarms of equipment health, and failure diagnosis support and (3) a system to perform health/life data analysis and maintenance decision support.

The project has developed further aspects related to each of the solution elements:

- 1) equipment status monitoring approaches and solutions –with special focus on vibration monitoring on rotatory machines (case study given by ALBA, related to our cooling systems);
- 2) algorithms/models/tools about weibull analysis and reliability centered maintenance (RCM);
- 3) data warehousing and business intelligence approach to asset management and maintenance – where a OSA-EAI standard Computerized Maintenance Management System (CMMS) is present.

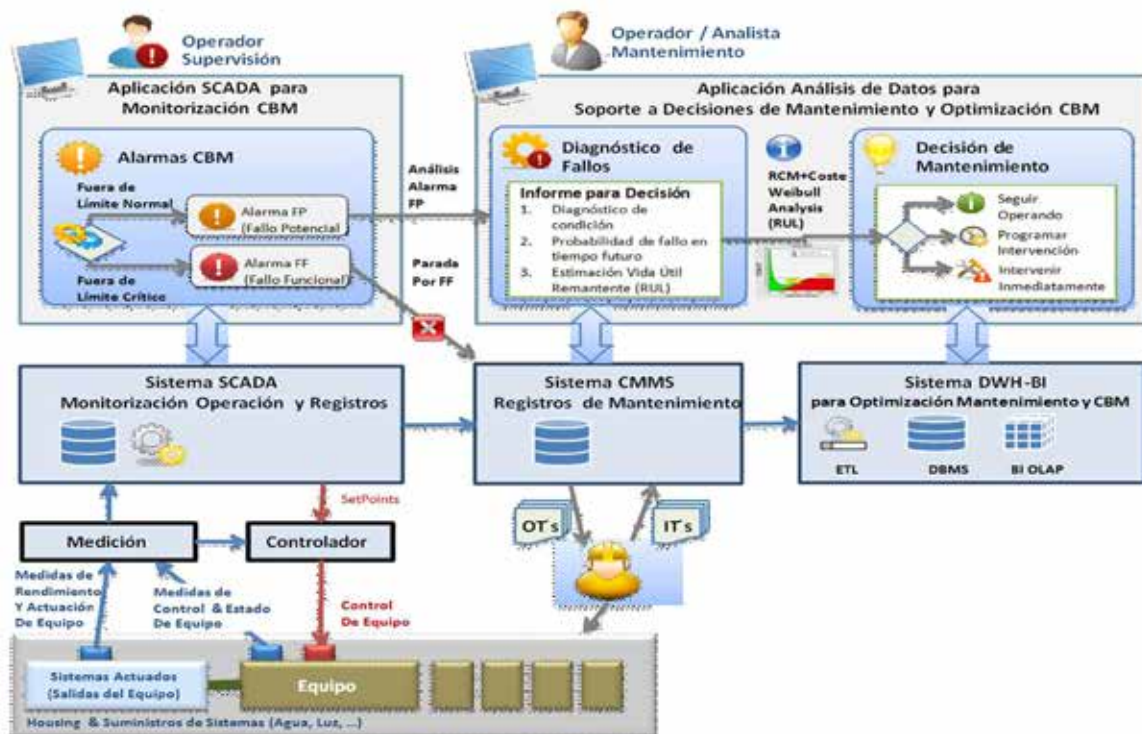


Figure 39: Design concept of the CBM for IC

## MODELLING THE ENERGETIC PERFORMANCE OF SYNCHROTRON ALBA'S COOLING SYSTEM

The topic of energy management has appeared recently in large-scale scientific facilities, to face the problem of the high impact that energy cost has on the overall running cost. In these facilities, there is a high consumption inherent to the activity, at the same time that there is a lack of energy efficiency studies that could optimize it. With the increase of the energy cost in the world and in the context of sustainable development, these installations have started thinking about developing energy management strategies to face this economic, societal and environmental issue. The Infrastructures Section in the Engineering Division at ALBA Synchrotron is deeply involved in the energy management, thanks to a recent design that integrates energy efficiency studies made during the construction phase. Representatives of the Infrastructures Section have participated to world meetings such as the «Energy for Sustainable Science» workshop in CERN (2013) to exchange experience about the energy management in scientific installations. By modeling the performance of our cooling system from the energy point of view, we have not only optimized the reliability and the stability of the control system, but also the yearly energy cost. Our annual consumption of energy is about 40 millions of kWh/year. This means an impact of about 23% of the overall running cost, and therefore, an important room for improvement. The charts detailing the distribution of this consumption were produced, highlighting that 53% of the

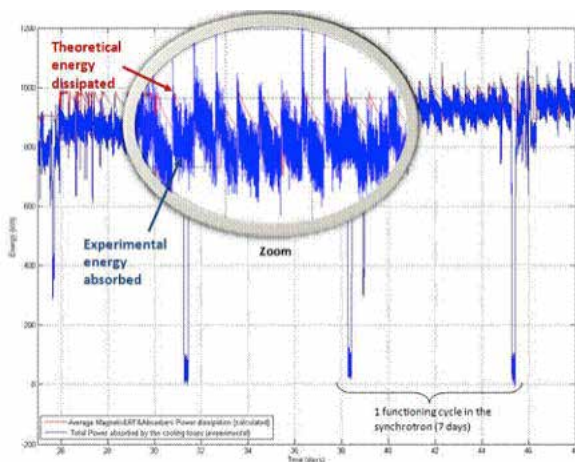


Figure 40: Comparison of the energy dissipated in the tunnel and the energy absorbed by the cooling system

energy required at ALBA is through electricity supply, while the remaining 47% comes from needs of cold water for the cooling system (cooling of the machine) and air conditioned system. However, the differences of prices of each type of energy in the contracts signed by ALBA make the electricity to be the major part of the budget (77%). During 2013, the detailed energy consumption map (see Figure 40) of our facility has been produced as a first necessary step for further improvements towards a complete energy efficiency optimization, which would represent an economic profit and high environmental benefits.

## ALBA COOLING SYSTEM UPGRADE

During the year 2013 the ALBA Cooling system suffered a problem of hydraulic stability. The problem was a constant decreasing of water flow in all cooling circuits, mainly in the Storage Ring and Booster. This behavior prevented the starting up of the accelerator systems, since 27th March to 29th May. A project was set up by a dedicated team and several actions were undertaken to understand and solve the problem. Were some of the relevant conclusions:

- The main cause of this decrease in water flow was due to the presence of air in the circuit.
- A particular characteristic of the cooling system is that all the return lines from the rings join progressively to form a common return pipe. This produces a hydraulic dependence between the four rings.
- The difference in the water flow decreasing Booster – Storage Ring versus Service Area – Experimental Area was due to the differences in the cooling interfaces (vertical separation between rings and consumptions) and due to the pressure reducers installed.
- It was realized that ALBA needed to increase their hydraulic diagnostic capability.
- Great water quantities did not pass through the filters but came back to the components through the three way temperature regulating valves or even went directly to the storage tank. The same problem existed with respect to the water quality, since the water that did not pass through the filter; also did not pass through the water treatment unit.
- Foreign bodies were found inside the hydraulic system. Subsequent chemical analysis confirmed the high content in Fe as well as Cu and Cr elements in the fibrous found in the Storage Ring inlet.

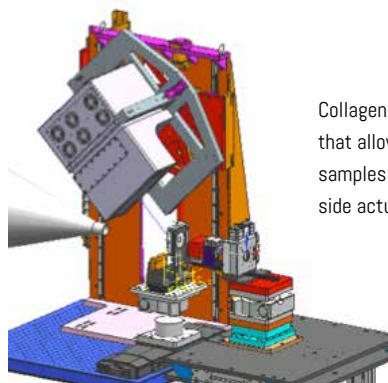
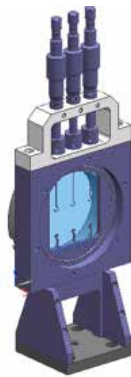
We implemented some actions during 2013 in order to improve our system, these were the main activities:

- To develop a model of the ALBA synchrotron cooling system in order to simulate numerically the steady state and transient behavior of the facility under typical operating conditions.
- First phase of the installation of electronic pressure measurement devices
- The flow circulation configuration of the Storage Ring and Booster circuits was changed from a 180°+180° to a 360° circulation. This action improved the minimum water flow velocities in the rings for removing air.
- Installed pressure reducers in the three RF cavities of the Storage Ring.
- Installed filters in critical consumptions at Service Area.
- Interchanged in/out in magnets and manifolds absorber of the Storage Ring and Booster, so that the regulating valve is at the input of the component.
- Performed test on pumps to determine pump curves for different operating frequencies.

## DESIGNS AND DEVELOPMENTS FOR ALBA'S BEAMLINES

### BL11 – NCD

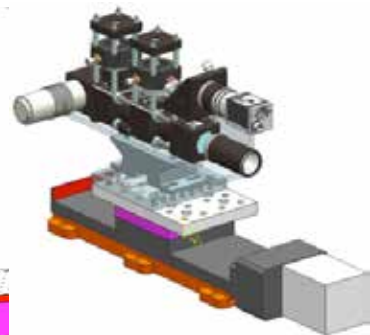
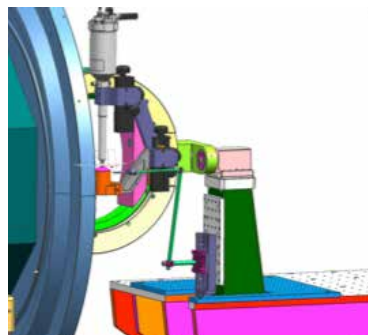
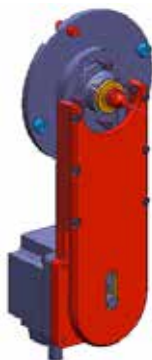
Provisional support aimed to put in operation the new WAXS. This set-up is mounted on the sample table, and consists of a manual positioning stage with vertical translation (600 mm of range) and pitch rotation (90° range).



Collagen cell, which is a sample holder that allows stretching biological samples under vacuum, by means of air side actuators.

### BL04 – MSPD

Capillary spinner for the powder diffraction end station, which is a sample spinner to rotate samples prepared in capillary at 6000 min<sup>-1</sup>.



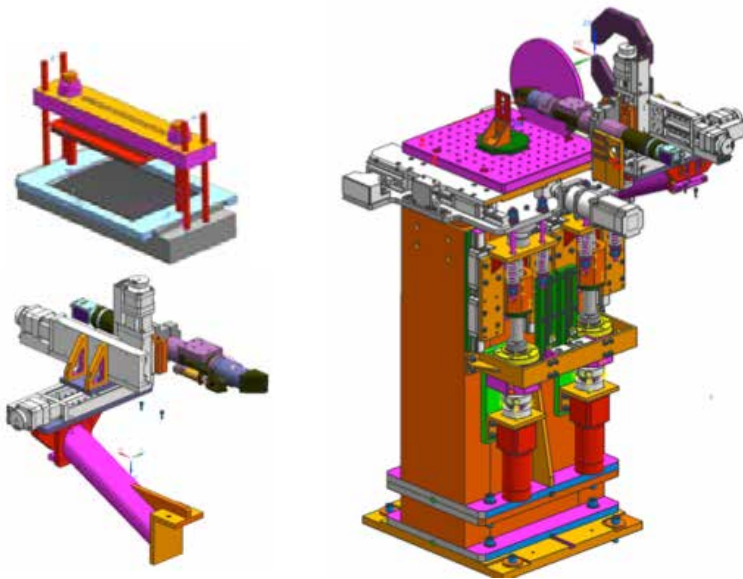
Upgrade of the beam stopper for the powder diffraction end station beam stopper. By making it manually adjustable (within a 100 mm range) it can work optimally for different experimental setups.

A new In-line camera positioning system for the high pressure end station has been also developed. It will be used to visualize the sample on the beam path by means of a pin hole through which the x-ray beam passes. The positioning system provides the proper alignment of the optics and the possibility to retract the pin hole.

## BL22 – CLAESS

Bender tool for the spectrometer. This is the tool for the proper mounting of the bender crystals to their support which interfaces with the bending mechanism.

New in-line camera view system: this is a set up for the accurate positioning of an in-line camera used to visualize the sample on the beam path by means of a pin hole which allows the x-ray beam to pass through. This camera will be used for cultural heritage experiments, for example.



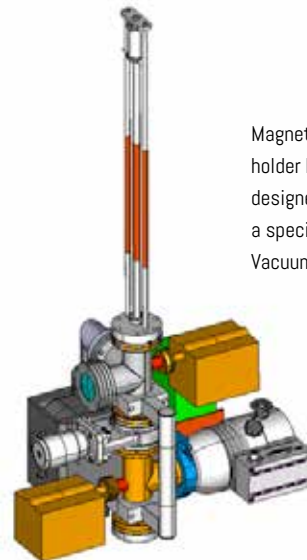
## BL24 – CIRCE



"Sample Parking". This is a retractable multiple sample holder which allows to load up to five sample from a single intervention.

This UHV suitcase is a portable vessel to be used for the loading, transportation and reinsertion of samples under UHV conditions allowing them to be moved between different experimental set-ups or end-stations. Equipped with its own ion pump, it has several hours autonomy.

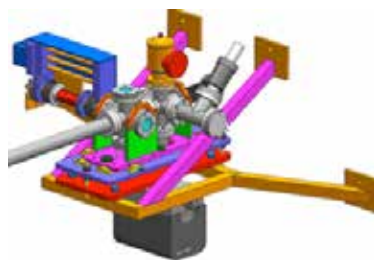
Magnetic field sample holder has been also designed for which a special Ultra High Vacuum suitcase.



## BL29 – BOREAS



New Transmission Diode set-up for BOREAS Beam-line. This device is used to detect light transmitted through the sample, at the XMCD end station. The device includes a retractile stage to remove the detector and a vacuum test & pumping stage.



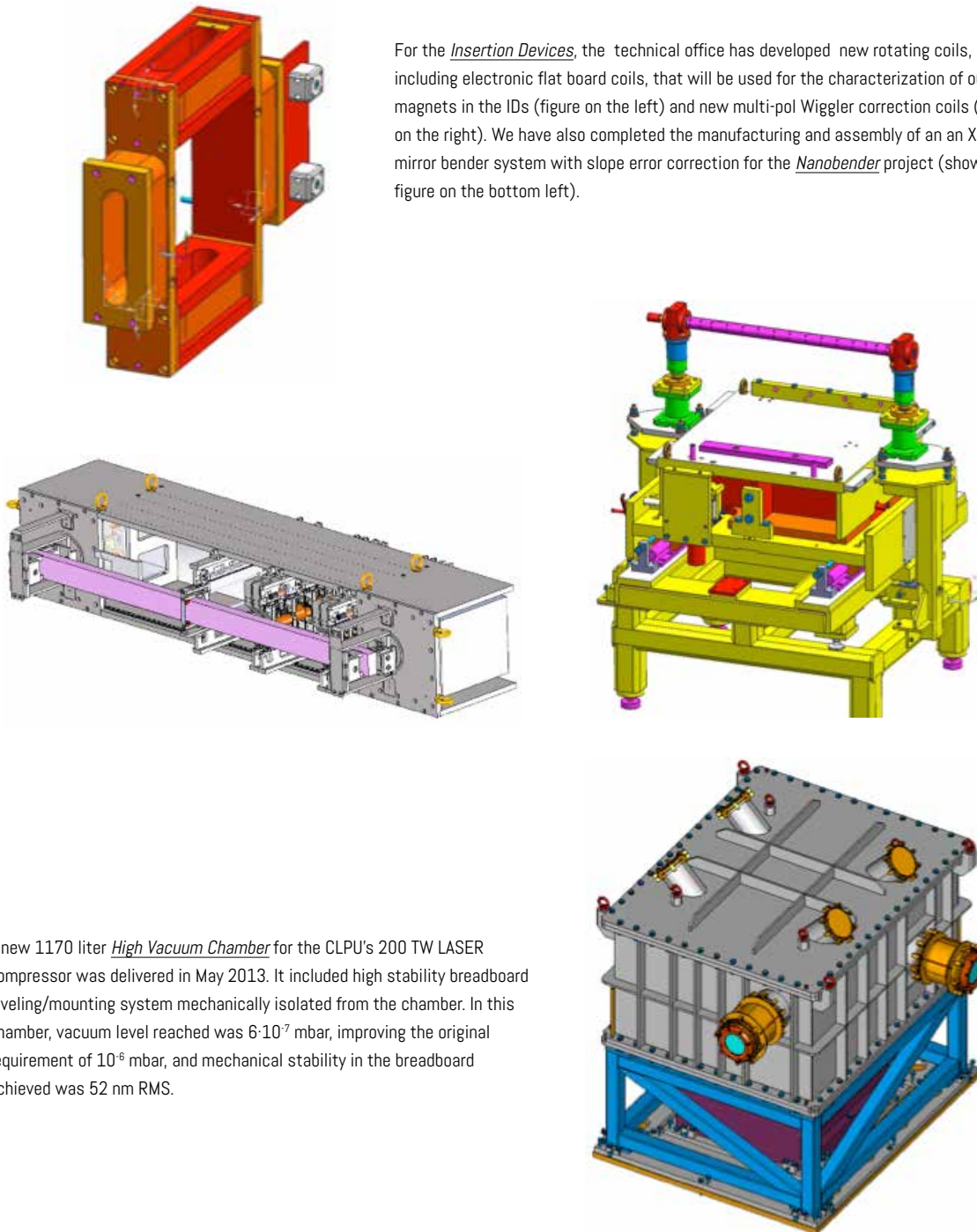
Complementary setup for fluorescence measurements in the same beam-line. This device has an specific electron shielding and thermal isolation both aimed to allow the direct mounting onto XMCD cryostat vessel avoiding to reach the dew point at the feed-through interface. Another development has been a provisional support for the preliminary end station check and commissioning.



New vacuum vessel is now available, allowing the integration of all end station equipment, and adding many ports for future upgrades. This is a versatile support which allows the mechanical assembly of the vacuum chamber and all surrounding components:  $\theta/2\theta$  rotary feed-through, Cryosample manipulator, load lock system, detectors and some vacuum equipment.

## OTHER DESIGNS AND DEVELOPMENTS

For the *Insertion Devices*, the technical office has developed new rotating coils, including electronic flat board coils, that will be used for the characterization of our magnets in the IDs (figure on the left) and new multi-pole Wiggler correction coils (shown on the right). We have also completed the manufacturing and assembly of an X-Ray mirror bender system with slope error correction for the *Nanobender* project (shown in figure on the bottom left).



A new 1170 liter *High Vacuum Chamber* for the CLPU's 200 TW LASER compressor was delivered in May 2013. It included high stability breadboard leveling/mounting system mechanically isolated from the chamber. In this chamber, vacuum level reached was  $6 \cdot 10^{-7}$  mbar, improving the original requirement of  $10^{-6}$  mbar, and mechanical stability in the breadboard achieved was 52 nm RMS.

## COLLABORATION WITH EXTERNAL INSTITUTIONS

DURING YEAR 2013 ALBA HAS CONTINUED AND EVEN STRENGTHENED ITS VOCATION FOR COLLABORATIVE EFFORTS WITH OTHER INSTITUTIONS, NOTABLY IN AN INTERNATIONAL FRAMEWORK. SOME PARTICULARLY RELEVANT ONES ARE MENTIONED BELOW, CHOSEN FOR THE INTENSITY OF THE EFFORT INVESTED AND/OR FOR THEIR STRATEGIC VALUE.





ALBA has undertaken and completed successfully a collaboration with Max-IV, building a new synchrotron light source in Sweden, to take care of the design and tendering preparation of the accelerator vacuum system. This project has involved intensive usage of ALBA expertise, with proper funding from the Max-IV side to compensate for it.



A very strategic collaboration is the one initiated with CERN, particularly within the CLIC project. Fully into the field of particle accelerators, CERN is an essential strategic partner for ALBA. Therefore further collaborative efforts with this key institution are being pursued.



One other collaboration which has implied intensive allocation of ALBA human resources and financial compensation by the external partner, has been the one performed with the Center for Ultra-short Pulsed Lasers (CLPU), located at Salamanca (Spain). In this case ALBA has taken care of doing the design and supervising the manufacturing and final installation on site of a vacuum chamber for a laser system. The project was a full success and both institutions are exploring the possibility of going further in the same spirit.



Partly through CERN itself, ALBA collaborates with the Sesame synchrotron light facility, located in Jordan. The contribution of ALBA is relevant for different Sesame project subsystems, and comes from a sustained effort in the past, with good prospects for continuing in the future.



ESRF is an institution with which ALBA has a long-standing relation, with particular emphasis on Computing and Controls activities. Collaboration has continued in 2013 and will continue in the future.



Year 2013 has seen an initiative of bilateral collaboration between ALBA and the Shanghai Synchrotron Radiation Facility (SSRF). A joint workshop was organized and held at ALBA in December 2013 with participation of SSRF scientists, in order to identify common interests and future specific collaboration projects.



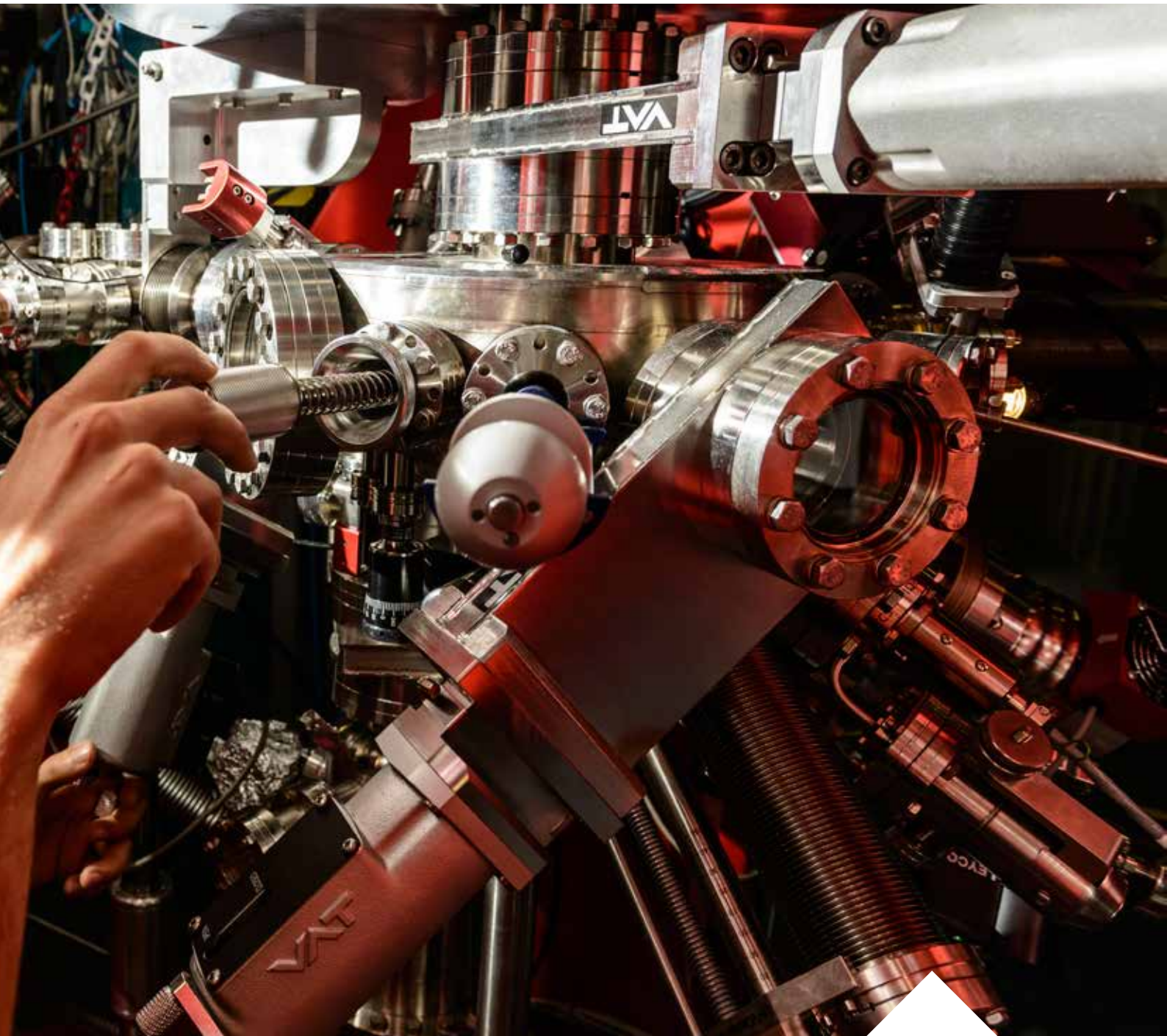
SOLEIL and ALBA have collaborated intensively during 2013, mainly in the field of Infrared microspectroscopy, wherein ALBA has been doing effort to advance on the design of the phase II beamline implementing this technique, with the help of SOLEIL scientists. Data acquisition software is another field in which both facilities interact very frequently.



ALBA has been collaborating in some developments by CIEMAT, in the field of accelerators, by using ALBA's capabilities to perform characterization of complex magnetic instruments.

# STUDENT TRAINING ACTIVITIES

ALBA HAS TAKEN, SINCE THE BEGINNING OF ITS ACTIVITY, A STRONG COMMITMENT ON CONTRIBUTING TO STUDENT EDUCATION AND PROMOTION OF SCIENTIFIC ACTIVITIES THEREIN. THIS EFFORT HAS TAKEN PLACE IN A VERY SUSTAINED WAY AT VERY DIFFERENT EDUCATION LEVELS: HIGH SCHOOL, UNIVERSITY UNDERGRADUATES, MASTER STUDENTS AND PhDs.



## PhDs. with data collected in ALBA

Eduardo Solano, from the Universitat Autònoma de Barcelona (UAB) and the Institut de Ciència de Materials de Barcelona (ICMAB-CSIC), obtained his PhD degree last November 2013 with a work about the synthesis of nanoparticles and the generation of new nanocomposite superconducting layers. Some of the measurements were acquired at BOREAS beamline in ALBA Synchrotron.

"Synthesis and characterisation of ferrite nanoparticles for  $\text{YBa}_2\text{Cu}_3\text{O}_{7-\delta}$  –

Nanocomposite superconducting layers: a neutron and synchrotron study", Eduardo Solano, directors: Susana Ricart Miró (ICMAB-CSIC) and Josep Ros Badosa (UAB).

As a part of his thesis, José Ignacio Baños, from the Universidad Complutense de Madrid and Instituto de Química Física Rocasolano (CSIC), solved the crystal structure of the complex between calmodulin and IP3 3-K using data taken at BL13-XALOC beamline.

"Structural Biology of inositol kinases, enzymes in charge of regulation of inositol phosphates", José Ignacio Baños Sanz, directors: Beatriz González Pérez and Juliana Sanz Aparicio, Universidad Complutense de Madrid and Instituto de Química Física Rocasolano (CSIC).

Taking as a somewhat arbitrary reference year 2006, at which ALBA had reached a certain critical mass in terms of staff and the facility construction was being started, ALBA has hosted about 107 student stays of very diverse types and durations.

Some remarkable achievements deserve some more specific description. During 2013 ALBA had one PhD thesis successfully finished, with full work developed within the facility. In addition, two PhD students are full-time dedicated to research at ALBA via the Marie Curie programme of the European Union. In the case of university undergraduate students, several stays were organized in the different areas of the facility. Opposite to what one could think intuitively, the possibilities for university students at ALBA go much further than just synchrotron science: accelerator physics and technology, engineering, computing and controls and even radiation safety are but some of the opportunities. The plan for 2014 are to further systematize this effort and arrange for public calls launched by ALBA in order to attract the most brilliant students of all branches of education.

Notably, 2013 saw the first edition of a series of training lectures addressed to high school teachers, with the purpose of handing over information useful for promotion of science and technology and fostering of scientific vocations at the classroom. The event was funded by La Pedrera foundation, via a competitive call for outreach projects. ALBA also collaborated with the Catalan science and technology foundation (FCRI) in the program "Science in the classroom", taking part in outreach lectures done at schools during the week of science.

Altogether it can be said that 2013 has been a year full of activity in relation to student training at ALBA. We are looking forward to 2014, when this effort shall be continued and intensified.

### 2013 STUDENT STAYS IN ALBA

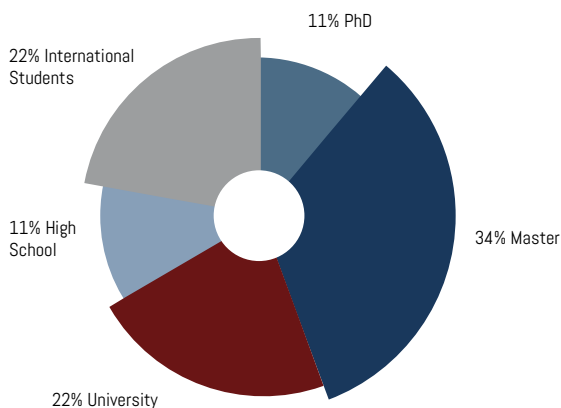
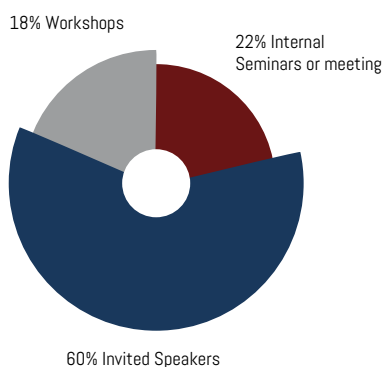


Fig. 41. Pie chart with the different type of student stays.



## 2013 EVENTS



Renowned specialists from international facilities and research centres have visited ALBA in order to promote scientific debates and exchange views and opinions with ALBA personnel. Internal seminars – addressed only to ALBA staff – have been also organized to enhance the awareness and knowledge of the different activities performed in ALBA's divisions.

ALBA has organized a total of 12 different workshops in 2013. Some of these workshops are part of international collaboration projects. ALBA has also hosted scientific meetings, such as the two annual Scientific Advisory Board Meetings, but also the 1st meeting of the Spanish Accelerators group and the 1st ALBA User Meeting, where more than a hundred of researchers attended. The ALBA Synchrotron has also continued disseminating its analytical possibilities into researchers who are still unfamiliar to synchrotron radiation techniques organizing technical workshops.

### - INTERNATIONAL COLLABORATION PROJECTS:

21/03/2013 - X-ray imaging WP8 follow-up meeting – BioStructX  
21-22/05/2013 - Sardana Workshop 2013  
23-24/05/2013 - 27th Tango Meeting Collaboration  
16-18/12/2013 - ALBA-SSRF Bilateral Workshop

### - SCIENTIFIC MEETINGS:

18/06/2013 - 16th Scientific Advisory Board Meeting  
11/07/2013 - 1st Meeting of the Spanish Accelerators Group  
03-06/09/2013 - ALBA User Meeting 2013 and VI AUSE Conference  
11/11/2013 - 17th Scientific Advisory Board Meeting

### - TECHNICAL WORKSHOPS:

03-05/04/2013 - Data retrieval and structure determination from synchrotron powder diffraction data  
03-04/06/2013 - XAS, XMCD and XMLD data analysis using CTM4XAS  
09/09/2013 - Workshop of biomedical applications of the synchrotron radiation  
14-15/11/2013 - New instrumentation for Nanoscience and Molecular

Caterina Biscari during the opening ceremony of the ALBA User Meeting 2013 and VI AUSE Conference.

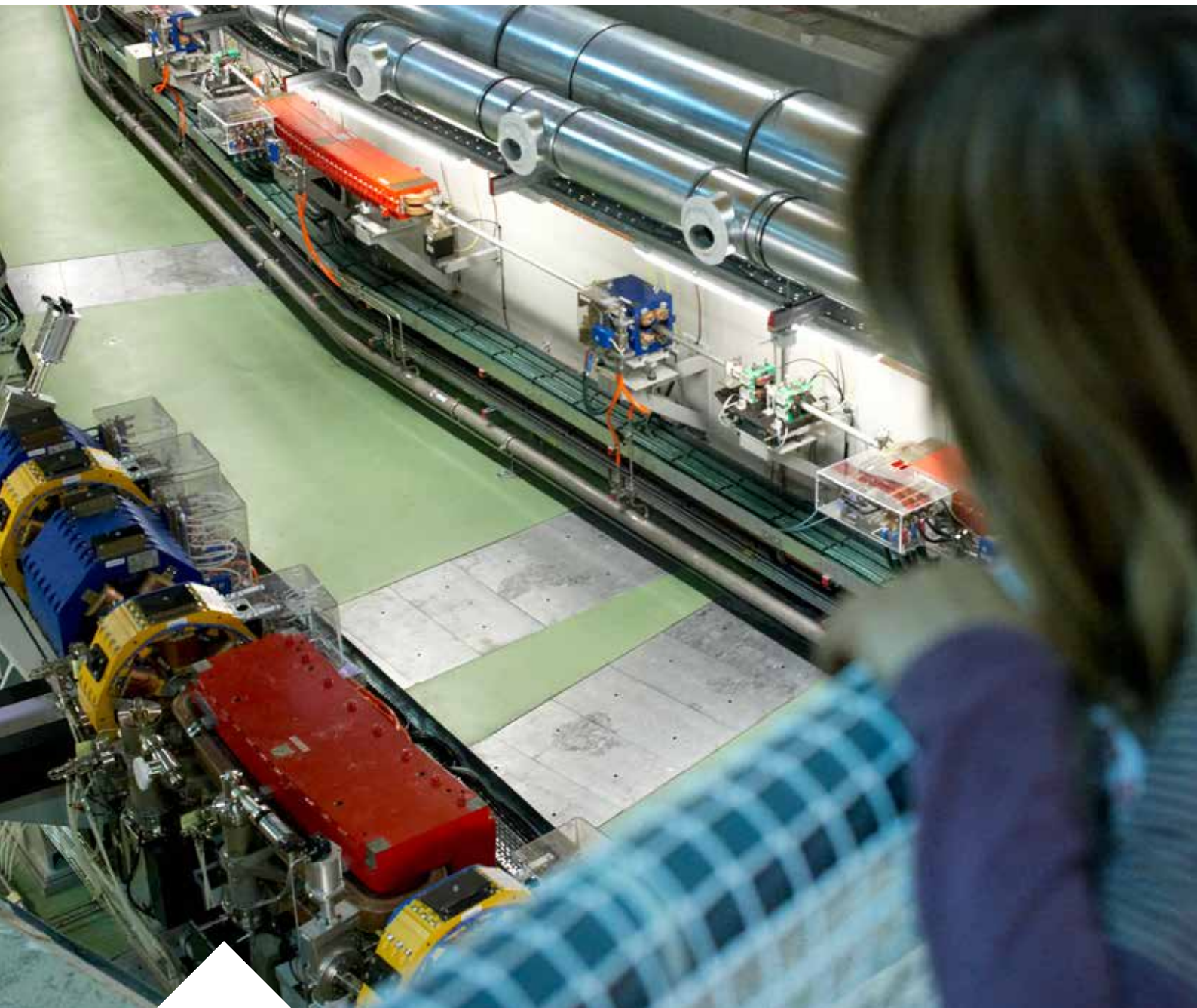
Image of the Maxwell Auditorium during the ALBA User Meeting 2013 and VI AUSE Conference.

At the poster session of the ALBA User Meeting 2013 and VI AUSE Conference.



# COMMUNICATIONS AND OUTREACH

THE ALBA SYNCHROTRON IS THE BIGGEST SCIENTIFIC FACILITY EVER BUILT IN SPAIN AND THIS FACT CAUSES A GREAT INTEREST OF THE SOCIETY AND THE MEDIA ABOUT THE RESEARCH PERFORMED IN ALBA. TO OVERCOME THESE NEEDS, ALBA CREATED IN 2013 THE COMMUNICATIONS AND OUTREACH OFFICE. ITS MAIN RESPONSIBILITIES ARE THE INTERNAL AND EXTERNAL COMMUNICATION OF THE INSTITUTION AND THE ORGANIZATION OF OUTREACH ACTIVITIES, SUCH AS THE ALBA OPEN DAY AND THE GUIDED TOURS INSIDE THE FACILITY.



---

During 2013, the ALBA Synchrotron has concentrated its outreach efforts on getting to know the society what a synchrotron is and which its main applications are. The ALBA Open Day and the Guided Tours Program are designed to accomplish these objectives.

The ALBA Synchrotron opened its doors to 1,584 people during the 2nd ALBA Open Day 2013. On December 2012, the 1st ALBA Open day had received 1,200 people. The visit was organized around a circuit with several exhibition areas, enabling visitors to see the devices through which the electrons pass, observe the interior of the accelerator's tunnel – which was only opened on occasion – and ask and talk to ALBA scientists and technicians.

Guided Tours have brought more than 3,500 people inside ALBA in 2013. These tours are organized in groups of 20-25 people and last approximately one hour and 30 minutes. Visitors can walk through the experimental hall and discover the different beamlines and equipment of the facility. High school students are the biggest group (37%) that has visited ALBA, followed by families (29%) – who were able to visit ALBA during summer holidays -. It is also remarkable the guided tours organized for other public or private institutions (professional and cultural associations).

GUIDED TOURS 2013

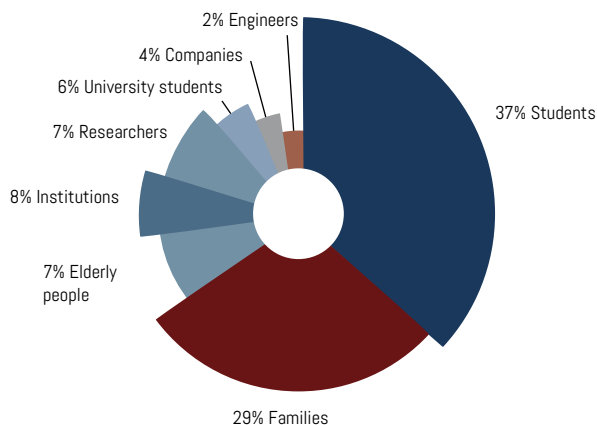




Image of the mayor of Barcelona, Xavier Trias, during his visit in ALBA.



More than 30 high school teachers participated at the seminar of synchrotron light.



Teachers during practical experiment in the seminar of synchrotron light.

## SPREADING ALBA'S ACTIVITIES

As part of the work developed for students, in 2013 the ALBA Synchrotron and the Catalunya-La Pedrera Foundation organized a seminar for high school teachers with the aim of increasing their knowledge of synchrotron light and its properties. The two-day seminar combined theoretic and practical contents, materials and examples to be used with students into the classroom and also a visit to ALBA's facilities.

The ALBA Synchrotron has enhanced its communication channels to improve the external and internal knowledge of the facility. The attention to media has been one of the main tasks developed, obtaining more than 40 direct mentions in mainstream Spanish media. One of the most successful cases has been the children cartoon "Descubre con Tadeo Jones", who devoted one chapter to our facility.

ALBA has also transformed its newsletter into the ALBA News magazine. Addressed to the scientific community interested in the use of synchrotron radiation, the ALBA News is a four-monthly magazine to inform the scientific community about the main activities of ALBA: news about the experiments performed in the different beamlines as well as in the accelerator complex, industrial collaborations, outreach activities,...

Regarding the internal communication, ALBA has also renovated the Management Board News, a newsletter for ALBA staff aimed at informing about the content of the Management Board Meetings.





**Management Board News**

**General News**

**Open Day 2013 looks for exhibitors**

**Meeting of Italian accelerator groups**

**Scientific and technological representatives of the Mediterranean Research Site visit ALBA**

**Collaborations**

**ALBA and JARA European Network**

**Industry News**

**CO2 and hydrogen in central ALBA**

**New industrial open to**

**Training programs**

**Science students in Cerning**

**Staff**

**New staff in ALBA**

**Staff leaving ALBA**

**Sincrotró a tota màquina**

**1**

**2**

**3**

**4**

**El sincrotró Alba il·lumina Part gòtic català**

**a Ciència**

**VEUREM ENTRENAR AL SINCROTRÓ ALBA EN UN DIA**

**EL PAIS CATALUÑA**

**El Sincrotrón Alba abre sus puertas**

**La instalación científica puntera organiza visitas guiadas para todo el público**

**Archivado en:**

**La oportunidad de conocer una instalación puntera como esta no se da cada día", comenta Joan Claveria, de 52 años y economista de profesión, pero aficionado a la ciencia. "Tengo curiosidad de ver qué se ha hecho con el dinero invertido y conocer qué experimentos hacen", añade Albert Parera, de 60 años y empleado de banca. Ambos han participado este miércoles por la mañana, junto a una veintena de personas más, en una visita guiada al Sincrotrón Alba, el acelerador de partículas situado en Cerdanyola del Vallès. Los gestores de la instalación aprovechan el mes de agosto, en que esta permanece cerrada para realizar tareas de mantenimiento, para organizar visitas guiadas al público en general. Es la segunda vez que se hace. En diciembre se realizó una jornada de puertas**

# FACTS & FIGURES

IN THIS FINAL SECTION, WE SUMMARIZE THE MAIN FACTS AND FIGURES OF THE ALBA SYNCHROTRON ACTIVITY IN 2013.



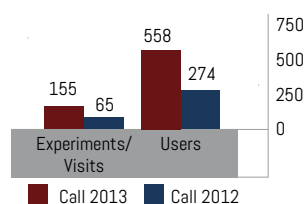
## USERS

For the first years of operation, the ALBA Synchrotron has launched two official User calls: 2012 (allocating experiments from May 2012 to March 2013) and 2013 (allocating experiments from April 2013 to March 2014). These proposals were evaluated by a panel, composed by international experts from different research areas, resulting on a ranking based on scientific excellence criteria. On 2012 and 2013 calls, the number of proposals received more than doubled the beamtime availability. Most of the granted experiments belong to Spanish institutions (82%). Macromolecular Crystallography has been the most demanded research area followed by Materials Sciences, Hard Condensed Matter, Chemistry, Biology, Soft Condensed Matter, Environment and Cultural Heritage and Methods and Instruments.

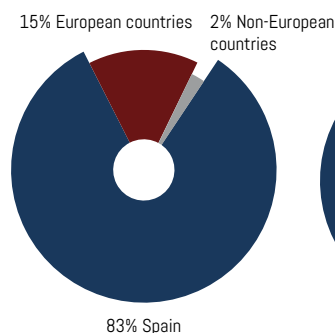
As the end of the 2013 cycle (in March 2014), the ALBA Synchrotron hosted a total of 220 official experiments and a total of 832 official users.

Most demanded beamlines have been BL13-XALOC (Macromolecular crystallography), followed by BL04-MSPD (Materials Science and Powder Diffraction), BL22-CLÆSS (Core Level Absorption and Emission Spectroscopies), BL29-BOREAS (Resonant Absorption and Scattering), BL11-NCD (Non-Crystalline Diffraction), BL24-CIRCE (Photoemission Spectroscopy and Microscopy) and BL09-MISTRAL (X-Ray Microscopy).

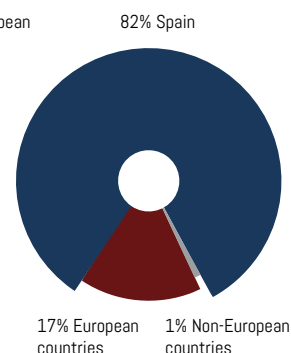
OFFICIAL USERS AND EXPERIMENTS



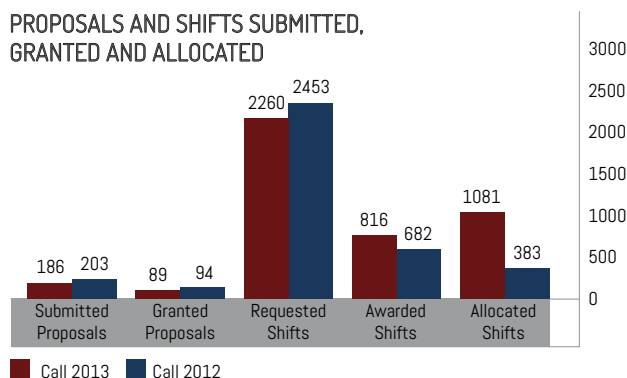
NATIONALITIES OF 2013 GRANTED PROPOSALS



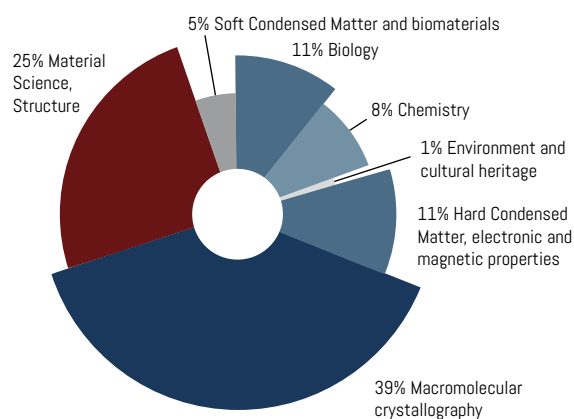
NATIONALITIES OF 2012 GRANTED PROPOSALS



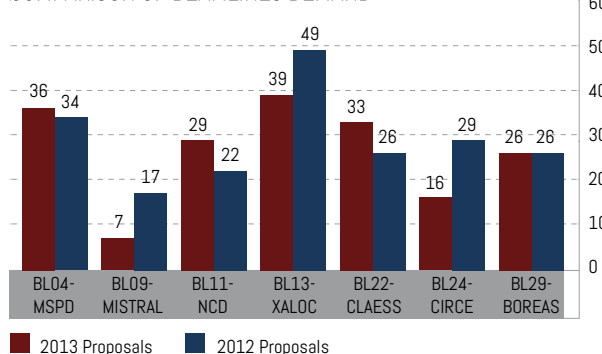
PROPOSALS AND SHIFTS SUBMITTED, GRANTED AND ALLOCATED



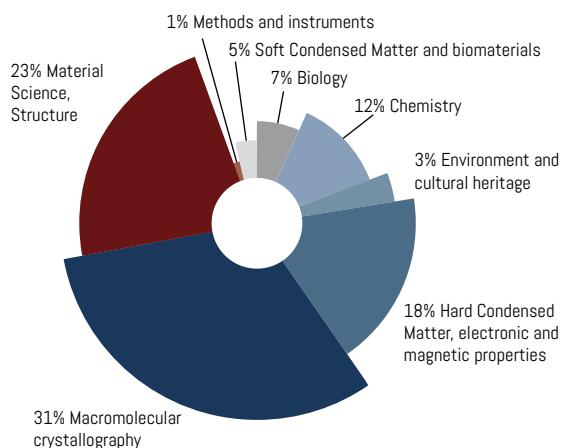
RESEARCH AREA OF 2012 GRANTED PROPOSALS



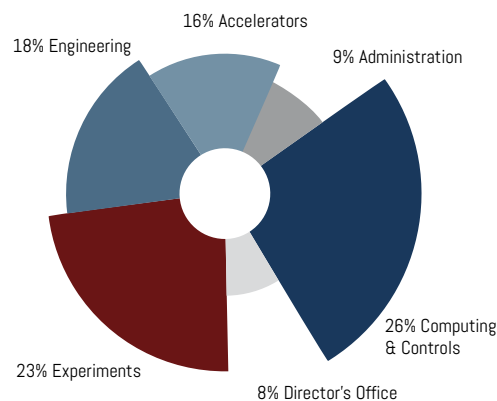
COMPARISON OF BEAMLINES DEMAND



## RESEARCH AREA OF 2013 GRANTED PROPOSALS



## ALBA STAFF - DISTRIBUTION OF DIVISIONS

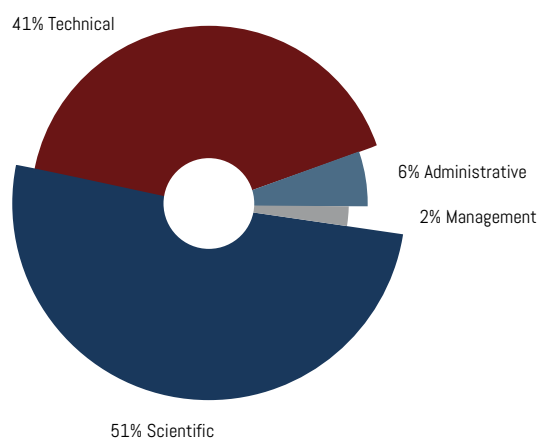


## MACHINE PERFORMANCE

The original schedule for 2013, including ca. 3500 h of beamtime for beamlines, had to be revised down to 3069 h. Taking as a basis this updated schedule, which was the one actually executed, the key performance figures are given below:

Scheduled hours for BLs	3069
Delivered hours for BLs	2971.5
Hours for machine development and optimization	1320
Mean Time Between failures (h)	25
Mean time to be back (h)	0.8

## ALBA STAFF - DISTRIBUTION OF CATEGORIES



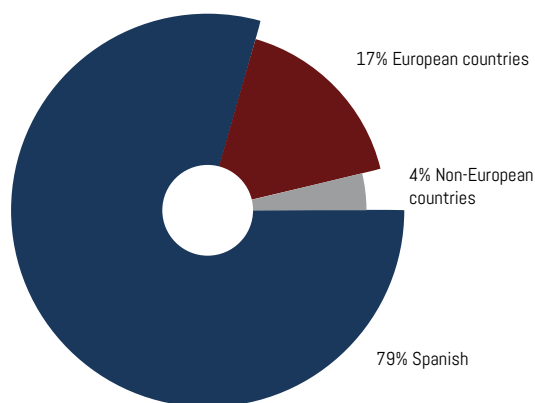
## HUMAN RESOURCES

As of 31st December 2013, the ALBA Synchrotron has 165 employees, organized in five different divisions: Accelerators (16%), Administration (9%), Computing & Controls (26%), Experiments (23%), Engineering (18%); in addition there is a director's office (8%).

The ALBA staff consists of 51% scientific staff, 41% technical and engineering staff, 6% administrative staff and 2% management staff.

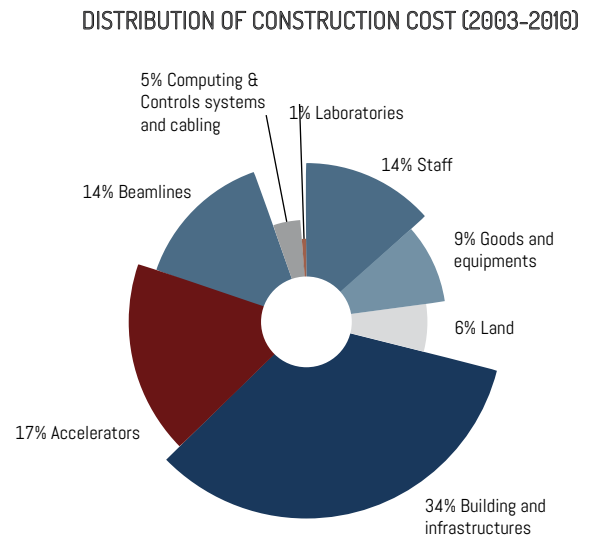
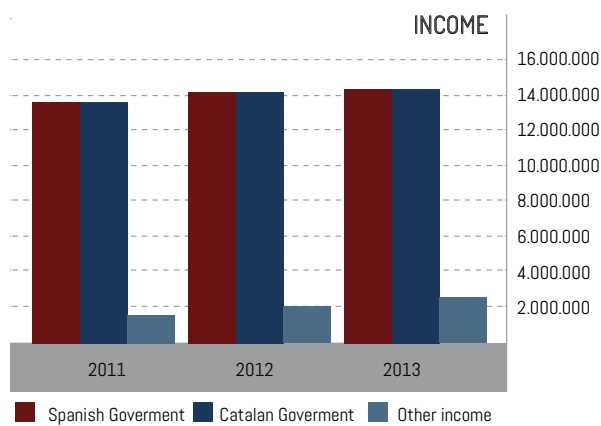
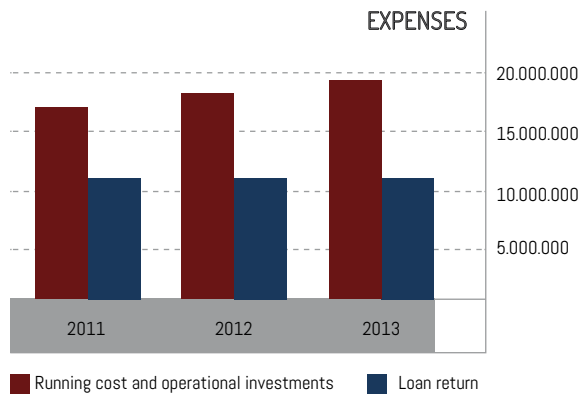
79% of staff is composed of Spanish people – in many cases people who have come back from other foreign countries -, 17% of staff is from other European countries and 4% from non-European ones.

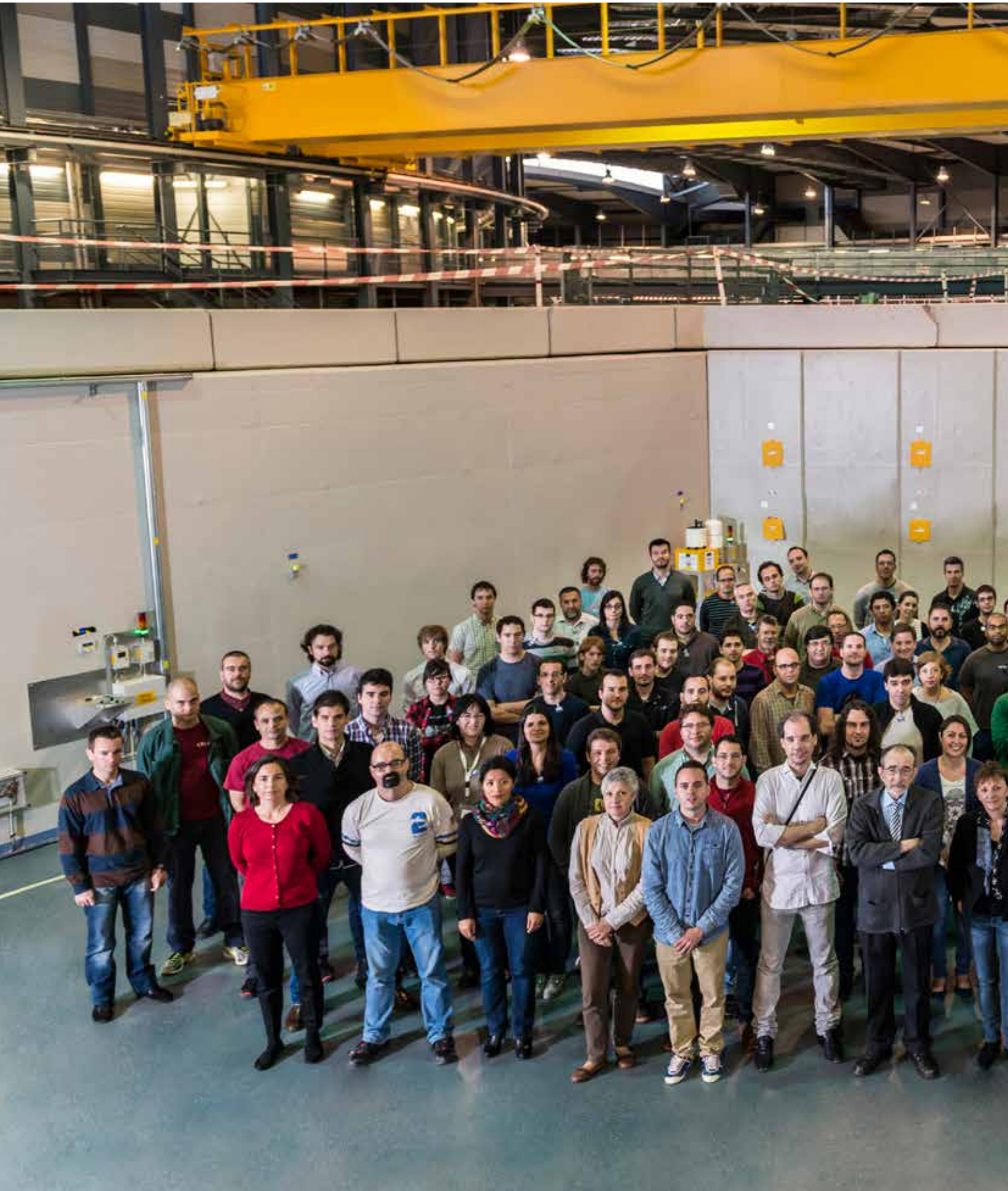
## ALBA STAFF - DISTRIBUTION OF NATIONALITIES



## BUDGET AND FUNDING

The total investment budget of ALBA during the period 2003-2010 has been 211 M€.













ALBA Synchrotron - Carretera BP 1413, de Cerdanyola del Vallès a Sant Cugat del Vallès, Km. 3,3  
08290 Cerdanyola del Vallès, Barcelona, Spain - Tel: +34 93 592 43 00 - [www.cells.es](http://www.cells.es)